ABSTRACT

Title of Dissertation: EVOLUTIONARY HISTORY AND CONSEQUENCES OF GENE FLOW IN BEARDED MANAKINS

Kevin Faulkner Philipson Bennett,
Doctor of Philosophy, 2023

Dissertation directed by: Adjunct Professor Michael J. Braun,
Department of Biology
Professor Gerald S. Wilkinson,
Department of Biology

Recent advances in DNA sequencing have revolutionized evolutionary biology by allowing for genome-scale studies of non-model organisms. We can now readily connect genotype with phenotype, i.e., identify the genetic basis of particular traits, a key goal in the study of evolution. In addition, genome-scale sequence analysis has shifted our understanding of the frequency and magnitude of gene flow in nature. Once viewed as important only for its role preventing divergence, the common view now is that in many taxa gene flow occurs among many lineages in the early stages of divergence. My dissertation focuses on gene flow in bearded manakins (genus *Manacus*), which are notable for their intense tandem courtship display, high degree of reproductive skew among males, and bright male plumage. In western Panama, yellow-collared *M. vitellinus* and white-collared *M. candei* interbreed in a narrow hybrid zone. Male *vitellinus* secondary sexual traits, including the yellow collar, have introgressed roughly 50 km west across the hybrid zone into *candei* populations and then stalled at the east bank of the

Río Changuinola, the region's largest river. Evidence from studies of male-male interaction and female choice implicate positive sexual selection for yellow collars as a driver of introgression. For thirty years since this situation was first described in detail, several key issues have remained unresolved, including why introgression has not continued across the river and what gene or genes are responsible for yellow coloration. In the first chapter, I reviewed the current state of knowledge of the *Manacus* hybrid zone system and proposed new hypotheses for some of the patterns exhibited by these populations. In the second chapter, I used reduced-representation genome sequencing to investigate whether reduced gene flow across the Río Changuinola alone can explain stalled trait introgression. I found that, although advantageous plumage traits have not introgressed far beyond the river, substantial gene flow is occurring, implicating an additional selective force or forces in preventing trait introgression. In the third chapter, I used whole-genome sequencing of all major *Manacus* lineages, including unpigmented *M. manacus* and pigmented *M. aurantiacus*, to explore the evolution and genetic basis of collar coloration. I identified the carotenoid metabolism gene beta-carotene oxygenase 2 (*BCO2*) as responsible for collar color differences between *vitellinus* and *candei* and uncovered evidence of past introgression introducing *aurantiacus BCO2* alleles into *vitellinus*. I argue that gene flow is likely to be a more common mechanism than previously appreciated for spreading sexual traits among species.

EVOLUTIONARY HISTORY AND CONSEQUENCES OF GENE FLOW IN BEARDED MANAKINS

by

Kevin Faulkner Philipson Bennett

Dissertation submitted to the Faculty of the Graduate School of the
University of Maryland, College Park, in partial fulfillment
of the requirements for the degree of
Doctor of Philosophy
2023

Advisory Committee:
Professor Gerald Wilkinson, Chair
Adjunct Professor Michael Braun, Co-Chair
Professor Karen Carleton
Assistant Professor Heidi Fisher
Professor Carlos Machado
Associate Professor Stephen Mount, Dean's Representative

Preface

Chapter One was published in 2021 as "Sexual selection and introgression in avian hybrid zones: spotlight on *Manacus*" in Integrative and Comparative Biology as part of the symposium "Manakin genomics: comparative studies of evolution and behavior in a unique clade of birds" (vol. 61, no. 4, pp. 1291-1309). It was conceived by me, Michael J. Braun, and Haw Chuan Lim. I wrote the manuscript with edits and comments from MJB and HCL. It is reproduced here (with the exception of Figure 1.2, which has been modified to include information relevant for Chapter Three) under the Oxford University Press self-reuse policy. Chapter Two is a submitted manuscript at the time of submission of the dissertation. Robb T. Brumfield, MJB, and I conceived and designed the study. Gerald S. Wilkinson and MJB supervised the research. I collected and analyzed the data in consultation with Peri E. Bolton. GSW, PEB, and MJB provided feedback on the analysis. I wrote the manuscript. GSW, PEB, RTB and MJB provided edits and comments. Chapter Three has been adapted from a collaborative manuscript in preparation, and I will be a co-first author. The project was conceived and designed by HCL, MJB, and me. HCL and I prepared and sequenced the genetic samples. HCL processed and filtered the *M. candei* and *M. vitellinus* DNA sequencing data and performed the principal components analysis in Appendix B. I performed the genomic windows analyses in consultation with HCL. I performed all analyses related to ancient introgression in *Manacus*. HCL and I collaboratively wrote the manuscript along with substantial input at all stages from MJB and Geoffrey E. Hill. The biochemical work, microscopy, and feather structural analyses were performed by Nicholas M. Justyn and Matthew J. Powers with supervision from GEH, and the associated section in the manuscript was written by NMJ and edited by me and HCL. MJB supervised the research. Contributors to particular methods are noted in the text.

Dedication

To Elijah, with the hope and expectation that the beauty and order and chaos of the natural world will enrich your life as it has mine. I love you.

Acknowledgements

First, many thanks to my early science mentors Tina Davies (high school), Judy Stone and Herb Wilson (undergrad), and Alan Clark, Peter Marra, Brian Evans, and Jason Munshi-South (master's), who collectively inspired and prepared me to become a scientist.

With immense gratitude, I thank Michael Braun for introducing me to and immersing me in the world of evolutionary genomics and for consistent support and encouragement over the last six years. With great appreciation, I thank Jerry Wilkinson for considerable good advice, direction, and patience. Many thanks to Karen Carleton, Heidi Fisher, Carlos Machado, and Steve Mount, all of whom substantially improved this dissertation and my academic experience at UMD. Thanks also to the Wilkinson Lab, including Danielle Adams, Kim Paczolt, and Edward Hurme, for their perspective and advice as these projects developed.

Thank you to the many Smithsonian scientists who helped me navigate the practical realities of laboratory and museum research, including Carole Baldwin, Chris Milensky, Chris Huddleston, Carla Dove, Faridah Dahlan, Jacob Saucier, Katie Murphy, Tripp McDonald, Mary Faith Flores, Carrie Craig, Jeff Hunt, Brian Coyle, Kate Rodriguez-Clark, Rebecca Dikow, Mike Trizna, Vanessa Gonzalez, Mirian Tsuchiya, and Matt Kweskin.

For indispensable assistance with field work, thank you to Adolfo Muñoz, Cesar Martinez, Marcelo Ábrego, Cesar Romero, Peri Bolton, Tom Parsons, and the Smithsonian Tropical Research Institute, including Owen McMillan, Raineldo Urriola, Isis Ochoa, and Taisha Parris.

I am grateful for the advice, support, and community of my network of friends and colleagues at UMD, including Shauna Rasband, Domenick Braccia, Nick Rachmaninoff, Vanessa Rubio Ramos, Anshuman Swain, Zabdiel Alvarado Martinez, Dave Weber, Miranda

Yourick, Stephanie Chia, Zeke Gonzalez, Joseph Mack, and Maria Colt, and the inspiring Manakin Genomics Coordination Network, including Chris Balakrishnan, Peri Bolton, Kira Long, Luke Anderson, Ben Vernasco, Elsie Shogren, Pearl Rivers, Andre Moncrieff, Lia Kajiki, Leilton Luna, Laura Schaedler, Alice Boyle, Emily DuVal, Mike Webster, Barney Schlinger, Leo Fusani, Matt Fuxjager, Bette Loiselle, and many more.

Finally, with profound love and gratitude, thank you to my parents, Jill Philipson and Charlie Bennett, my brother Drew Bennett, my mother- and father-in law, Debby and Tony Urbanelli, and my wife Katy Bennett, for many unwavering years of love and support.

Table of Contents

Preface ... ii
Dedication ... iii
Acknowledgements ... iv
Table of Contents ... vi
List of Tables ... vii
List of Figures ... viii
Introduction ... 1
Chapter 1. Sexual selection and introgression in avian hybrid zones: spotlight on *Manacus* ... 4
- Abstract ... 4
- Introduction ... 4
- Manakins ... 9
- Hybridization, sexual selection, and introgression in *Manacus* ... 11
- Outstanding issues in the *Manacus* system ... 19
- Opportunities for future research with *Manacus* ... 27
- Conclusions ... 35
- Acknowledgements ... 36

Chapter 2. Impact of a riverine barrier on genomic introgression of a sexually selected trait ... 37
- Abstract ... 37
- Introduction ... 38
- Methods ... 42
- Results ... 46
- Discussion ... 50
- Acknowledgements ... 59

Chapter 3. Repeated introgression of an ornamental male plumage trait in manakins ... 60
- Abstract ... 60
- Introduction ... 60
- Colorful feathers have a single carotenoid and a distinct microstructure ... 62
- *BCO2* is responsible for yellow collar pigmentation in hybrid manakins ... 64
- *BCO2* shows signatures of past interspecies introgression ... 69
- Conclusions ... 71
- Acknowledgements ... 72

Appendix A. Supplementary material for Chapter 2 ... 73
Appendix B. Supplementary material for Chapter 3 ... 88
- Feather analyses ... 88
- Resequencing and outlier analysis ... 97
- Ancient *BCO2* gene flow ... 112

References ... 116

List of Tables

Table	**Page**
Table 1.1 Five non-mutually exclusive hypotheses explaining incomplete trait introgression across the *Manacus* hybrid zone in Panama	20
Table 2.1. AMOVA results partitioning variation within and between sampling locations and between riverbanks	48
Table S2.1. Manakin samples sequenced for Chapter Two	76
Table S2.2. Geographic and genetic distance between manakin populations	84
Table S2.3 AMOVA results partitioning variation within and between and between riverbanks of the Río Teribe	85
Table S2.4. Geographic and genetic distance between all-male samples of manakin populations	86
Table S2.5. AMOVA results partitioning all-male variation within and between and between riverbanks	87
Table S3.1. Summary of museum specimens sampled to perform feather analyses	88
Table S3.2. Results from statistical models contrasting carotenoid and reflectance data among manakin species	94
Table S3.3. Samples used for genome resequencing	100
Table S3.4. Genomic neighborhoods containing outlier regions	107
Table S3.5. Sample information for ancient *Manacus* gene flow analyses	113

List of Figures

Figure	**Page**
Figure 1.1. Relationships of manakins (Pipridae)	10
Figure 1.2. An overview of *Manacus*	12
Figure 1.3. Proposed model for stalled introgression of *Manacus* yellow plumage	24
Figure 2.1. The hybrid zone between *Manacus vitellinus* and *M. candei*	41
Figure 2.2. Geographic structure in cross-river manakin populations	47
Figure 2.3. Population structure in cross-river manakins populations	49
Figure 3.1. Biochemical, microscopic, and spectrophotometric analysis of *Manacus* feathers	63
Figure 3.2. Differentiation and introgression analyses between white-collared and yellow-collared *M. candei*	67
Figure 3.3. Gene trees in *Manacus* at three loci on Chromosome 24	70
Figure 3.4. Introgression D-statistic fd between *M. vitellinus* and *M. aurantiacus*	71
Figure S2.1. Number of genetic clusters inferred from admixture analysis	73
Figure S2.2. Cross-validation of discriminant analysis of principal components (DAPC)	74
Figure S2.3. Genetic structure in manakin populations using a male-only dataset	75
Figure S3.1. Representative HPLC chromatograms of pigment extractions detected at 450 nm using UV-vis	93
Figure S3.2. The effect of increasing feather lutein concentration on various color metrics	96
Figure S3.3. Barb width of manakin collar feathers	97
Figure S3.4. Plot of principal component axes 1 and 5	102
Figure S3.5. Density plot of differentiation and introgression statistics	103
Figure S3.6. Relationships between average nucleotide diversity of white-and yellow-collared *M. candei* and two differentiation statistics	104

Figure S3.7. Venn diagram showing the number of outlier windows supported summary statistics 106

Figure S3.8. Differentiation and introgression statistics in and around genomic neighborhood 9 109

Figure S3.9. Introgression blocks in yellow-collared vs. white-collared *M. candei* 110

Figure S3.10. Differentiation and introgression statistics in and around genomic neighborhood 19 111

Figure S3.11. Concentration of dSNPs nearby and within *BCO2* 112

Figure S3.12. Information used to determine sites cutoff in fd analysis 115

Introduction

Gene flow is the movement of genetic information between populations or species (Slatkin 1985). It was originally considered important mainly for its role in preventing speciation (Dobzhansky 1937; Mayr 1963), but more recent research, particularly using modern sequencing methods, has highlighted the profound ways that gene flow can impact evolution. Introgression between species has played an integral role in the evolution and diversification of entire clades, including African Rift Lake cichlids (Meier et al. 2019), *Heliconius* butterflies (Enciso-Romero et al. 2017; Edelman et al. 2019), and Mediterranean wall lizards (Yang et al. 2021), among others. Introgression of particular genes has been implicated in key evolutionary innovations, including pesticide resistance in *Anopheles* mosquitos (Grau-Bové et al. 2020), seasonal camouflage pelage in snowshoe hares (Jones et al. 2018), and high-altitude tolerance in hominins (Huerta-Sánchez et al. 2014).

Such introgression events often cannot be investigated directly because they have occurred in the past and positive selection has swept introgressed alleles to fixation in the recipient species. As a result, identifying these events has mostly come from instances where the genetic basis of a trait is known, and the gene tree can be compared to the species tree for incongruences (e.g., Edelman et al. 2019; Baiz et al. 2021; Suvorov et al. 2022). However, to investigate selective forces facilitating or impeding introgression, research into ongoing hybridization and introgression is necessary.

In this dissertation, I focused on hybridization and gene flow in *Manacus*, a genus of birds in the Neotropical manakin family Pipridae in which females provide all parental care and male reproductive investment is devoted entirely to mating. This situation creates intense sexual selection that has caused males to evolve special ornamentation and elaborate mating displays.

The five major lineages (including four named species) form a "superspecies," in which species replace each other geographically and form narrow hybrid zones where they come into contact. Two *Manacus* species with differences in plumage coloration of adult males hybridize in northwestern Panama: *M. candei* which has a white collar and yellow belly and *M. vitellinus* which has a yellow collar and olive-green belly. The yellow collar of *M. vitellinus* males has introgressed ~50 km across the genomic center of the hybrid zone, producing hybrid populations that look like *vitellinus* but are genomically like parental populations of *candei* (Parsons et al. 1993; Brumfield et al. 2001; Parchman et al. 2013; Long et al. in review). Introgression has proceeded as far as the east bank of the Río Changuinola, the largest river in the region (Parsons et al. 1993; Brumfield et al. 2001; Bennett et al. 2021). The yellow collar is a phylogenetic novelty (Brumfield and Braun 2001) preferred by females in mixed leks where males of both colors occur (Stein and Uy 2006b). Many males with yellow collars are more aggressive than males with white collars, regardless of whether their genomes are *vitellinus*-like or *candei*-like (McDonald et al. 2001). Thus, both intrasexual competition and intersexual choice appear to be driving the spread of key traits from one species into another in this system.

Chapter One reviews research in the *Manacus* hybrid zone system, identifies questions that remain to be answered, and proposes hypotheses to test. Among the questions addressed are (1) why yellow collars have not continued to spread across the Changuinola despite apparently being advantageous for female mate choice, (2) what gene or genes are responsible for coloration differences between species, and (3) whether yellow collars have evolved once or multiple times within *Manacus*. Chapter Two uses restriction site-associated DNA sequencing (RADseq), a reduced-representation method for efficiently genotyping thousands of loci across the genome, to address question (1) above. Chapter Three uses whole-genome sequencing of multiple

individuals from the hybrid zone region and the other major lineages within *Manacus* to address questions (2) and (3) above. Through this body of research, my co-authors and I shed light on the role of geographic barriers in preventing trait introgression, the genetic targets of sexual selection, and the mechanisms governing the evolution of sexual traits.

Chapter 1. Sexual selection and introgression in avian hybrid zones: spotlight on *Manacus*

Abstract

Hybrid zones offer a window into the processes and outcomes of evolution, from species formation or fusion to genomic underpinnings of specific traits and isolating mechanisms. Sexual selection is believed to be an important factor in speciation processes, and hybrid zones present special opportunities to probe its impact. The manakins (Aves, Pipridae) are a promising group in which to study the interplay of sexual selection and natural hybridization: they show substantial variation across the family in the strength of sexual selection they experience, they readily hybridize within and between genera, and they appear to have formed hybrid species, a rare event in birds. A hybrid zone between two manakins in the genus Manacus is unusual in that plumage and behavioral traits of one species have introgressed asymmetrically into populations of the second species through positive sexual selection, then apparently stalled at a river barrier. This is one of a handful of documented examples of asymmetric sexual trait introgression with a known selective mechanism. It offers opportunities to examine reproductive isolation, introgression, plumage color evolution, and natural factors enhancing or constraining the effects of sexual selection in real time. Here, we review previous work in this system, propose new hypotheses for observed patterns, and recommend approaches to test them.

Introduction

Although evolutionary change is constantly ongoing in nature, it is difficult to observe directly because salient changes often develop over the course of many generations. Consequently, the causative processes must often be inferred from current patterns of variation

within and among populations. Hybrid zones, regions where differentiated populations or species come into contact and interbreed, present special opportunities to overcome this limitation (Barton and Hewitt 1985). Hybrid zones can be thought of as natural laboratories of evolution, where genetic and ecological interactions between differentiated populations can be studied in real time (Hewitt 1988; Harrison 1993). Hybrid zones may also promote active evolutionary change: they give rise to new genetic diversity (e.g., Barton et al. 1983; Rieseberg et al. 1990; Elgvin et al. 2017; Barrera-Guzmán et al. 2018; Gazda et al. 2020a), accelerate speciation by reinforcing reproductive isolation (e.g., Zouros and d'Entremont 1980; Hoskin et al. 2005; Rosser et al. 2019; Roberts and Mendelson 2020), and provide conduits for gene flow between populations (e.g., Liu et al. 2015b; Dowell et al. 2018; Irisarri et al. 2018; Jones et al. 2018; Edelman et al. 2019). As a result, hybrid zones have become a rapidly growing focus of research on diversification processes as more hybrid zones have been discovered and new genomic tools have facilitated their detailed genetic characterization (Gompert et al. 2017).

Birds have been prominent in the new wave of research on diversification processes. Studies of avian hybridizations and polymorphisms have uncovered candidate genes for migratory orientation (Delmore et al. 2015; Toews et al. 2019), carotenoid coloration, melanin coloration, and plumage patterning (Lehtonen et al. 2012; Poelstra et al. 2014; Toews et al. 2016; Wang et al. 2020), demonstrated the importance of chromosomal inversions in locking together disparate traits into so-called supergenes (Poelstra et al. 2014; Küpper et al. 2016; Lamichhaney et al. 2016; Tuttle et al. 2016), and highlighted the propensity of hybridization to facilitate the rise of new inversions (Hooper and Price 2017). Avian systems have provided rich insights into how numerous factors such as genetic incompatibility, physiology, ecology, mate choice, altitudinal migration, vocal learning, and cognition can influence levels of hybridization and

hybrid zone movement in response to climate change (e.g., Bronson et al. 2003, 2005; Reudink et al. 2007; Sattler et al. 2007; Olson et al. 2010; Davidson et al. 2013; McQuillan and Rice 2015; McQuillan et al. 2018; Wagner et al. 2020). Still other systems with multiple instances of secondary contact illustrate how disparate ecological contexts and historical contingencies can produce dramatically different outcomes, ranging from massively introgressive hybridization to complete maintenance of reproductive isolation (e.g., Kingston et al. 2012, 2014, 2017).

Amid recent advances in avian hybrid zone research, a topic prime for more attention is the interplay between hybridization and sexual selection. Sexual selection is caused by differential reproductive success among individuals arising from variation in the ability to obtain mates or fertilizations (Andersson 1994). It is widely believed to be an important driver of speciation in birds and other organisms (Andersson 1994; Price 2008). Theory posits that when two species in secondary contact differ in a sexual signal, postmating isolating factors (e.g., reduced hybrid viability) can select for divergence in traits that underlie premating isolation mechanisms, reinforcing sexual signals or the discrimination of the receiver, thus causing the species boundary to be strengthened (Wallace 1889; Fisher 1930; Dobzhansky 1937; Liou and Price 1994; Coyne and Orr 2004). Indeed, divergence via mate choice has accelerated isolation in darters (Roberts and Mendelson 2020), butterflies (Rosser et al. 2019), tree frogs (Hoskin et al. 2005), and fruit flies (Zouros and d'Entremont 1980), among others.

However, evidence for speciation by reinforcement in birds has been mixed. Support for the theory includes character displacement of sexual signals, where song or plumage have diverged more in sympatry than in allopatry (e.g., Sætre et al. 1997; Seddon 2005; Kirschel et al. 2009). Evidence against this hypothesis comes from cases where discrimination among vocal signals is reduced in contact (Lipshutz et al. 2017) or where divergent plumage types fail to

produce assortative mating (Brelsford and Irwin 2009). In a review of 17 avian hybrid zones, Hudson and Price (2014) found no correlation between plumage differences and assortative mating. The picture that emerges is one in which divergent sexual signals can contribute to speciation in some avian systems, while in others they have no effect or fail to prevent collapse of isolating mechanisms upon secondary contact. Understanding the factors that govern these patterns and whether one or the other predominates demands focused and incisive research.

A third possible outcome when hybridizing species differ in a sexual signal is asymmetric introgression of the sexual trait from one species into the other. As with any adaptive trait, whether introgression can occur depends on the strength of selection, number of genes involved, and degree of physical linkage among them. Traits under strong selection and controlled by a single gene or a suite of genes locked together by an inversion might be expected to introgress easily. In such cases, a sweep to fixation in the recipient population could occur quickly, obscuring evidence of the introgression event (Barton 1979). Nevertheless, the recent rapid advance of sequencing technology and genomic analysis has led to the revelation that introgression is actually quite common across the tree of life. Notable examples include mimicry pattern genes in *Heliconius* butterflies (Edelman et al. 2019; Kozak et al. 2021), coat color in snowshoe hares (Jones et al. 2018), spectral tuning genes in African cichlids (Irisarri et al. 2018), warfarin resistance in mice (Liu et al. 2015b), and venom types in rattlesnakes (Dowell et al. 2018), among many others.

Introgression driven by sexual selection, however, has been much more rarely observed. Whether this is attributable to an actual difference in the propensity of naturally versus sexually selected traits to introgress is unclear, but because sexual traits are often involved in premating isolation, they may be less likely to introgress. In addition, ascertaining the selective advantage

of a sexual trait requires lengthy observations in the field or laboratory, and the genetic basis of sexual traits is still poorly understood compared to other adaptive traits (Wilkinson et al. 2015).

Some of the best examples of asymmetric introgression of sexual signals come from birds. However, to date there are only a handful of known examples in birds and even fewer in which selective mechanisms contributing to introgression have been identified. In White Wagtail (*Motacilla alba*) subspecies in Siberia, clines for head plumage traits are displaced from the genomic center of the hybrid zone (Semenov et al. 2017, 2021). The cline discordance in these populations appears to be consistent with a model of partial dominance and epistatic interactions between two genomic regions (Semenov et al. 2021), but with assortative mating of plumage forms preventing further cline movement (Semenov et al. 2017, 2021). Long-tailed Finch (*Poephila acuticauda*) subspecies in Australia show a bill color cline displaced from the genomic hybrid zone, but the mechanism creating the pattern remains to be uncovered (Hooper et al. 2019). In the sex role-reversed Northern and Wattled Jacanas (*Jacana spinosa* and *J. jacana*) in Panama, female body size predicts reproductive success (Emlen and Wrege 2004), and the cline for body size is shifted relative to the hybrid zone (Lipshutz et al. 2019). Body size is likely controlled by multiple genes of small effect, however, so this pattern may result from introgression from the larger *spinosa* into *jacana* or selection on standing genetic variation (Lipshutz et al. 2019). In Red-backed Fairy-wrens (*Malurus melanocephalus*), females of both red-backed and orange-backed forms preferentially seek out red-backed males for extra-pair matings, which has driven the introgression of the red-backed trait into orange-backed populations (Karubian 2002; Baldassarre and Webster 2013; Baldassarre et al. 2014). In bearded manakins (genus *Manacus*), males with golden collar plumage are preferred by females and behave more aggressively than those with white collars, causing several sexual traits to

introgress across a hybrid zone between two species (Parsons et al. 1993; Brumfield et al. 2001; McDonald et al. 2001; Stein and Uy 2006b). These latter two systems, in addition to showing displaced clines for sexually selected traits, have clear evidence for selective mechanisms contributing to introgression. Because introgression has not progressed to fixation in the recipient populations of these study systems, they contain a range of phenotypes and genomic backgrounds, and the processes of introgression and selection may be ongoing. As such, they are excellent opportunities to study the interplay of sexual selection and hybridization. Below, we review work to date on the *Manacus* system and manakins generally as a model for studying sexual selection and hybridization in wild birds, then outline promising avenues for future research.

Manakins

Manakins (family Pipridae) comprise~55 species in 17 genera that inhabit humid Neotropical forests. They are remarkable for their elaborate courtship displays, ornamentation, and social behavior. These traits are generated by intense sexual selection stemming from the birds' polygynous breeding system (Snow 2004). Males of many manakin species gather in aggregations called leks to display for females (Kirwan and Green 2011). These leks often contain smaller courts where one or more males perform courtship displays (Kirwan and Green 2011). Males of some species are known to experience highly uneven reproductive success, with one or a few males receiving the majority of all matings on a lek in a season (Lill 1974; Foster 1977; Théry 1992; Shorey 2002). A well-resolved phylogeny including all genera and nearly all manakin species was recently published (Leite et al. 2021). The phylogeny demonstrates a clear

progression in complexity of both ornamentation and display, from early branching monomorphic clades with simple lek organization and behavior to later branching clades with elaborate male plumage ornamentation, lek organization and display behavior (Figure 1.1). All these features of manakin biology have made them an excellent model system for sexual selection research.

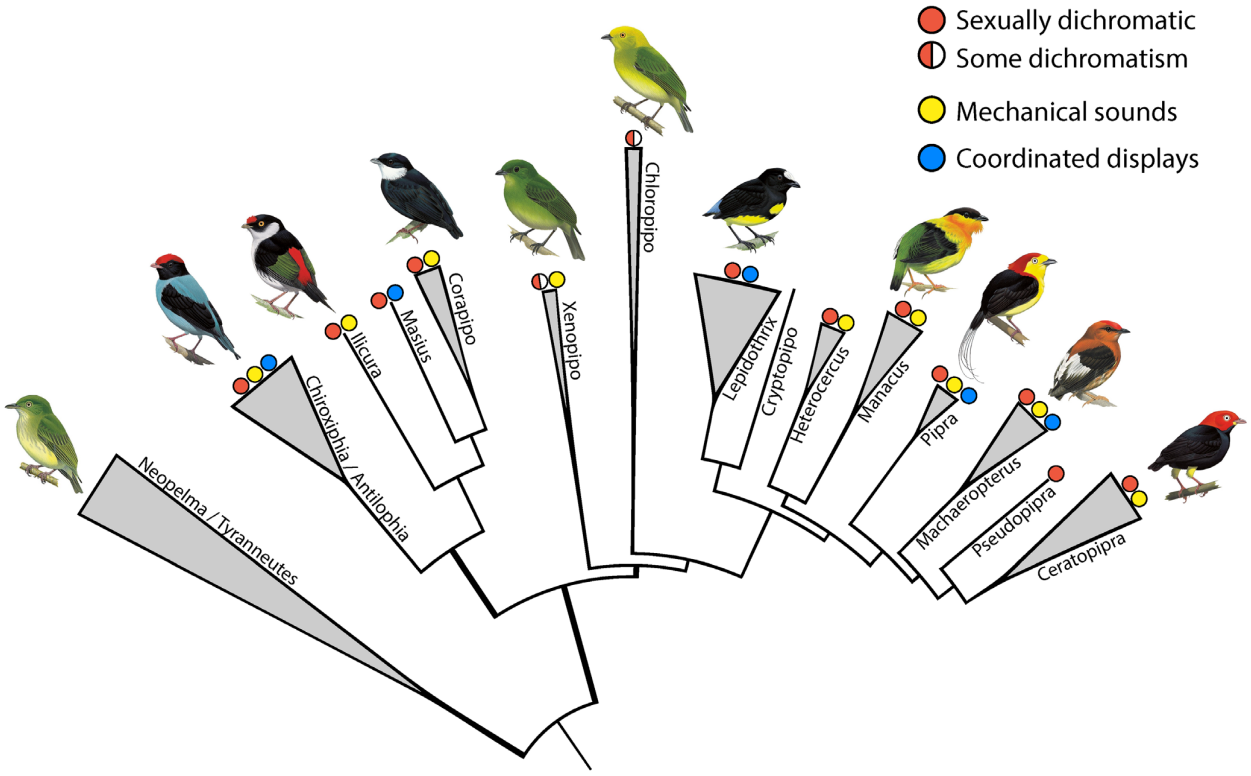

Figure 1.1. Relationships of manakins (Pipridae), adapted from the molecular phylogeny of Leite et al. (2021). Branch tips represent the 17 manakin genera with males of 11 representative species illustrated. Species show a range of plumage ornamentation, lek organization, and courtship display complexity. The oldest genera tend to be sexually monochromatic with simpler displays, while two more recent radiations have produced species that are sexually dichromatic and often elaborately ornamented with more complex displays, including mechanical sounds and/or coordination between males (Prum 1994, 1998; L. Day pers. comm.). Because displays have not been characterized for some species, display complexity traits are coded as present/absent by genus. Phylogeny reproduced from Leite et al. (2021) with permission from Elsevier. Illustrations reproduced with permission from Lynx Edicions.

Several interesting patterns of hybridization are on display in the family Pipridae. Many manakin genera are thought to have diverged in forest refugia in the Plio-Pleistocene and radiated as habitat expanded (Haffer 1969). This scenario is consistent with recent molecular

estimates of their age (Harvey et al. 2020). Similar to other avian radiations, the resulting young species tend to form parapatric distributions and can frequently hybridize with one another. For example, several cases of hybridization among species and color forms in the genera *Lepidothrix* and *Pipra* in Amazonia have been described (Haffer 1970; Stotz 1993; Weir et al. 2015; Sampaio et al. 2020). In addition, at least nine cases of intergeneric hybridization are known in manakins (Graves 1993; Marini and Hackett 2002; Alves et al. 2016), following a pattern of frequent intergeneric hybridization in clades with high degrees of sexual dimorphism (Sibley 1957; Parkes 1961). Finally, crossing between Opal-crowned and Snow-capped Manakins (*Lepidothrix iris* and *L. nattereri*) has produced the Golden-crowned Manakin (*L. vilasboasi*) in central Amazonia (Barrera-Guzmán et al. 2018), in what may be a rare example of hybrid speciation in birds.

Hybridization, sexual selection, and introgression in *Manacus*

The genus Manacus

A particularly promising system for untangling the effects of hybridization and sexual selection is the genus Manacus. The various forms in this species complex differ mainly in secondary sexual traits of males (Figure 1.2) and males are known to be under intense sexual selection (Lill 1974; Stein and Uy 2006b). At least three hybrid zones exist in the complex, which invites replicate studies of dynamic speciation processes.

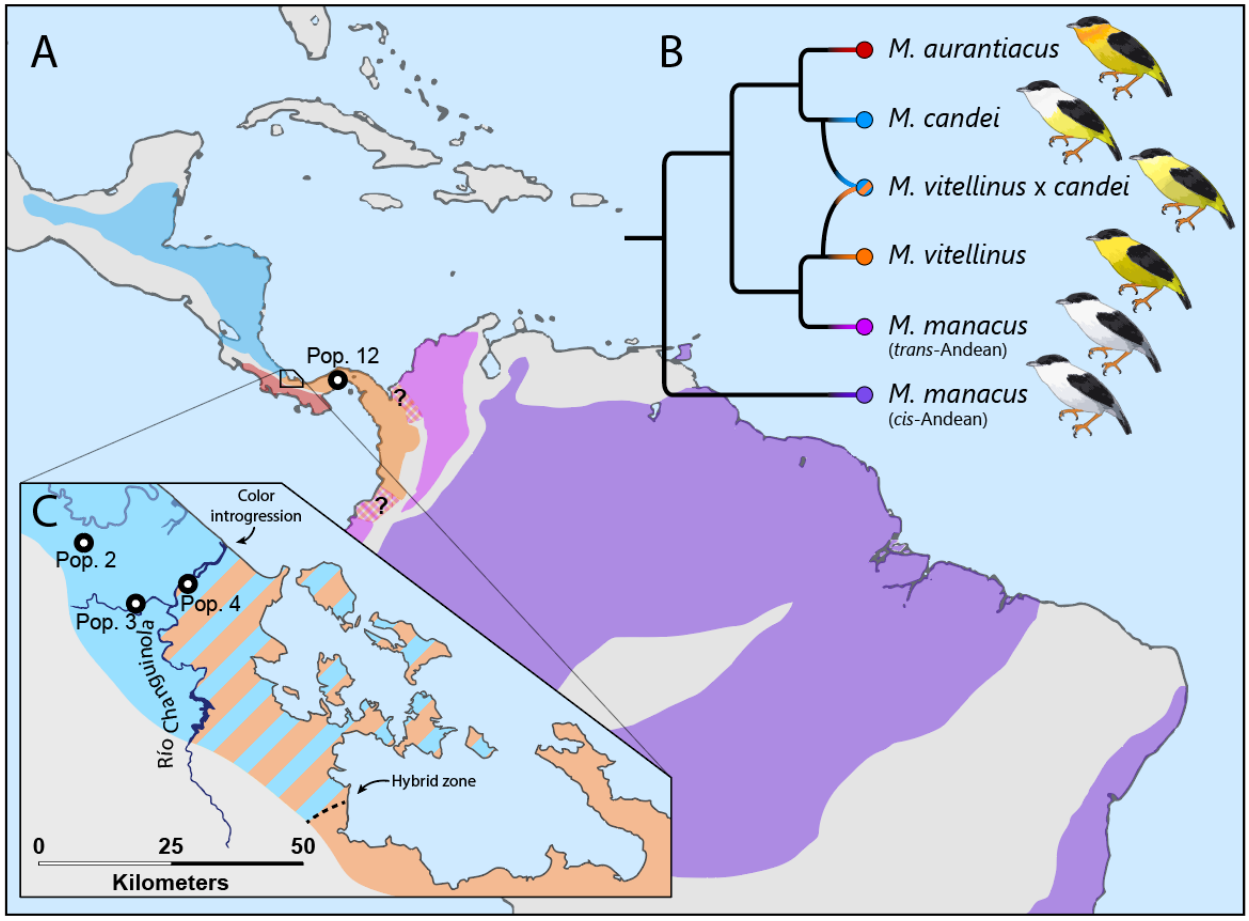

Figure 1.2. An overview of *Manacus*. A. Geographic distribution of major *Manacus* lineages. Question marks indicate the location of apparent but uncharacterized hybrid zones between *M. vitellinus* and *M. manacus*. B. Phylogeny of *Manacus* from Harvey et al. (2020). C. Hybrid zone and plumage introgression region between *M. vitellinus* and *M. candei*. Labeled populations indicate sampling sites from Chapter 3. Sampling site numbers are based on Brumfield et al. (2001). In Chapter Three, I refer to populations 2, 3, 4, and 12 as parental *candei*, WCC, YCC, and parental *vitellinus*, respectively.

Like several other manakin genera mentioned above, the four species of Manacus replace each other geographically, with each occupying well-recognized areas of endemism in Neotropical forests—White-collared Manakins (*M. candei*) in northern Caribbean Central America, Orange-collared Manakins (*M. aurantiacus*) in the humid lowlands of southwestern Costa Rica and southwestern Panama, Golden-collared Manakins (*M. vitellinus*) in other humid regions of Panama and western Colombia and White-bearded Manakins (*M. manacus*) in *trans*-Andean northern Colombia and southwestern Colombia, as well as *cis*-Andean humid regions of

Amazonia and the Atlantic Forest (Figure 1.2). This is a classic Neotropical distributional pattern often attributed to allopatric divergence in forest refugia during dry climatic periods of the Pleistocene and post-Pleistocene (Haffer 1967). A recent molecular estimate puts the age of the oldest extant lineages within *Manacus* at 2 MYA (Harvey et al. 2020), in line with Pleistocene divergence. *Manacus* species hybridize commonly wherever their ranges abut—*candei* with *vitellinus* in Caribbean western Panama and *vitellinus* with *manacus* in both northern Colombia and southwestern Colombia (Haffer 1967). This fact suggests that they have not developed reciprocally exclusive pre-mating isolating mechanisms (Mayr 1963). Their failure to occur in sympatry is also consistent with the possibility that they exclude each other through ecological competition, and modeling suggests that hybridization and competition acting in concert can limit sympatry even more strongly (Goldberg and Lande 2006). Generations of biologists have considered such patterns to constitute strong evidence of allopatric speciation in progress, with hybridization occurring upon secondary contact (e.g., Barton and Hewitt 1985; Newton 2003; Price 2008).

The intense sexual selection to which male *Manacus* are subjected has produced displays that are some of the most complex among manakins (Lindsay et al. 2015; Day et al. 2021). Display behavior is similar among the four species. Males clear a roughly one-meter circular area of all leaf litter as a display court, framed by several small upright saplings. Court-clearing among manakins is unique to *Manacus*, and this behavior has been hypothesized to aid in defense against predators (Cestari and Pizo 2014), enhancing the conspicuousness of the courtship display (Uy and Endler 2004), or both. When displaying, males jump acrobatically between saplings and rapidly strike their wings together over their backs to make a variety of snapping sounds (Chapman 1935; Skutch 1969; Lill 1974). Interested females will join in the

display without snapping, and the two will "ping pong" back and forth over the court (see Bennett, Lim, and Braun 2021 Supplementary Video).

Male *Manacus* have evolved numerous morphological specializations associated with their display and acoustic signaling (Schlinger et al. 2013; Bodony et al. 2016). Their throat feathers are elongated and can be erected into a "beard," which juts out under the mandible during display. Some flight feathers are modified with a thickened shaft and an unusual curvature, which are likely involved in producing a whirring sound males make in flight. Their leg muscles are hypertrophied to enable their long-distance jumps of up to a meter between saplings. Their wing bones are flattened to produce the loud snapping sounds they make during display. The muscle contraction needed to produce the wing snaps is an extraordinary physiological feat—it involves the fastest recorded limb muscle contraction in a vertebrate (Fuxjager et al. 2016) and among the fastest heart rates ever recorded in a bird or mammal (Barske et al. 2011). As such, it has required specialization of skeletal muscles, motor neurons, androgens, and androgen receptors (Schlinger et al. 2013; Bodony et al. 2016). In fact, the *Manacus* display has become a model system for understanding how neurophysiology supports the evolution of complex behaviors (Fuxjager and Schuppe 2018).

The hybrid zone between *Manacus candei* and *M. vitellinus*

Peters (1927) described a fifth species of *Manacus*, *M.* "*cerritus*," from the region of western Panama between the ranges of *candei* and *vitellinus*. However, Eisenmann suspected this highly variable population was the result of hybridization (Haffer 1967), which ultimately proved to be the case. Parsons, Olson, and Braun (1993) first characterized the unusual structure of this hybrid zone, showing that transitions in two male plumage characters, collar, and belly color, did not coincide with clines for morphometric traits and molecular markers, but were

displaced at least 40 km to the west. This results in a "plumage introgression zone" in which males look like yellow-collared *vitellinus* but are morphometrically and genetically like white-collared *candei* (Figure 1.2). The change from yellow to white plumage traits occurs abruptly across the largest river in the region, the Río Changuinola. The fact that the two displaced clines involved male secondary sexual traits in birds known to be under intense sexual selection in a lek breeding system led Parsons, Olson, and Braun (1993) to propose that positive sexual selection was responsible for driving these traits across the hybrid zone from one species into the other.

Butlin and Neems (1994) suggested that the apparent shift of Manacus color clines might be an artifact of greater cline width, nonlinear color scales, or genetic dominance of vitellinus traits. Brumfield et al. (2001) confirmed the hybrid zone structure with additional molecular markers and denser population sampling, replacing the semi-quantitative plumage color scores of Parsons, Olson, and Braun (1993) with spectrophotometric color measurements. They showed that the clines for collar and belly color were significantly shifted from other genetic and morphometric clines, with centers ~50 km to the west, making broader clines and nonlinear color scales untenable explanations. Genetic dominance also seems untenable; using a simple model of complete dominance for vitellinus alleles, at least 12 unlinked loci would have to be involved in collar color determination to produce the observed cline shifts and phenotypic frequencies of yellow and white birds (Parsons et al. 1994; Brumfield et al. 2001). Billo (2011) showed that vocalizations of birds with *vitellinus*-like plumage in the plumage introgression zone match those of *candei*, adding behavioral characters to the suite of traits that are concordant with the genetically and morphometrically defined hybrid zone.

Determining the age of hybridizing taxa and whether or not they are sister in a phylogenetic sense can inform important questions on genomic divergence, potential barriers to

introgression, species status, and reticulate evolution. A well-resolved phylogeny and age estimates for the species and subspecies of *Manacus* were long elusive, largely due to confounding copies of mitochondrial DNA in the nuclear genome (Braun et al., unpublished data). However, early estimates of phylogeny did indicate that *candei* and *vitellinus* were not sister taxa (Brumfield and Braun 2001; Brumfield et al. 2008). Recent phylogenomic studies have finally produced a well-supported phylogeny, confirming that *candei* and *vitellinus* are not sister, and providing an age estimate for their divergence of ~1.6 MYA (Leite et al. 2021; Harvey et al. 2020).

No formal age estimate of the hybrid zone itself has been published, but the Bocas del Toro archipelago situated just offshore from the hybrid zone may offer some clues. Wetmore (1972) referred manakin populations on these islands to *M. vitellinus cerritus*, which suggests they are derived from the mainland populations with introgressed plumage traits. The islands separated from the mainland sequentially starting ~5200 years ago (Anderson and Handley 2002). Assuming that the island populations were formed by these vicariance events, the hybrid zone must be at least as old. Recent dispersal to the islands seems much less likely. One island population with an introgressed phenotype is nearly 2 km over water from its nearest neighbor today (Billo 2011), a challenging dispersal barrier for an understory bird (Moore et al. 2008).

Additional studies have probed the genetic structure of this hybrid zone in more detail. Yuri et al. (2009) compared geographic clines between diagnostic and non-diagnostic molecular markers, reasoning that alternative diagnostic alleles are more likely to be selected against in hybrids and thus may yield underestimates of overall gene flow. They found that clines in non-diagnostic markers were wider on average, and several were significantly shifted in position towards *candei* from the genomic center of the hybrid zone. These observations are consistent

with the idea that neutral and positively selected alleles may be able to introgress more freely across this hybrid zone than the narrow coincident clines in diagnostic markers would suggest.

Parchman et al. (2013) examined genomic clines in 59,100 single nucleotide polymorphisms (SNPs) and mapped many of them to a de novo genome assembly for *M. vitellinus*. They found substantial genetic differentiation between parental *candei* and *vitellinus* populations overall (mean $F_{ST} = 0.26$), and a high degree of heterogeneity in differentiation across genomic regions (F_{ST} range 0.09–0.61). F_{ST} outliers were widely (although not universally) distributed throughout the genome. Estimates of genomic cline parameters were also highly variable across the genome, and introgression at many loci differed significantly from the genome-wide average. Genetic differentiation was correlated with the absolute values of introgression parameters in admixed individuals, consistent with many outlier loci being associated with reproductive isolation through effects on hybrid fitness or assortative mating in the hybrid zone. These results confirm and extend earlier studies (Parsons et al. 1993; Brumfield et al. 2001; Yuri et al. 2009) and suggest that speciation in these manakins involves a porous genome, where the consequences of adaptation or reproductive isolation are restricted to narrow chromosomal regions that may nevertheless be fairly numerous and widely distributed throughout the genome (Yeaman 2013), evoking a genomic landscape associated with divergence with gene flow models (Wu 2001; Via 2009).

While Parchman et al. (2013) detected a wide range of intermediacy in hybrids, genomic hybrid indices were heavily skewed towards *candei* in populations that display *vitellinus* plumage traits northwest of the genomic center of the hybrid zone (Figure 1.2). Taken together with the relatively high genome-wide F_{ST} between parental *vitellinus* and *candei* populations, this pattern suggests that chromosomal regions containing genes responsible for introgressing

traits should be readily identifiable, because they will bear signatures of *vitellinus* ancestry that contrast strongly with the *candei*-like genomic background of hybrid populations northwest of the genomic transition zone.

Sexual selection and asymmetric trait introgression in *Manacus*

If sexual selection is responsible for the observed asymmetric introgression of male traits, it could act through male–male competition, female choice, or both. Examining the propensity of vitellinus, candei, and introgressed candei males to attack taxidermic mounts of male manakins on their display courts, McDonald et al. (2001) found that *vitellinus* males are more aggressive than *candei* and that introgressed *candei* males with yellow collars are more aggressive than either parental species. Since aggression has previously been correlated with mating success in *M. manacus* (Shorey 2002), this finding raises the possibility that males with *vitellinus* plumage could increase their mating success through aggression, e.g., by gaining access to the best display court sites.

The *vitellinus* plumage phenotype could also have introgressed via female choice for yellow collars. Stein and Uy (2006a) showed that the brightness of *vitellinus* males' collar plumage predicts their mating success, supporting this idea. Stein and Uy (2006b) next measured male mating success in mixed leks in the narrow upper reaches of the Río Changuinola, where males of both color forms co-occur. They found that yellow-collared males were more successful overall than white-collared males, suggesting that females in this region prefer males with yellow collars.

Finally, plumage introgression could have proceeded via selection on correlated traits involved in courtship display. Barske et al. (2011) demonstrated that vitellinus females choose mates partly on the basis of minute differences in the speed with which males perform various

display components. Miles et al. (2018) tested for differences between the two species in one display element, the roll-snap, in which a male strikes its wings together over its back in a rapid series, creating a loud buzz. They found that *vitellinus* produces faster series than *candei* without sacrificing the duration of the entire roll-snap. Female preference for roll-snap speed has not been tested directly, but Miles et al. (2018) demonstrated that the roll-snap pushes males to their physiological limits, indicating a trait likely to be under strong selection.

These studies open the possibility that one or a combination of male competition, female preference for plumage, and female preference for display could be responsible for trait introgression across the *Manacus* hybrid zone. The correlated male traits could be under direct selection individually, could be pleiotropic effects of a single gene, or could experience indirect selection through physical linkage or genomic coupling (Butlin and Smadja 2018; Nosil et al. 2021).

Outstanding issues in the *Manacus* system

Why has plumage introgression stalled?

A significant question remaining for the *Manacus* system is why, with clear evidence of positive sexual selection, the introgressing vitellinus plumage traits have not progressed beyond the east bank of the Río Changuinola. Field surveys in 2016–2020 (K. Bennett, K. Long, and M. Braun, pers. obs.) revealed that the limit of introgression has not advanced since the system was first carefully studied more than 25 years ago (Parsons et al. 1993), nor indeed since candei was first detected in Panama more than 40 years ago (Ridgely and Gwynne 1989). If these traits are globally advantageous, theory predicts that they should sweep to fixation in *candei* (Barton 1979;

Hewitt 1988). Below we describe several non-mutually exclusive hypotheses to explain the observed pattern (Table 1.1).

Table 1.1. Five non-mutually exclusive hypotheses explaining incomplete trait introgression across the *Manacus* hybrid zone in Panama.

Hypothesis	**Description**	**First proposed**
Hypothesis 1	Dispersal constraint: the Río Changuinola prevents dispersal, and thus gene flow, between white- and yellow-collared populations. Such limited gene flow would also contribute to the hypotheses below.	Brumfield (1999); Brumfield et al. (2001)
Hypothesis 2	Frequency-dependent selection: female preference for yellow collars is frequency-dependent, such that yellow collars are only favored when they are the more common color in a lek. The Río Changuinola prevents yellow-collared birds from becoming common in populations west of the river.	Brumfield et al. (2001); Stein and Uy (2006)
Hypothesis 3	Geographic variation in optimal display habitat: because of differences in forest lighting/color conditions, white-collared males are optimized for greatest conspicuousness in forests west of the Río Changuinola, while yellow-collared males are more conspicuous east of the river.	Brumfield et al. (2001); Uy and Stein (2007)
Hypothesis 4	Display conspicuousness and male site selection: males have established leks in forest patches that optimize the conspicuousness of their own coloring. Males dispersing across the Río Changuinola will be at a disadvantage whether they join an existing lek or attempt to display on their own.	Uy and Stein (2007), expanded upon in this review
Hypothesis 5	Geographic variation in female preference: females west of the Río Changuinola prefer white-collared males.	This review

Hypothesis 1: Dispersal constraints. The simplest explanation is that the Río Changuinola constrains westward dispersal of yellow birds, preventing opportunities for further interbreeding between color forms. Rivers have long been considered major dispersal barriers to animals in tropical forests, and rivers often form the boundaries of species' distributions in the New World tropics (Wallace 1852; Weir et al. 2015; Naka and Brumfield 2018). Clearly, the Río Changuinola presents some obstacle to dispersal; leks on opposite sides of the lower river, where

the annual floodplain is nearly half a kilometer wide, consist of all yellow males on the east bank and all white males on the west bank (Parsons et al. 1993). However, the river's narrow upper reaches can be less than 100 m wide, a distance *vitellinus* is physically capable of covering over water (Moore et al. 2008). Indeed, mixed leks exist in these headwater areas, with males of each color found on the opposite bank from their predominant range (McDonald et al. 2001; Stein and Uy 2006b), demonstrating that cross-river dispersal does occur. Brumfield (1999) used 13 microsatellite markers to estimate gene flow between *Manacus* populations across the lower, middle, and upper reaches of the river, and found that it presented only a mild barrier to gene flow. Thus, lack of dispersal across the river appears insufficient to explain why introgression has stalled.

Hypothesis 2: Frequency-dependent selection. Since gene flow between populations on either side of the Río Changuinola should allow for continued introgression of vitellinus plumage traits, selection against yellow birds west of the river may be constraining such introgression. Stein and Uy (2006b) measured mating success of yellow- and white-collared birds in leks with mixed proportions of collar colors on both sides of the river. They found that yellow-collared males were more successful overall and suggested that their advantage over white-collared males increased as the frequency of yellow males in the lek increased. In other words, where yellow males were more common, they were more successful. Stein and Uy (2006b) described this as an example of positive frequency-dependent selection (FDS). Negative FDS in sexual selection has occasionally been invoked as a mechanism for maintaining polymorphisms in a population (O'Donald and Majerus 1984; Gross et al. 1991; Frost 2006), or maintaining hybrid zones by subjecting unfamiliar males to more competition (Rohwer 1973), but examples of positive FDS on sexual traits have not been described. However, this hypothesis could be understood in the

context of mother species versus father species and the observation that crossing typically occurs between the females of the rarer form and the male of the commoner form (Wirtz 1999), which is the opposite of the situation arising when a yellow male disperses west across the river. A limitation of Stein and Uy's (2006b) study, however, is that they did not actually show that white-collared males were more successful where yellow collars were rare. Instead, they lacked sufficient observations from such leks. In fact, in leks where white collars predominated, Stein and Uy (2006b) observed only two copulations in total: one with a white male and one with a yellow male. While Stein and Uy (2006b) convincingly demonstrated female preference for yellow collars, further observations are necessary to evaluate their hypothesis of positive FDS.

Hypothesis 3: Geographic variation in optimal habitat for conspicuous display. Uy and Stein (2007) proposed yet another mechanism for stalled introgression, extending the ideas of Endler and Théry (1996), who observed that displaying birds in tropical forests, including two manakin species, use sites that optimize the contrast of their plumage against the visual background. Uy and Stein (2007) posited that there must be an adaptive benefit to displaying against certain backgrounds over others and that this phenomenon could be relevant in the *Manacus* hybrid zone. They measured the color of white- and yellow-collared male plumage and the color of the ground in display courts in allopatric Golden-collared and White-collared Manakin leks, as well as leks in the plumage introgression zone, then used a general avian visual model to predict the contrast of plumage to background color in these courts. They found that, on courts of allopatric Golden-collared Manakin and those in the plumage introgression zone, yellow plumage was more conspicuous than white plumage, whereas in White-collared Manakin courts, white plumage was more conspicuous. Uy and Stein (2007) inferred from these data that there was a geographic shift in the color of the forest floor or ambient light, creating conditions

where yellow-collared and white-collared birds were favored by sexual selection in their respective ranges, but that further introgression of the yellow collar would not be favored.

The idea that introgression of plumage color traits may be constrained by the color of the birds' habitat is intriguing. If true, it would be powerful evidence for the importance of the visual environment in shaping not just bird behavior, but their evolutionary trajectories. However, the study areas where Uy and Stein (2007) obtained background color measurements for parental white-collared and golden-collared populations were separated by hundreds of kilometers from the area of plumage transition where collar color changes abruptly across a river. As an initial matter, color measurements of plumage and background should be compared at a finer geographic scale—ideally in leks on either bank of the Río Changuinola where the plumage transition occurs.

Hypothesis 4: Display conspicuousness and male site selection. If plumage and court colors along the river confirm Uy and Stein's (2007) results, such a pattern would also be consistent with males choosing sites that maximize their conspicuousness, as argued by Endler and Théry (1996). Under this hypothesis, yellow-collared and white-collared males would be motivated to display where their respective plumages are most conspicuous, rather than conspicuousness being a byproduct of the color of the forest floor in a region. Notably, this explanation does not require any abrupt environmental transitions at the Río Changuinola that would cause a shift in soil color or appearance, while still providing an explanation for why introgression has stalled. Under this model, when a yellow bird disperses across the river it must join an existing lek or display alone (Figure 1.3). In either case, it would be at a disadvantage. Existing leks west of the river would be formed at sites selected by white-collared birds where white is presumed advantageous, while a yellow male displaying alone would be at a

disadvantage due to small lek size (Alatalo et al. 1992). As a result, white males would remain more successful west of the river, and trait introgression would stall. For now, this hypothesis is speculative, but it presents perhaps a more likely explanation for Uy and Stein's (2007) results.

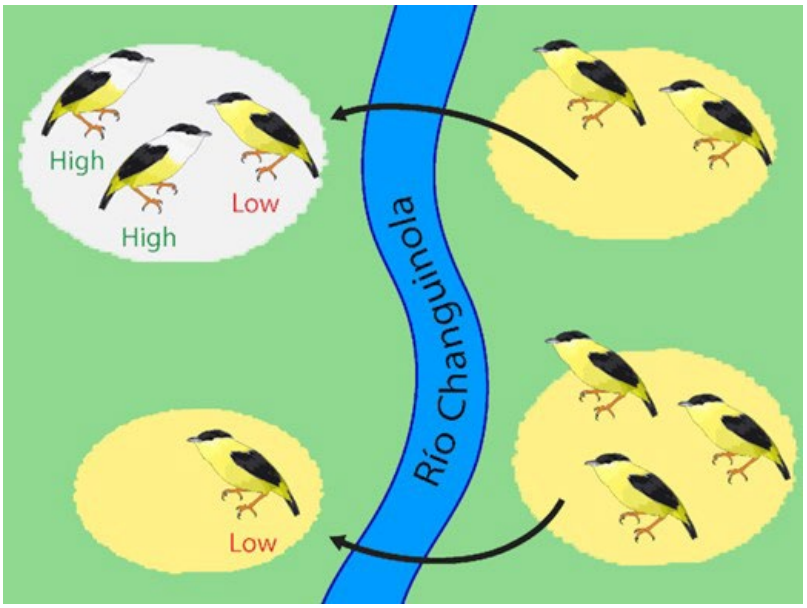

Figure 1.3. Proposed model for stalled introgression of *Manacus* yellow plumage (Hypothesis 4). This model assumes males form leks and choose display sites based on ambient conditions that enhance their conspicuousness. When a yellow male disperses across the river, it must either join an existing lek where white males are more conspicuous or display on its own, which is disadvantageous in lekking species. As a result, yellow males are unsuccessful relative to white males and the river barrier to plumage trait introgression is amplified. Colored patches represent lek habitats favorable to that color. Relative mating success of each individual's plumage color is shown below the lek.

Hypothesis 5: Geographic variation in female preference. The foregoing hypotheses assume uniform preference for one or more of the introgressing vitellinus traits by females of both species. Another possibility is that females west of the Rio Changuinola simply prefer the traits of male *candei*. This hypothesis can be tested directly in the headwaters region where mixed leks occur by amassing more data on mate choice. Observational field tests in pure white-collared populations are not possible of course, but experimental tests of female preference could be designed that would allow this hypothesis to be assessed over a much wider geographic region.

Are yellow-collared males more aggressive?

Sexual selection in the *Manacus* hybrid zone may be acting via male plumage, display, or aggression, but the extent to which Manacus parental species and hybrids show differences in aggression is unresolved. McDonald et al. (2001) first tested aggression in *Manacus* using mount presentations and found that *vitellinus* males are more aggressive than *candei* and that males in the region of plumage introgression are more aggressive than either parental species. Stein and Uy (2006b) performed similar experiments in mixed-color leks along the upper Río Changuinola and found no difference in aggression between white- and yellow-collared males. Billo (2011), in contrast, tested male responses to recorded vocalizations and found that males in the genomic center of the hybrid zone were most responsive, while no differences were found among *vitellinus*, *candei*, or males in the region of plumage introgression. Since these studies were conducted in different populations and/or using different methods, we cannot yet say definitively that aggression has or has not introgressed to any extent. Disentangling the effects of male competition, female plumage preferences, and female display preferences will require greater understanding of male aggression in the parental species and admixed populations. Future studies should build on the work of McDonald et al. (2001) and Stein and Uy (2006b) by repeating mount presentation experiments in multiple leks of all three populations.

Many of the studies mentioned in this and the preceding section were performed under challenging field conditions when no roads or hotels existed in crucial regions of the hybrid zone. Improved infrastructure (roads, hotels, cell service) and advances in monitoring technology, such as compact motion-sensor cameras, should facilitate replicating the studies discussed above and conducting new ones with more leks, individuals, and total observation effort.

Sympatric speciation in *Manacus*

Generations of biologists have considered species distribution patterns like those found in *Manacus* to constitute strong evidence of allopatric speciation in progress, with hybridization occurring upon secondary contact (e.g., Barton and Hewitt 1985; Newton 2003; Price 2008). It was, thus, surprising when a recent paper proposed sympatric speciation in Manacus (Miles et al. 2018). Sympatric speciation is believed to be extraordinarily rare in birds; the only plausible examples involve special cases where temporal, ecological, or behavioral segregation has promoted reproductive isolation and allowed divergence within local populations (Price 2008). No such special conditions exist for *Manacus*. The proposal of Miles, Goller, and Fuxjager (2018) was based on phylogeographic models (e.g., Lemmon and Lemmon 2008) that they used to reconstruct the ranges of the common ancestors of extant species of *Manacus*. There are several potential issues with this modeling exercise. First, Miles, Goller, and Fuxjager (2018) used a phylogeny for Manacus derived from Leite et al. (2021) that does not include all the relevant taxa. *Cis*- and *trans*-Andean populations of *M. manacus* are known to be deeply divergent from each other; in fact, the *trans*-Andean population is actually more closely related to *vitellinus* than to *cis*-Andean *M. manacus* (Brumfield and Braun 2001; Brumfield et al. 2008; Harvey et al. 2020). Inclusion of a *trans*-Andean *M. manacus* terminal sister to *vitellinus* in the phylogeny would have produced an additional common ancestor presumably with a different reconstructed range. Second, the phylogeographic modeling used a continuous Brownian motion process to reconstruct putative ranges for common ancestors that existed at various points in time. Given the potential for discontinuities such as forest refugia, sea level fluctuation and range expansion or contraction through time, apparent overlap of reconstructed ancestral ranges seems inconclusive on the issue of sympatric speciation. Third, no mechanism is provided that would

explain how or why *Manacus* species came to occupy their current exclusively allopatric or parapatric distributions if they actually arose in sympatry. Any conceivable mechanism would presumably require strong disruptive selection linked to both premating and postmating isolation, which is at odds with the existence of present-day hybrid zones. On the other hand, it is important to note that current or past contact between *Manacus* populations provides the opportunity for gene flow as well as reinforcement of reproductive and/or ecological isolating mechanisms. Further analysis will be needed to construct a convincing case that sympatric speciation occurred in *Manacus*.

Opportunities for future research with *Manacus*

What factors maintain the narrow transition zone?

Available evidence suggests that the *Manacus* hybrid zone has existed for at least 5000 years (see above), yet geographic clines for many genetic markers are still quite narrow; indeed, cline widths for six of seven classic nuclear and mitochondrial markers were 11 km or less (Brumfield et al. 2001; Yuri et al. 2009). The genomic transition is situated in a forested region with no obvious dispersal barriers, and the birds are capable of flying substantial distances (Moore et al. 2008). This evidence is inconsistent with neutral introgression; rather, it indicates that the narrow genomic transition zone is likely maintained by some form of selection against hybrids (e.g., Barton and Hewitt 1985). Selection could, in principle, be exogenous or endogenous, but there are no obvious ecological gradients in the region; the narrow cline widths mentioned above and numerous F_{ST} outlier loci widely distributed throughout the genome (Parchman et al. 2013) suggest that endogenous selection based on genetic incompatibilities is more likely.

Recombination breaks down the associations between postmating barriers (i.e., selection against hybrids) and premating barriers (i.e., assortative mating preferences) that are necessary to maintain a species boundary (Felsenstein 1981), but one trait can be responsible for both ("magic traits," reviewed by Servedio et al. 2011) or genes for the traits can be protected against recombination by inversions (Edelman et al. 2019), often on the Z chromosome (e.g., Sæther et al. 2007). Field and laboratory studies are needed to confirm postmating and premating contributors to reproductive isolation in the *Manacus* hybrid zone. Observations on hatching success, fledging success and survivorship can distinguish developmental issues from fitness issues that arise later in life. Comparison of parasite load of hybrids and parentals could reveal immune system dysfunction. Genome scans of hybrids could reveal signatures of selection and help identify candidate genes for impaired functions. Observations of mating patterns of genetically characterized birds in the genomic transition zone could address the possibility of assortative mating and help identify genotypes or phenotypes associated with female preference and whether they fall on the Z chromosome as predicted.

Because ~25 years have passed since the zone was first carefully studied, a new transect survey is in order to assess whether the zone has moved, which has been observed in a number of hybrid zones (Buggs 2007) and has important implications for zone dynamics (Rheindt and Edwards 2011). Brumfield et al. (2001) mentioned evidence from historical specimens that morphometric clines may have moved eastward over the preceding 100 years. Next generation sequencing technology now makes it feasible and highly desirable to add genomic data from those historical specimens. Genetic data from a transect across the hybrid zone could also uncover associations between genomic loci and quantitative traits that have not introgressed,

such as beard and tail length (Parsons et al. 1993; Brumfield et al. 2001), providing additional insight on how genotype connects to phenotype for important plumage features.

The genetic basis of collar color

Many of the yellows, oranges, pinks, and reds of bird plumage come from carotenoid pigments (Brush 1990). Carotenoids are synthesized by plants and ingested by birds, and then deposited into growing feathers. These pigments are often used in sexual signaling. Certain colors may be preferred by females (Hill 1991, 2006; Stein and Uy 2006b; Burley and Coopersmith 2010), serve as badges of status (Pryke and Andersson 2003; Murphy et al. 2009), and/or as honest signals of fitness (Hill 1991; reviewed by Møller et al. 2000). Our understanding of sexual selection would therefore benefit considerably from further elucidation of the genetic and mechanistic bases for carotenoid coloration in birds. Only recently have such genes begun to emerge as genomic methods have become more accessible and interest in the genetics of carotenoids coloration has surged (Toews et al. 2017; Funk and Taylor 2019).

Carotenoids are hydrophobic and require chaperone proteins for transportation and selective uptake by cells (Sakudoh et al. 2013). In birds, scavenger receptor proteins, which have previously been shown to carry out this function (Kiefer et al. 2002), have a role in determining plumage color. In domestic canaries (*Serinus canaria*) and Yellow-rumped Warblers (*Setophaga coronata*), scavenger receptor proteins *SCARB1* and *SCARF2*, respectively, have been implicated in plumage polymorphisms involving yellow feathers (Brelsford et al. 2017; Toomey et al. 2017).

Once carotenoids are inside cells, they can be deposited as pigments in growing feathers or broken down into colorless products by metabolic enzymes like carotenoid oxygenases (dela Seña et al. 2016). In this class of genes, *BCO2* has been implicated in carotenoid color

polymorphisms of several birds, including chickens (Eriksson et al. 2008), canaries (Gazda et al. 2020a,b), and warblers (Toews et al. 2016; Baiz et al. 2021).

Some yellow dietary carotenoids are converted in birds to keto-carotenoids, producing orange and red plumage (Brush 1990). Recently, the ketolase that performs this conversion has been traced to *CYP2J19*, based on studies showing this gene to be associated with yellow-to-red shifts in finches (Mundy et al. 2016; Hooper et al. 2019), canaries (Lopes et al. 2016), fairy-wrens (Khalil et al. 2020), and flickers (Aguillon et al. 2021).

Finally, Aguillon, Walsh, and Lovette (2021) and Wang et al. (2020) recently showed that genes previously only known to be associated with melanin variation in birds also control patches of carotenoid-pigmented feathers in Northern Flickers (*Colaptes auratus*) and Hermit/Townsend's Warblers (*Setophaga occidentalis*, *S. townsendi*), respectively. These findings suggest that some genes previously thought to control melanin coloration could instead be regulating color patterning more broadly. One of the genes uncovered by Aguillon, Walsh, and Lovette (2021), *CAMKV*, is in the *MAPK* signalling pathway. The *MAPK* and *Wnt* pathways have broad regulatory functions but also involve several genes with specific connections to melanin coloration in birds, such as *RAS-GRF1* (Poelstra et al. 2015), *NDP* (Vickrey et al. 2018), *FST* (Lehtonen et al. 2012; Toews et al. 2016; Toomey et al. 2018), and *Wnt-11b* (Toews et al. 2016). This finding points to the possibility that *MAPK*, *Wnt*, or other broad developmental gene pathways may control patterning of carotenoid pigments in addition to melanin.

Because of the natural mixing of genomes that occurs in hybrid zones—successive crossing and backcrossing—they are ideal systems for investigating the genetic bases of traits. *Manacus* populations in the region of introgression are predicted to have the *vitellinus* allele for collar color in a *candei* genetic background. Genome-wide association-mapping for this trait and

genome scans measuring differentiation between populations differing mainly in this trait should uncover genomic regions containing the allele(s) responsible for producing the yellow color.

Pigmented collars in *Manacus*: convergence or introgression?

Two of the four Manacus species (*vitellinus* and *aurantiacus*) show carotenoid pigmentation in their collars, while the other two have white collars (Figure 1.2). The propensity for hybridization in the genus, along with the apparent selective advantage of yellow over white collars in the *vitellinus* x *candei* hybrid zone, opens the possibility that the trait arose once and spread between *vitellinus* and *aurantiacus* via introgression. A pigmented collar is a derived trait on the *Manacus* phylogeny (Brumfield and Braun 2001), and while *vitellinus* and *aurantiacus* are not currently known to come into contact, their ranges may not be more than 20 km apart in western Panama (Angehr and Dean 2010). Carotenoid-pigmented collars could have arisen in either species and passed to the other via introgression if, as proposed by Miles, Goller, and Fuxjager (2018), there was historical gene flow among the *Manacus* lineages as they diverged. A similar scenario was recently uncovered among parulid warblers, which exchanged an allele for a gene involved in carotenoid pigmentation during the group's diversification (Baiz et al. 2021). Also of note in this regard is another manakin species complex with a yellow/white switch in plumage of the crown, a likely sexual ornament (Barrera-Guzmán et al. 2018).

The two *Manacus* species' collars do not look identical: *aurantiacus* males have richer orange highlights while *vitellinus* collars are uniform yellow. Orange plumage may be produced by either dietary or converted keto-carotenoids. One study has proposed that orange feathers of *aurantiacus* may contain the keto-carotenoid rhodoxanthin (Hudon et al. 2012), but this has not been confirmed or even tested. Carotenoids extracted from museum skins of *vitellinus* and *aurantiacus* males could be identified chemically to test this hypothesis. If the two species'

pigmentation is caused by different carotenoids, they are likely to have separate genetic mechanisms and thus evolutionary origins. A finding that their collars contain the same carotenoid at different concentrations, for example, could suggest that the two species share a genetic mechanism for the trait.

The genetic basis for collar color in *Manacus* has yet to be identified, but, as we describe above, the conditions in the *Manacus* hybrid zone are ideal to study this question. Once the gene(s) responsible for the white-yellow polymorphism between the two hybridizing species is identified, the same genomic region(s) should be sequenced for *aurantiacus* to determine whether pigmented collars in *Manacus* have a single evolutionary origin, or whether the trait has arisen twice in the genus independently.

Genetic basis of belly color

The yellow collar of *vitellinus* has introgressed to fixation in *candei* populations east of the Río Changuinola (Brumfield et al. 2001), and thus has been the subject of most subsequent research into the driver(s) of introgression in this system. The dark belly of *vitellinus*, however, has introgressed nearly as completely in a pattern also indicating selection (Brumfield et al. 2001) but has received no further attention in the last two decades. Adult *vitellinus* and hybrid males have an olive green belly, and juvenile males and females are uniformly olive green. This green color could be produced by melanin deposited on top of carotenoids, darkening the yellow to appear olive. The genetic basis of melanin variation in bird feathers has been remarkably consistent across taxa. Just a handful of genes have turned out to be responsible for such variation, most notably MC1R (e.g., Theron et al. 2001; Lamichhaney et al. 2016; Stryjewski and Sorenson 2017), ASIP (e.g., Toews et al. 2016; Stryjewski and Sorenson 2017; Abolins-Abols et al. 2018), and FST (Lehtonen et al. 2012; Toews et al. 2016; Toomey et al. 2018). However,

because manakin populations on the east bank of the river show substantial variation in belly color (Brumfield et al. 2001), multiple loci may be controlling this trait.

Why melanism might be advantageous is unclear, but one possible mechanism is via aggression. Melanin coloration has been linked to increased aggression across a wide phylogenetic range of bird species through the melanocortin pathway's pleiotropic effects on behavior (Ducrest et al. 2008). This connection could explain introgression of dark belly plumage and also reconcile the results of McDonald et al. (2001) and Stein and Uy (2006b). McDonald et al. (2001) found that yellow-collared males were more aggressive than white-collared males, while Stein and Uy (2006b) found no difference. However, Stein and Uy's (2006b) experiments were conducted in the narrow upper reaches of the Río Changuinola, where most individuals have the bright yellow belly of *candei* (K. Bennett and M. Braun, pers. obs.). Introgression of the dark belly could be decoupled from the yellow collar and proceeding via the separate mechanism of aggression. For now, this idea is merely speculative, but it recommends further work, such as DNA sequencing and aggression assays in admixed populations with a range of phenotypes.

Female preference for male ornamentation: the role of retinal carotenoids

An enormous body of work has been devoted to understanding why ornaments are favored by sexual selection (see Andersson 1994; Prum 2017; Hill 2019), and intense debate has revolved around whether ornaments are honest signals of mate quality or not. Research in the *Manacus* system can contribute to this debate by delving into why yellow collars are favored (if they are under direct selection). Recent work suggests one possible avenue: retinal carotenoids.

In addition to coloring bird feathers, carotenoids play an additional important role in vertebrate spectral tuning; they accumulate in retinal oil droplets and modify the spectrum and

intensity of light passing through the retina, improving and fine-tuning color vision (Toomey and Corbo 2017). Recently, Caves et al. (2020) showed that intraspecific variation in Zebra Finch retinal carotenoid content was sufficient to affect birds' ability to discriminate colors from a biologically relevant color spectrum. This observation raises the question of whether variation in retinal carotenoid content could affect female preference for pigmented male plumage. Previous work has shown that *vitellinus* females discriminate between males on the basis of their plumage brightness (Stein and Uy 2006a). Other recent work has linked a single gene to canary bill, plumage, and retinal carotenoid accumulation (Gazda et al. 2020b,a). Combining these pieces of evidence, it is possible that yellow collars in the *Manacus* hybrid zone are controlled by a locus simultaneously affecting the accumulation of carotenoids in retinal oil droplets, thereby enhancing female perception of, and thus preference for, yellow collars. Under this hypothesis, females possessing the yellow allele would prefer yellow males, driving the introgression of the allele. This situation—a male ornament and female preference controlled by the same allele—would be precisely the conditions predicted to favor a "runaway" process (Fisher 1930). This idea is speculative—no previous evidence has linked retinal carotenoids to mate choice, but the *Manacus* hybrid zone is a promising system to test this idea.

Comparative studies in *Manacus*

Two additional characteristics of the *Manacus* system enhance its usefulness as a model for sexual selection and introgression. The superspecies structure of the genus and geography of the hybrid zone in Panama combine to create natural replicates and a potential time series that will facilitate valuable comparative studies. Where *M. vitellinus* contacts *M. manacus* in Colombia, there are two additional hybrid zones (Figure 1.2; Haffer 1967; Brumfield and Braun 2001). These South American hybrid zones, however, have never been characterized genetically

or behaviorally, nor has there been any attempt to determine whether plumage or other traits have introgressed asymmetrically. These hybrid zones offer the attractive opportunity to study independent replicates of hybridization upon secondary contact of yellow-collared and white-collared *Manacus* species.

In addition, populations on the continental islands of Bocas del Toro in Panama may provide a window into the history of the hybrid zone. This archipelago lies just offshore of the region of *vitellinus* plumage introgression. The manakins on the islands, like those in the region of introgression, show *vitellinus*-like plumage, but are morphometrically like *candei* and give *candei*-like vocalizations (Billo 2011). The islands separated from the mainland sequentially between 5200 and 1000 years ago (Anderson and Handley 2002) and may thus harbor a time series of introgressed populations as they became isolated. The manakins on one small island, Escudo de Veraguas, have evolved rapidly to present an example of insular gigantism. They are substantially larger and darker than the birds on the other islands or the mainland and have been treated as a distinct subspecies, *M. v. amitinus* (Wetmore 1959). Future studies of the genomics, morphology and behavior of these island populations may produce insights on the longitudinal dynamics of this system.

Conclusions

The *Manacus* system is one of only a handful of well-studied cases of positive sexual selection driving introgression across a hybrid zone. Because introgression of phenotypically prominent traits has not yet swept to fixation, these cases afford us rare opportunities to study evolutionary processes in action. Nevertheless, similar circumstances almost certainly exist in other systems where cryptic traits have gone undetected or selective sweeps have obscured the

history of introgression. As more hybrid zones are discovered and studied using increasingly sophisticated genomic and field techniques, we predict that this phenomenon will be described elsewhere, perhaps many more times. As the field progresses, the *Manacus* hybrid zone will serve as an important point of reference for predictions and hypotheses about patterns and processes in these systems. Extending our knowledge of the *Manacus* system will thus provide a crucial foundation for future research into the interplay of hybridization and sexual selection.

Acknowledgements

For helpful discussion, inspiring insight, indispensable assistance, and hard work, we thank our many colleagues, collaborators, and friends, including but not limited to Tom Parsons, Robb Brumfield, David McDonald, Tamaki Yuri, Jerry Wilkinson, Karen Carleton, Heidi Fisher, Carlos Machado, Steve Mount, Lil Camacho, Maria Leone, Owen McMillan, Sarah Kingston, Kira Long, Jeff Brawn, Ovidio Jaramillo, Antonio Pineda, Cesar Romero, Robert Jernigan, Tom Parchman, Bette Loiselle, Emily DuVal, Alice Boyle, Chris Balakrishnan, Peri Bolton, Wes Warren, Morgan Wirthlin, Claudio Mello, Mike Webster, Barney Schlinger, Matt Fuxjager, Tim Billo, Leo Fusani, Geoff Hill, Rick Prum, Marina Anciães, Marco Pizo, Cesar Cestari, Lilian Manica, and many other active participants in the Manakin Genomics Research Coordination Network. Finally, we thank Trevor Price, Scott Taylor, and an anonymous reviewer for their insightful comments that improved the paper.

Chapter 2. Impact of a riverine barrier on genomic population structure and introgression of a sexually selected trait

Abstract

Gene flow connects populations and facilitates the exchange of alleles, impacting speciation and adaptation. A robust debate has explored whether and how geographic barriers to gene flow can drive species divergence, but the impact of barriers on the spread of advantageous alleles has received less attention. Theory predicts that universally advantageous alleles should sweep to fixation rapidly, but very few empirical studies have investigated such a situation in the presence of a geographic barrier. In western Panama, lekking golden-collared and white-collared manakins (*Manacus vitellinus* and *M. candei*, respectively) interbreed in a narrow hybrid zone across which males' brilliant yellow collar plumage has introgressed from *vitellinus* into *candei* under sexual selection. Plumage introgression is sharply limited across the lower reaches of the widest river in the region, but both color morphs occur on both riverbanks at its headwaters. In this study, my collaborators and I used ~12,000 single nucleotide polymorphisms (SNPs) to assess genetic differentiation, infer gene flow, and evaluate the river's ability to constrain further introgression. We found that, while the river did show a clear effect of structuring genetic variation, particularly along its wide lower reaches, it was not sufficient to prevent extensive gene flow at its narrow headwaters. These results are consistent with a model in which the river impedes gene flow enough for other selective forces to prevent trait introgression, rather than as a sufficient barrier to prevent gene flow altogether. We argue that even modest barriers can constrain selective sweeps by interacting with the existing selective landscape.

Introduction

Gene flow is the movement of genetic information within and between populations or species (Slatkin 1985). It has long been recognized as one of the major forces of evolution for its role in preventing divergence or local adaptation (Dobzhansky 1937; Mayr 1963) and introducing new, potentially adaptive alleles into recipient populations (Wright 1931). Recently, a revolution in DNA sequencing and sequence analysis has caused a shift in our understanding of gene flow between species. Once believed to be rare or at least evolutionarily unimportant in animals (Arnold 1997), biologists now recognize that hybridization is common even between largely isolated lineages (Taylor and Larson 2019) and that gene flow often plays important roles in the evolution and diversification of species. Outcomes can include range shifts that favor the better adapted species (Haas and Brodin 2005; Olson et al. 2010; Taylor et al. 2014), introgression of particular adaptive alleles and traits (Huerta-Sánchez et al. 2014; Liu et al. 2015b; Jones et al. 2018; Edelman et al. 2019), hybrid speciation (Brelsford et al. 2011; Hermansen et al. 2011), trait elaboration (Eliason et al. 2023), and collapse of two populations into one (Taylor et al. 2006; Kleindorfer et al. 2014; Kearns et al. 2018).

Cessation of gene flow, e.g., due to a geographic barrier, has typically been considered the first step toward divergence and eventual speciation. If a sedentary population arises on a volcanic island, for example, isolation may be essentially complete and speciation will proceed through local adaptation and genetic drift (Sendell-Price et al. 2021; Wiens et al. 2022). In a more connected landscape, gene flow and geographic barriers can interact in more complex ways. Gene flow between semi-isolated populations can be mediated by species' dispersal ability (Irwin 2002; Burney and Brumfield 2009; Smith et al. 2014) and habitat stability (Johnson et al. 2023), and may not be consistent across the genome (Toews and Brelsford 2012; Martin and

Jiggins 2017). A single clade may even display multiple different patterns of genetic divergence across barriers, with the outcome dependent on the history of the barrier, niche divergence of the populations (Pyron and Burbrink 2009), and other environmental or stochastic factors (Kingston et al. 2017; DeRaad et al. 2023). As a general pattern, however, geographic barriers often coincide with population divergence (Wallace 1852; Jordan 1908; Mayr 1942; Capparella 1988; Ayres and Clutton-Brock 1992; Harvey and Brumfield 2015), and where barriers dissipate, gene flow increases (Haffer 1974; Peres et al. 1996; Naka et al. 2012; Weir et al. 2015).

The pattern of geographic barriers separating phenotypically and genetically diverged populations is well-described, but the role of the barriers themselves in generating these patterns has not been fully resolved. Large South American rivers, for example, are classic examples of geographic barriers delimiting species and population boundaries (Wallace 1852; Bates 1892; Hellmayr 1910; Parker et al. 1985; Ayres and Clutton-Brock 1992; Naka et al. 2012). The formation of these rivers was initially hypothesized to have functioned as vicariant forces that split populations leading to speciation in allopatry (Sick 1967; Capparella 1988), but that view has been complicated by more recent genetic evidence (Smith et al. 2014; Naka and Brumfield 2018; Kopuchian et al. 2020). The picture that has emerged is one where ecological specialization and limited dispersal ability drive divergence, while landscape features, such as rivers, determine range boundaries (Burney and Brumfield 2009; Naka et al. 2012; Salisbury et al. 2012; Smith et al. 2014; Naka and Pil 2020). Under this model, the reduction in gene flow across rivers is a secondary feature of these systems, necessary but not sufficient to maintain species boundaries.

These examples typically involve genome-wide divergence and gene flow. Much less empirical work has focused on how geographic barriers can affect the spread of particular traits

and alleles under positive selection. Theory predicts that an advantageous allele can sweep through a population or even across a hybrid zone to fixation (Fisher 1937; Hewitt 1988; Barton and Gale 1993). In the case of a strongly advantageous allele, a sweep should also be able to overcome barriers to gene flow (Barton and Gale 1993). The extent to which geographic barriers have a role to play in this scenario remains unclear. Under any simple model, if migrants can cross the barrier, a globally advantageous allele should continue to spread.

New cases of historical trait introgression continue to be uncovered through genome-scale analyses (Taylor and Larson 2019), highlighting the increasing relevance of this topic. Introgression of bird coloration is a particularly rich area of research (Funk and Taylor 2019; Orteu and Jiggins 2020). Recent studies have reported a variety of outcomes, including partial introgression (Semenov et al. 2021), fixation of introgressed traits in new species (Baiz et al. 2021), and possible isolation of introgressed populations leading to incipient hybrid speciation (DeRaad et al. 2023). Evaluating the evolutionary forces facilitating or constraining such introgression is a new frontier for hybridization and speciation research. In this study, my collaborators and I used a hybrid zone between two species of manakin (Aves: Pipridae) in Panama exhibiting asymmetric sexual plumage color introgression to investigate the role of geographic barriers in the spread or hinderance of trait introgression.

Manakins are a family of suboscine passerine birds that inhabit tropical forests from Mexico to Brazil (Snow 2004; Kirwan and Green 2011). The evolution of the group is characterized by intense sexual selection stemming from their lek breeding system, where males display in aggregations ("leks") and are evaluated by choosy females. Reproductive success in a lek is highly skewed to a small number of males (Lill 1974; Foster 1977; Théry 1992; Shorey 2002), leading to strong selection for traits that are important for mate choice.

In western Panama, golden-collared and white-collared manakins (*Manacus vitellinus* and *M. candei*, respectively) interbreed in a narrow hybrid zone (Figure 2.1). In the face of apparently strong selection against hybrids, as evidenced by the steep transition in genetic markers at the genomic center of the hybrid zone (Brumfield et al., 2001), introgression of male plumage traits has nonetheless proceeded from *vitellinus* into *candei*. The male *vitellinus* traits of yellow collars and green bellies have spread roughly 50 km west beyond the genomic center, producing an introgression zone where *Manacus* populations are genetically like *candei* but resemble *vitellinus* in male plumage (Parsons et al. 1993; Brumfield et al. 2001; Parchman et al. 2013). Behavioral studies have found that males with yellow collars are more aggressive than white-collared males (McDonald et al. 2001) and that females choose to mate with yellow-collared males more often when both colors occur in a lek (Stein and Uy 2006b). These studies suggest that female choice and/or male competition have driven introgression of male traits through sexual selection.

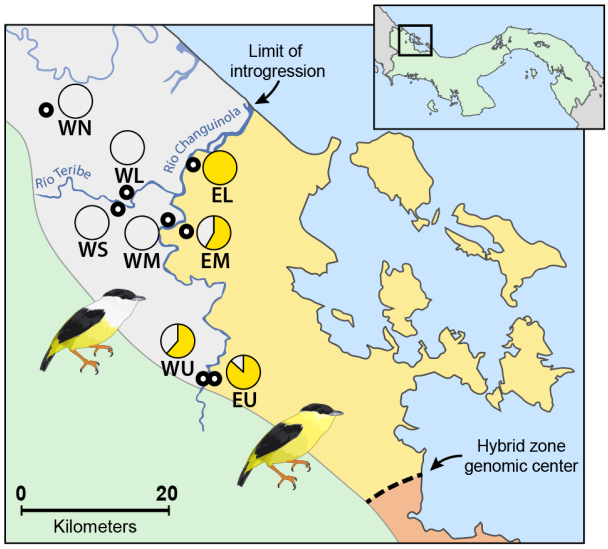

Figure 2.1. The hybrid zone between *Manacus vitellinus* and *M. candei* with the sampling design for this study. Parental *vitellinus* range is in orange; parental *candei* is in gray; and the plumage introgression region is in yellow. Manakin sampling localities are named on the basis of their position relative to the Río Changuinola (W for west, E for east), their position along that river (L for lower, M for middle, U for upper), and their position relative to the Río Teribe (N for north, S for south). Pie charts represent the

proportion of adult male color morphotypes (yellow- and white-collared) in each sampling location. Inset map shows the location of the study area in western Panama.

When sexual selection is intense, alleles that influence expression of an advantageous male trait would be predicted to rapidly spread to fixation (Prado et al. 2009). However, introgression of *vitellinus* plumage traits appears to have stalled at the Río Changuinola, the largest river in western Panama. Manakins are small, sedentary forest understory birds, so they are expected to show low dispersal capability (Salisbury et al. 2012). However, the Changuinola is narrow in its upper reaches, with some stretches of suitable habitat separated by less than 100 m, well within the physical dispersal capabilities of this species (Moore et al. 2008). This unusual situation prompts the question of whether the river's role as a dispersal barrier alone is enough to explain the observed pattern of trait introgression, or whether it interacts with other pre-existing ecological or selective forces. That question has never been addressed with genome-scale data (but see Brumfield 1999). In this study, we measured population genetic structure at a genomic scale to evaluate the role of the Río Changuinola in isolating manakin populations and impeding a selective sweep.

Methods

Sampling and sequencing

Sampling occurred between 1991 and 1997 during collecting expeditions by the Smithsonian Institution's National Museum of Natural History (NMNH) and targeted manakin sampling along the Río Changuinola. Sampling sites are named based on their position along the Río Changuinola (E for east, W for west, L for lower, M for middle, U for upper) and the Río Teribe (N for north, S for south). Samples consisted of tissue isolated from euthanized birds or blood taken from live birds captured by passive mistnetting (Appendix A, Table S2.1). DNA was

isolated by phenol-chloroform extraction and ethanol precipitation using two methods: RTB followed the protocol described in Brumfield (1999) and I used a Gene Prep automated extractor (Autogen Inc.). I measured DNA concentrations using a Qubit 4 fluorometer (ThermoFisher Scientific). In all, I used samples from 191 birds from eight sampling locations for sequencing (Figure 2.1).

I prepared restriction site-associated DNA sequencing (RADseq) libraries using the SbfI restriction enzyme and following a modified version of the Etter et al. (2011) protocol. Libraries were sequenced across two lanes of Illumina HiSeq 4000 flow cells in 150 bp paired-end reads by Azenta Life Sciences and Novogene Corp. I trimmed and demultiplexed raw reads using process_radtags in Stacks v2.6 (Rochette et al. 2019), aligned reads to the *M. vitellinus* reference genome (ASM171598v3) using bwa mem v0.7.1 (Li 2013), assembled reads into contiguous sequences and called variants using gstacks in Stacks 2.6.

Next, I produced a VCF file containing genotype information for single-nucleotide polymorphisms (SNPs). I first ran the populations program in Stacks to make an unfiltered VCF file. Next, using VCFtools v0.1.16 (https://vcftools.github.io/index.html), I removed insertions/deletions (indels), set genotype quality and depth cutoffs (--minGQ 40, --minDP 4, --maxDP 60), removed sites with singleton alleles, and removed sites missing data in greater than 75% of all individuals. Next, I iteratively filtered out low-quality individuals and SNPs as recommended by O'Leary et al. (2018). I removed individuals with uncalled genotypes at greater than 90% of all SNPs, then sites still missing data from more than 10% of all individuals, then individuals still missing genotypes in more than 40% of all SNPs. I used these cutoffs after examining distributions of individual or site missingness at each step. Finally, I thinned the dataset by removing SNPs within 5 kb of one another based on previous estimates of linkage

distance in some of these same manakin populations (Parchman et al. 2013). The resulting VCF file containing 12,375 SNPs and 173 individuals (Appendix A, Table S2.1) was used for the following analyses.

Genetic analysis

Some birds were sexed in the field based on plumage and breeding condition. For all other birds and to confirm the sexes recorded in the field, I measured sequencing coverage on several Z-chromosome and autosome scaffolds using BEDTools v2.28 coverage (Quinlan and Hall 2010). Birds with roughly equal Z-chromosome and autosome coverage I called males, while birds with roughly half-coverage on Z-chromosomes I called females. Two individuals with very low-quality sequences were left unsexed and were among the samples removed from subsequent analyses during the filtering steps described above.

I employed several methods to test for effects of the Río Changuinola on genetic structuring of manakin populations. First, I tested for an effect of isolation-by-distance (IBD) by calculating pairwise F_{ST} (Weir and Cockerham 1984) and geographic distances between all pairs of sampling locations using the *dist* and *pairwise.WCfst* functions, the latter from the hierfstat package v0.5-11 (Goudet and Jombart 2022) in R v4.2 (R Core Team 2021). To assess significance while controlling for autocorrelation, I performed a Mantel correlation test in R using the ade4 package v1.7-22 (Chessel et al. 2004) and 1000 permutations.

To test whether F_{ST} between cross-river populations was significantly higher than expected given geographic distances, I performed a randomization test wherein I randomly sampled from all pairwise comparisons between sampling locations and arbitrarily labeled each pair as either cross-river or same-bank. I took the difference between mean cross-river and same-bank residuals from a regression line calculated for this sample and repeated the process 10,000

times to generate a null distribution. I then estimated the probability that observed differences exceeded a random expectation by comparing the difference in observed mean residuals to the null distribution.

Next, I performed an analysis of molecular variance (AMOVA) using the poppr package v2.9.3 (Kamvar et al. 2014) in R to test for within-population, between-population, and between-riverbank effects contributing to overall genetic variation in the dataset. I tested for significance of the associated variance (σ) contributions by performing a randomization test with 9,999 replicates using the *randtest* function from the ade4 package.

To compare the effects of the Río Changuinola and the smaller Río Teribe, which runs into the Changuinola from the west between WL and WM (Figure 2.1), I repeated the same- and opposite-bank randomization test and AMOVA for sampling localities west of the Changuinola, treating the Teribe as the barrier to test.

To summarize the genetic variation across samples and the genetic clustering of manakin populations, I performed a principal components analysis (PCA) and a discriminant analysis of principal components (DAPC) (Jombart et al. 2010). I used the *glPcaFast* function from the adegenet package v2.1.10 (Jombart 2008) in R to calculate principal components from the SNP data. I then used those PCs to infer genetic clusters in the data using the *dapc* function in adegenet. I identified the optimal number of PCs to retain in the discriminant function using cross-validation with the *xvalDapc* function, which tests the ability of different numbers of retained PCs to assign 10% of the samples to clusters based on a training set of 90% of the samples. Based on the cross-validation results (Appendix A, Figure S2.1), I retained 50 PCs.

To assign ancestry coefficients from inferred genetic clusters to individuals, I ran an admixture analysis in R using the *snmf* function in the package LEA v3.10.2 (Frichot and

François 2015). This method estimates proportions of genetic clusters in the data that make up the genomes of each individual using sparse non-negative matrix factorization. K = 2 minimized cross-entropy (Appendix A, Figure S2.2), so I ran the analysis for two genetic clusters.

Due to different methods and purposes for collecting samples from the sampling locations represented in this study (see Brumfield 1999), the proportion of males and females present in the dataset varied widely by site (Appendix A, Table S2.1). Female birds typically disperse further than males (Greenwood 1980; Clarke et al. 1997), and male manakins have been shown to be more closely related than females within leks, possibly for indirect fitness benefits (Concannon et al. 2012; Fusani et al. 2018). Therefore, to avoid biasing population structure estimates, I repeated all of the above analyses, including the Mantel test, residuals randomization test, AMOVA, PCA, DAPC, and admixture analysis using a sample of only males.

The code used for these analyses is available at https://github.com/kfpbennett/cross-river.

Results

Color distribution

The filtered dataset contained genetic data from 173 total individuals, including 43 yellow-collared males, 74 white-collared males, 18 immature green males, and 38 females. Several adult males had collar colors characteristic of the opposite riverbank from where they were captured. Five of 12 (42%) adult males in EM had white collars; two of 15 (13%) adult males in EU had white collars; and eight of 13 (62%) adult males in WU had yellow collars (Figure 2.1). The rest of the adult males (15 in EL, 20 in WN, 18 in WL, 13 in WS, and 11 in WM) had the expected collar color for their side of the river, i.e., white to the west and yellow to

the east. The adult male tallies above include one green male from WU that had several yellow collar feathers.

Population structure

The Mantel test revealed a significant effect of distance ($\rho = 0.44$, $p = 0.026$; Figure 2.2a), meaning genetic similarity was positively related to geographic proximity between manakin sampling sites. However, the randomization test of residuals also revealed a riverbank effect that was independent of distance ($p = 0.002$, Figure 2.2b).

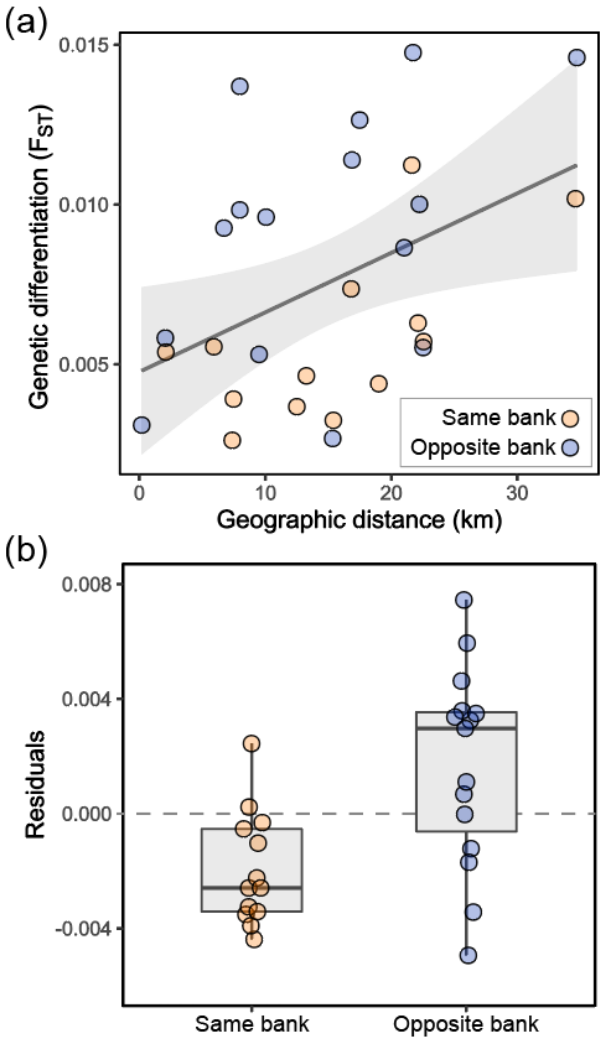

Figure 2.2. Geographic structure in manakin populations. **(a)** Genetic differentiation between pairs of manakin populations as a function of geographic distance. Pairs on the same bank of the Río Changuinola are in orange; pairs on opposite banks are in blue. There was a significant effect of Isolation by distance (IBD) (Mantel test $\rho = 0.44$, $p = 0.026$). **(b)** Residuals of the relationship shown in (a) separated into

same- or opposite-riverbank comparisons. This difference represents a significant departure from IBD (randomization test $p = 0.002$).

Average pairwise F_{ST} between all sampling locations was quite low at 0.0075 ± 0.0037. The two cross-river comparisons with lowest F_{ST} values were between WU and EU and between WU and EM, indicating less cross-river population structure in the upper reaches of the Río Changuinola. In fact, F_{ST} between populations WU and EM (0.0027), which are separated by 15.4 km and the river, was lower than F_{ST} between EM and the closest same-bank population EU (0.0032), which are 15.5 km apart through mostly connected habitat (Appendix A, Table S2.2).

The AMOVA revealed that overall genetic variance was mostly contributed by within-population variation, with a small but significant between-population effect and a small non-significant riverbank effect ($p = 0.0922$, Table 2.1). To test the extent to which the WU sampling location contributed to the AMOVA results, I repeated the analysis excluding only that sampling locality. When WU was excluded from the AMOVA, the estimated riverbank effect was twice as large and highly significant ($p < 0.0001$, Table 2.1).

Table 2.1. AMOVA results partitioning variation within populations (i.e., sampling locations), between locations, and between riverbanks. The test was performed on the full dataset and after excluding the western up-river sampling location WU.

	Component	Sigma	% Variance Explained	P-Value
Full dataset	Within-population	1143.17	96.61	< 0.0001
	Between-population	22.53	1.90	< 0.0001
	Between-riverbank	17.56	1.48	0.0922
Excluding WU	Within-population	1133.03	96.15	< 0.0001
	Between-population	16.82	1.43	< 0.0001
	Between-riverbank	28.55	2.42	< 0.0001

The same- and opposite-bank randomization test ($p = 0.23$) and AMOVA ($p = 0.51$) revealed no effect of the smaller Río Teribe in structuring manakin populations (Appendix A, Table S2.3).

I summarized genetic variation in the dataset by calculating principal components. The first PC, which explained 2.2% of the total genetic variance, separated individuals mostly by riverbank, except for WU which had mostly positive PC1 values (Figure 2.3a). The DAPC using the first 50 principal components also separated populations by riverbank with the exception of WU, which clustered with the eastern sampling locations (Figure 2.3b).

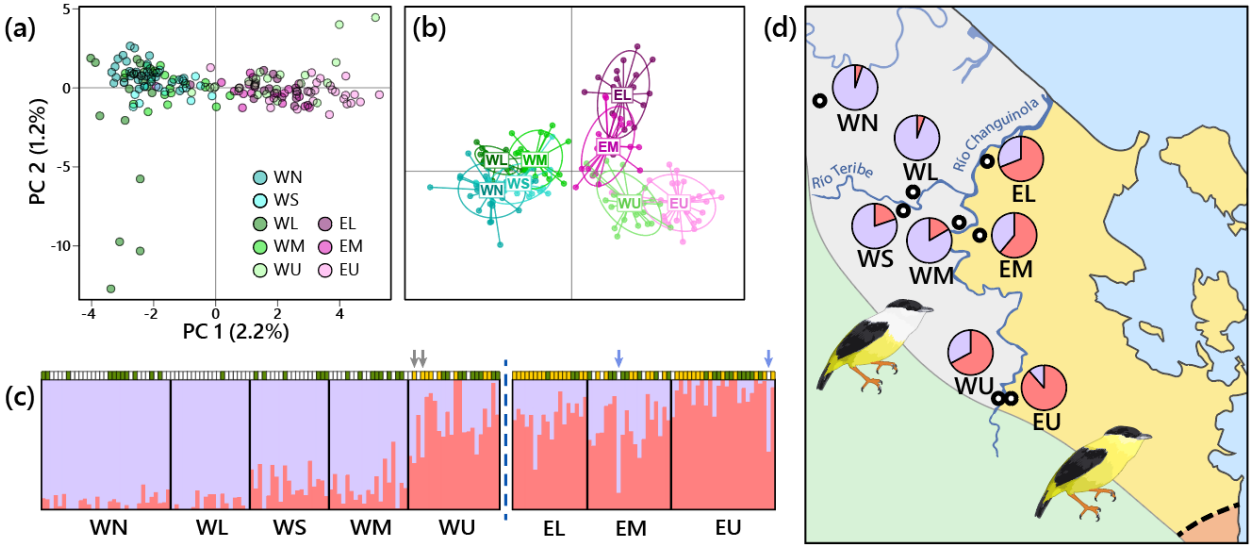

Figure 2.3. Population structure in manakins. **(a)** Principal component analysis (PCA) with individuals colored by sampling location. **(b)** Discriminant analysis of principal components using the first 50 PCs. **(c)** Admixture analysis. Blue dashed line represents the Río Changuinola. Colors above each bar indicate an individual's collar color. Arrows indicate examples of males with opposite collar colors from the predominant color on their riverbank. Gray arrows indicate such males that nevertheless have typical ancestry proportions for their riverbank; blue arrows indicate males with ancestry proportions typical of the opposite riverbank. **(d)** Proportions of ancestry clusters inferred in (c) by geographic location.

The admixture analysis revealed that the two genetic clusters inferred from the data were in large part confined to opposite riverbanks (Figure 2.3c,d), consistent with the PCA and DAPC. However, consistent with other results, WU contained a large proportion of ancestry from the

genetic cluster otherwise associated with eastern populations. Manakins from the two western sampling locations south of the Rio Teribe, WS and WM, had greater ancestry from the eastern cluster than nearby populations north of the Teribe, WN and WL (Figure 2.3c,d). There was also a general northwest-to-southeast trend of increasing ancestry derived from the eastern cluster (Figure 2.3d).

The male-only dataset yielded substantively similar results to the dataset including both sexes. The Mantel test revealed a significant distance effect ($\rho = 0.47$, $p = 0.024$, see Appendix A, Table S2.4 for pairwise F_{ST}), and the randomization test revealed an effect of riverbank independent of distance ($p = 0.0002$). The AMOVA riverbank effect was significant even including WU in the male-only dataset ($p = 0.0365$, Appendix A, Table S2.5). The PCA, DAPC, and admixture analyses showed similar patterns between the two datasets (Appendix A, Figure S2.3).

Discussion

Color distribution and population structure

The distribution of collar colors along the Río Changuinola indicates that some amount of cross-river migration occurs in these populations, especially across the upper reaches of the river. It is notable that collars of adult males in the sample from WU were proportionally more yellow than white. In mid-river populations EM and WM, the eastern males were proportionally more white-collared (42%) than the western males were yellow-collared (0%). The EM males also had proportionally more white collars than the upriver EU males (Figure 2.1), suggesting that the white-collared phenotype in EM results at least partly from cross-river migration rather than gene flow or dispersal from EU alone. There is likely some degree of variability between leks

and sampling years, as Stein and Uy (2006b), working in leks nearby WU roughly 10 years after this study's samples were collected, observed eight out of 26 (31%) yellow-collared adult males. Nevertheless, these results indicate that the Río Changuinola is not a complete barrier to movement of color morphotypes in either direction.

The results of the population genetic analyses all pointed to a modest but real structuring effect of the Río Changuinola that weakened in the upper reaches where the river narrows. Overall genetic variation was quite low, with an average pairwise F_{ST} of 0.0075. For comparison, Parchman et al. (2013) estimated F_{ST} between parental *M. vitellinus* and *M. candei* populations at 0.259. In spite of a significant distance effect, pairs of populations on opposite riverbanks were significantly more differentiated given their geographic distance than same-bank population pairs (Figure 2.2). The AMOVA showed a significant river effect explaining 2.42% of the total genetic variance when the west upriver population WU was excluded but no significant river effect when WU was included (Table 2.1). The largest axis of variation in both the PCA and DAPC separated sampling locations by riverbank except for WU, which clustered with other individuals from east of the river (Figure 2.3a,b). The first principal component, which, except for WU, tended to cluster individuals by riverbank, explained 2.2% of the total genetic variation. Similarly, the admixture analysis identified two genetic clusters, one more prevalent west of the river and the other more prevalent to the east (Figure 2.3c,d). Again, birds from WU were estimated to contain a larger proportion of ancestry from the eastern cluster. Together with observations of collar color distributions, these results indicate that not only are birds crossing the river in both directions, but gene flow is occurring, particularly from the yellow-collared eastern upriver populations into white-collared western populations.

There are several possible alternative explanations for these results. First, signals of differentiation could be driven by genes underlying the plumage coloration trait itself, rather than overall genetic variation. This seems unlikely for two reasons. Several studies have evaluated genetics of populations across the *Manacus* hybrid and introgression zones and found that yellow-collared populations on the east bank of the Río Changuinola genetically resemble *M. candei* (Parsons et al. 1993; Brumfield et al. 2001; Yuri et al. 2009; Parchman et al. 2013), indicating a very low proportion of the genome contributed by introgressed DNA from *vitellinus* (Long et al. in review). In addition, the overwhelming majority of recent studies on bird plumage coloration have concluded that simple color polymorphisms between closely related species are influenced by just one or a handful of genes (Funk and Taylor 2019; Price-Waldman and Stoddard 2021). If one of the RAD loci in the dataset were located in such a gene, its effect would be diluted by thousands of other loci.

Another possible explanation for these results is that they reflect pre-existing genetic variation across the landscape from northwest to southeast that has been somewhat discretized by the river, and similarities between populations reflect pre-existing genetic similarity rather than gene flow. Supporting this idea, manakins from the furthest northwest location WN had the most "western" cluster ancestry in the admixture results, while the furthest southeast EU had the most "eastern" cluster ancestry (Figure 2.3d). In addition, my collaborators and I found a significant effect of distance, suggesting that populations in close proximity even across the river should be more genetically similar. This effect may account for some of the observed patterns. For example, the "western" ancestry present in EL (Figure 2.3d) could indicate a pre-existing signal of alleles from the northwest due to geographic proximity rather than gene flow.

However, some results are only consistent with an isolating effect of the Río Changuinola and a weakening of that effect as the river narrows towards its headwaters. Genetic structure was lowest where the river was narrow and greatest where it was wide, even across very short geographic distances. For example, the third-highest pairwise F_{ST} value (0.0137) was between EL and WL which were separated by only 8 km, the eighth-closest out of 28 pairs of sampling locations (Appendix A, Table S2.2). In the west, even the smaller Río Teribe may be affecting population structure, with the southern WS and WM sampling locations showing more eastern ancestry than nearby WN and WL in the north (Figure 2.3d), though this difference did not correspond to a significant river effect (Appendix A, Table S2.3).

In addition, collar color distribution along the river only supports the gene flow explanation. Color introgression from *vitellinus* presumably post-dates establishment of the river course, so the substantial numbers of yellow-collared males found west of the river must result from cross-river migration. Notably, several of the adult males with "opposite-color" collars, i.e., white to the east and yellow to the west, were assigned ancestry proportions typical of the opposite riverbank (Figure 2.3c), indicating possible cross-river migrants. Conversely, there were other opposite-color males with ancestry proportions typical of their own side of the river (Figure 2.3c), pointing to recombination of color alleles into the opposite-riverbank genetic background. These observations are evidence for both recent cross-river dispersal and effective gene flow via breeding post-dispersal. Such an outcome is consistent with previous findings that isolation typically breaks down and gene flow increases in river headwaters (Wallace 1852; Peres et al. 1996; Haffer 1997; Naka et al. 2012; Weir et al. 2015).

While river course changes ("avulsions") can effectively transplant individuals across rivers (Ruokolainen et al. 2019) , this phenomenon is almost certainly not responsible for the

distribution of collar colors across the Changuinola. Where the river is narrow and both colors are found on either bank, it flows through steep foothills of the Cordillera Central and is unlikely to have gone through many course changes. The wide lower extent of the river is on a flat coastal plain and may periodically change course, but in that region manakin color forms are restricted to opposite riverbanks.

Implications for color introgression

These results show that the Río Changuinola impedes but does not prevent gene flow between manakin populations. This finding sheds new light on the *Manacus* system, which has developed into a model system for studying introgression of sexual traits (Parsons et al. 1993; Brumfield et al. 2001; McDonald et al. 2001; Stein and Uy 2006b; Uy and Stein 2007; Yuri et al. 2009; Concannon et al. 2012; Parchman et al. 2013; Bennett et al. 2021; Long et al. in review). This result is consistent with previous observations of yellow-collared and white-collared males on opposite sides of the river from their normal range (McDonald et al. 2001; Stein and Uy 2006b), but it complicates the picture of a strongly selected trait quickly spreading until it is hindered by a geographic barrier.

One possibility is that introgression is recent, and this system happens to have been studied during a pause at the river before color introgression proceeds west with sufficient accumulation of alleles for yellow collars. This scenario is unlikely for several reasons. First, there has been no noticeable change in collar color across the river since these populations were first studied by scientists thirty years ago (Long et al. in review). Second, there is evidence that introgression is at least several thousand years old. Manakins on the Bocas del Toro archipelago (Figure 2.1) have yellow collars. Birds from the main cluster of islands have been proposed to derive from *candei* populations (Parsons et al. 1993; Bennett et al. 2021), a scenario supported

by morphometric and behavioral data (Billo 2011) and recent microsatellite data (Barske et al. 2023). The oldest of these islands separated from the mainland by post-glacial flooding between 7,000 and 8,000 years ago (Titcomb and O'Dea 2020). If island manakins were yellow when they were isolated–a more likely scenario than multiple mainland-island and island-island dispersal events–color introgression must be more than 7,000 years old. After hundreds of generations, a strongly advantageous trait would be expected to continue introgression beyond the river.

Another possibility is that selection favoring yellow-collared males is weak, and the combination of the river preventing frequent migration and genetic drift counteracting selection prevents further introgression west of the river. Results from the only behavioral study conducted in mixed-color leks upriver contradict this idea. Stein and Uy (2006b) recorded 14 copulations by yellow-collared males and three copulations by white-collared males in observations of 13 white- and 13 yellow-collared males across six mixed-color leks. Previous studies in *Manacus* have indicated that mating skew can be extremely high, with three males receiving more than 90% of all matings at one *M. manacus* lek in Trinidad (Lill 1974). More behavioral research is needed to confirm the strength of the preference for yellow collars.

On the other hand, yellow collars may not be favored west of the river. There have been several mechanisms previously proposed along these lines. First, Stein and Uy (2006b) argued that, because they observed more frequent copulations by yellow males in mixed leks with the highest proportion of yellow collars, female preference for yellow collars is positively frequency-dependent. In other words, females' preference for the yellow collar, and thus its selective advantage, is dependent on yellow collars being common in the lek. Because dispersal across the river is presumably relatively rare, yellow males never become common enough to be

favored, and the trait ceases to spread. It is difficult to assess the strength of this hypothesis because Stein and Uy (2006b) did not observe many matings by either color morph in leks where yellow collars were rare. Additional behavioral observations in up-river populations will help resolve this question and are more tractable now that roads have been built that provide access to these habitats (Bennett et al. 2021).

Second, Uy and Stein (2007) proposed an explanation, further developed by Bennett, Lim, and Braun (2021), dependent on the light environment in display courts. Uy and Stein (2007) found that yellow plumage appears more conspicuous than white plumage in the hybrid zone and allopatric golden-collared habitats, whereas white plumage appears more conspicuous than yellow plumage in the allopatric white-collared habitat. Under their interpretation, a shift in the color of the forest floor across the river could be responsible for yellow collars being disfavored to the west. Under the interpretation of Bennett, Lim, and Braun (2021), manakins could be choosing lekking areas with lighting conditions that favor their plumage. Thus, when a yellow-collared male disperses across the river, it either joins an existing lek site chosen by white birds for light conditions favorable to white or selects a new site with light conditions favorable to yellow, but displays alone, which is not advantageous for a lekking bird (Alatalo et al. 1992). In either case, yellow alleles are less likely to spread.

Third, Bennett, Lim, and Braun (2021) proposed that female preference for collar color could turn over across the river. Under this idea, pre-existing variation, e.g., in aspects of female perception that affect mate choice, varies geographically such that different mate preferences predominate on either bank. For example, differences in female retinal carotenoids could impact spectral tuning in such a way as to affect perception of and preference for male color (discussed by Bennett, Lim, and Braun 2021). When hybridization between *candei* and *vitellinus* began,

candei females close to the hybrid zone preferred yellow-collared males, but as introgression reached the river and those males dispersed across to the west bank, females they encountered were predisposed to prefer white-collared males. Again, additional behavioral studies of male mating success in mixed-color leks along the Río Changuinola could evaluate and distinguish between these hypotheses. Recent evidence indicates that other traits of *vitellinus*, including green bellies (Long et al. in review) and display behaviors (Barske et al. 2023), are also introgressing beyond the genomic center of this hybrid zone. Studying the dynamics of introgression in these traits will sharpen initial inferences based on yellow collar introgression.

Conclusions

In each of the above scenarios, the role of the Río Changuinola as a partial barrier to gene flow is necessary but not sufficient to prevent a selective sweep from continuing. Instead, the river's impact on gene flow interacts with existing variation in the selection landscape. It is unclear whether this scenario is common in nature. High-throughput sequencing is rapidly uncovering both cryptic diversity within species and the genetic basis of traits (Funk and Taylor 2019; Taylor and Larson 2019; Orteu and Jiggins 2020; Price-Waldman and Stoddard 2021). As the evolutionary origins of more traits are investigated, more instances of ancient introgression will be uncovered.

Several different outcomes are possible when alleles of one hybridizing species are favored by both species. For example, yellow plumage in *Setophaga* warblers appears to have spread between species and become fixed multiple times (Baiz et al. 2021). On the other hand, introgressing red plumage in Red-backed Fairywrens has failed to spread throughout the orange-backed subspecies despite a known selective mechanism (Baldassarre and Webster 2013; Baldassarre et al. 2014). In that case, the authors proposed that geographic region of poor habitat

suitability may be constraining further introgression (Baldassarre et al. 2014). In several other recent avian examples, it is not yet known whether introgression is ongoing or has stalled (Hooper et al. 2019; Lipshutz et al. 2019; Metzler et al. 2021; Semenov et al. 2021). Outside of birds, adaptive introgression of resistance to seed predators in *Helianthus* sunflowers was proposed to be limited due to pleiotropic effects of resistance genes or reduced impact of the predator in other populations (Whitney et al. 2006), but this instance of introgression has recently been called into question altogether (Owens et al. 2021). Johnson et al. (2015) hypothesized that introgression of alleles due to asymmetric mate choice in spotted salamanders may still be ongoing but that it may be limited by the Mississippi River in the future. Many other hybrid zones have been evaluated in a geographic context (e.g., Jaarola et al. 1997; Martinsen et al. 2001; Payseur et al. 2004; Bímová et al. 2011; Carneiro et al. 2013; Delmore et al. 2013; Arntzen et al. 2017; Ryan et al. 2017; Menon et al. 2020; Sequeira et al. 2020, 2022), but hardly any have attempted to explain the geographic extent of putatively introgressing genomic loci (see, e.g., Teeter et al. 2010; Stewart et al. 2016; Pflugbeil et al. 2021).

The forces permitting or constraining trait introgression remain to be adequately addressed in these and other systems. The present study provides one framework for such research. In *Manacus*, a combination of reduced gene flow at a geographic barrier and one or more of several selective mechanisms interact to constrain trait introgression. Further research on the dynamics of introgression in this and other systems will clarify whether the situation in *Manacus* is a typical mechanism in nature for constraining gene flow.

Acknowledgements

For helpful feedback and productive discussions, I thank Carlos Machado, Kira Long, Andre Moncrieff, Pearl Rivers, Camilo Alfonso, Diego Cueva, Danielle Adams, and Kim Paczolt. The work was strengthened by able field assistance from Antonio Pineda, Sr. and Antonio Pineda, Jr. For logistical support with fieldwork, I thank the Chiriquí Land Company and the Smithsonian Tropical Research Institute, including María Leone, Gloria Maggiori, and Eldridge Bermingham. I thank Panama's Ministerio de Ambiente (MiAmbiente, formerly INRENARE) for fieldwork permits and NMNH staff, including Chris Milensky and Chris Huddleston, for providing access to genetic samples.

Chapter 3. Repeated introgression of an ornamental male plumage trait in manakins

Abstract

Sexual selection is among the most influential and idiosyncratic forces of evolution. Some of the most distinctive and unusual traits found in nature have resulted from sexual selection, but how and why it produces such traits is still a topic of intense debate. Insights into the genetic architecture of sexual traits will shed light on this question, but only recently have the tools become available to explore this architecture in free-living organisms. An unusual hybrid zone in Panama between lekking white-collared and golden-collared manakins presents a promising opportunity to probe the phenotypic targets of sexual selection, its genetic underpinnings, and its evolutionary trajectory at multiple timescales. By sequencing whole genomes of fourteen individuals from four species and performing biochemical and spectrophotometric analysis of feathers, my collaborators and I identified the molecular and microstructural bases of a coloration trait under strong sexual selection, identified regulation of the carotenoid-metabolizing enzyme *BCO2* as responsible for color differences, and uncovered evidence of two separate inter-species introgression events involving this gene. These results demonstrate the remarkably small toolkit of genes acted on by sexual selection to affect coloration and provide two rare examples of inter-species introgression of a sexual trait.

Introduction

Sexual selection is a pervasive force in shaping biodiversity, and it can operate both in concert and in conflict with natural selection (Andersson 1994). Sexual selection can promote rapid diversification of extravagant phenotypes and accelerate molecular evolution. Moreover,

sexual selection for traits involved in mating displays can move organisms away from fitness optima dictated by natural selection (Rowe and Rundle 2021) To gain insight into the evolution of sexually selected traits, it is essential to understand the genetic architecture of these traits, but we lack such information for virtually all natural systems.

Sexual selection is a particularly powerful selective agent in shaping the phenotypes of Neotropical manakins (Pipridae). In these taxa, females provide all parental care and male reproductive investment is devoted entirely to mating (Ligon 1999; Emlen and Wrege 2004). Females are 'choosy' and most matings in local populations go to a few males, leading to the most intense sexual selection known in nature (Shorey 2002). In Panama, golden-collared and white collared manakins (*Manacus vitellinus* and *M. candei*, respectively) form a narrow hybrid zone, which appears to be maintained by strong selection against hybrids (Brumfield et al. 2001; Long et al. in review). Nevertheless, bright yellow collar plumage of *vitellinus* adult males has introgressed roughly 50 km beyond the genomic hybrid zone into *candei* populations through intrasexual and/or intersexual selection (McDonald et al. 2001; Stein and Uy 2006b; Bennett et al. 2021). At the furthest extent of trait introgression, there exist populations that are geographically close and genetically similar but differ in plumage coloration (Parsons et al. 1993; Brumfield et al. 2001; Parchman et al. 2013; Long et al. in review). Hereafter, I refer to these populations as WCC (white-collared *candei*) and YCC (yellow-collared *candei*). In this study, my collaborators and I take advantage of the hybrid zone as well as plumage variation among all *Manacus* species to identify molecular and genetic bases of plumage coloration in a group of birds where color is a key sexual phenotype (McDonald et al. 2001; Stein and Uy 2006a,b).

Colorful feathers have a single carotenoid and a distinct microstructure

There are four species of *Manacus* possessing different adult male collar and belly plumage, including bright whites, vibrant yellows, saturated oranges, olive greens, and greys (Figure 1.2B). NMJ, MJP, and GEH used light microscopy, reflectance spectroscopy, and High-Performance Liquid Chromatography (HPLC) to characterize pigments and mechanisms of color production in these plumage patches (Appendix B, Table S3.1).

The concentration of a single carotenoid pigment—lutein—determines the coloration of collar plumage (Figure 3.1A, Appendix B, Figure S3.1). White-bearded manakin (*M. manacus*) and *M. candei* collar feathers had no lutein; yellow collar feathers of *M. vitellinus* and YCC had intermediate lutein levels; and orange-collared manakin (*M. aurantiacus*) collar feathers had the highest lutein concentrations. Spectrophotometric analysis of pigmented collar feathers showed that increased lutein concentration was positively correlated with yellow and carotenoid-specific saturation, but not hue (Figure 3.1C,E, Appendix B, Figure S3.2), as expected if coloration is the product of a single carotenoid pigment.

Unlike collar feathers, color variation of belly feathers was determined largely by presence or absence of lutein and melanin, rather than variation in pigment concentration. Gray belly feathers of *M. manacus* had no lutein; dark olive green bellies of *vitellinus* had some; and olive to yellow bellies of *aurantiacus*, *candei*, and YCCs had the most lutein (Figure 3.1A, Appendix B, Table S3.2). In yellow belly feathers of *M. candei*, both the barbs and barbules were yellow, and contained only lutein (Figure 3.1A, Appendix B, Figure S3.1). Both the olive green belly feathers of *M. vitellinus* and the grey feathers of *M. manacus* had melanosomes deposited in the barbules (Figure 3.1D). The combination of yellow barbs and black barbules creates an olive green plumage patch in *M. vitellinus*, while the combination of white barbs and

black barbules produces grey belly plumage in *M. manacus*. The presence of melanosomes in the barbules of the YCCs was sporadic (Figure 3.1D), making the belly feathers less olive green in some individuals and indicating that the introgression of green belly coloration across the hybrid zone was incomplete, as previously reported (Brumfield et al. 2001). Thus, presence or absence of lutein in feather barbs and barbules, combined with the presence or absence of melanosomes in barbules, explains the range of belly color variation observed in *Manacus* males.

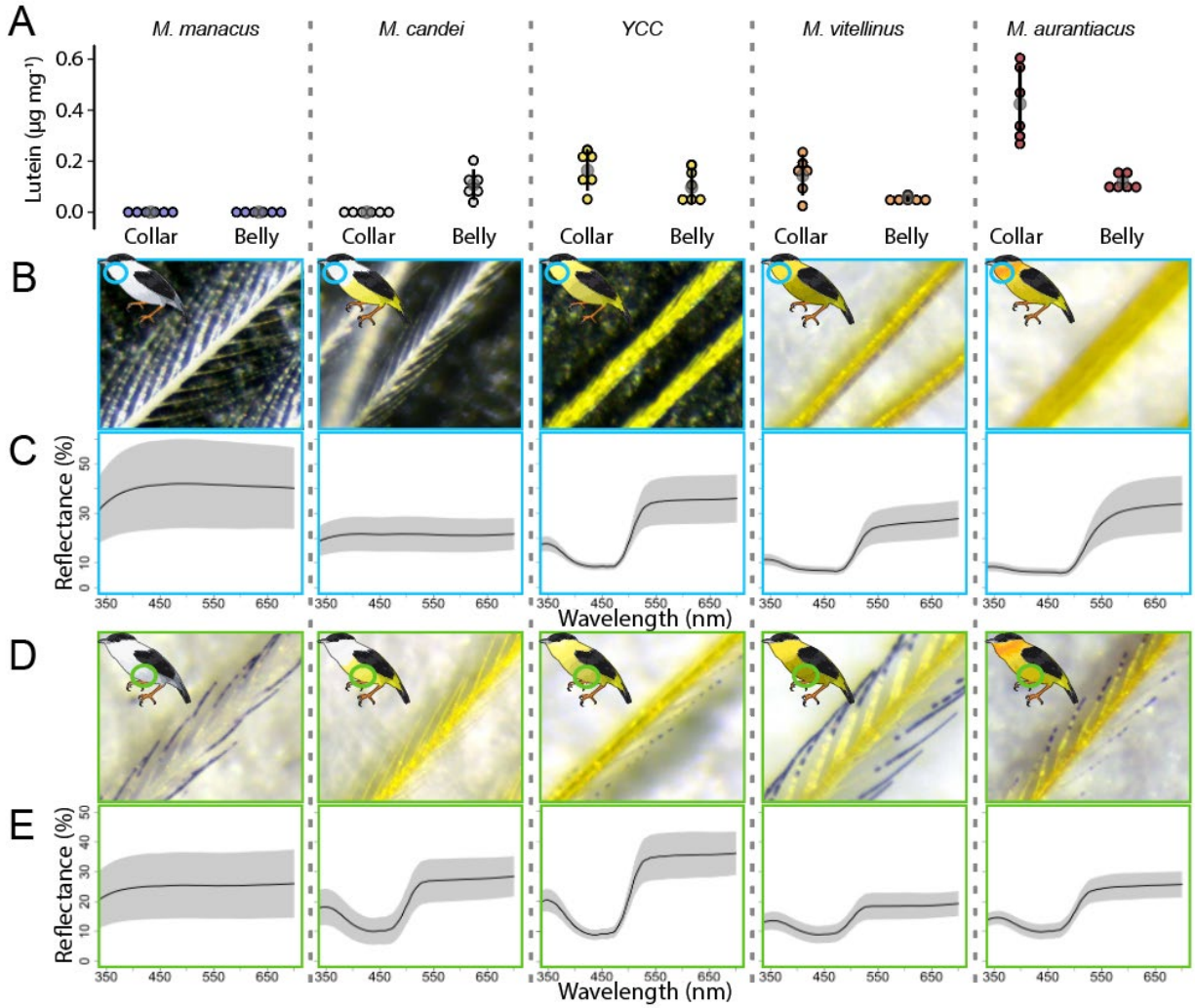

Figure 3.1. Biochemical, microscopic, and spectrophotometric analysis of *Manacus* feathers. A. Concentrations of the dietary carotenoid lutein from collars and bellies of *Manacus* males. B. and D. Microscope images of *Manacus* collars and bellies, respectively. C and E. Reflectance spectra for *Manacus* collars and bellies, respectively. A shift in reflectance peak location, rather than height, would indicate a change in hue. YCC refers to a population of *M. candei* that has yellow collars due to introgression from *M. vitellinus*.

To determine if feather structure differs among species in addition to color, NMJ examined feathers for microstructural modifications. White feathers had barbs and barbules typical of avian contour feathers, while yellow *M. vitellinus* and orange *M. aurantiacus* feathers lacked barbules (Figure 3.1B), consistent with previous evidence in pigmented feathers (Brush and Seifried 1968; Olson 1970; Troy and Brush 1983; Potticary et al. 2020). The barbs of pigmented collar feathers were also significantly wider than those of white collar feathers (Figure 3.1B, Appendix B, Figure S3.3). YCCs had an intermediate morphology and smaller barbules. The presence of lutein in yellow feathers may be partly responsible for the lack of/smaller barbules, because carotenoids are known to inhibit angiogenesis (Sugawara et al. 2006; Guruvayoorappan and Kuttan 2007), a process that is important for the full formation of the hierarchical branches of feathers (Lin et al. 2013). However, deposition of carotenoids is unlikely to be the sole factor causing structural differences in *Manacus*. Yellow collar feathers of YCCs, which had lutein concentrations similar to parental *vitellinus*, had small barbules, and yellow belly feathers of *M. candei*, which had similar lutein concentrations as *vitellinus* collars, had barbs of normal width and fully formed barbules (Figure 3.1B, D). This evidence suggests the unique microstructure of pigmented feathers has been refined by selection, supported by previous evidence that broad barbs and reduced barbules may elevate color saturation and reduce diffuse scattering, respectively (Hill 1994; Potticary et al. 2020).

BCO2 is responsible for yellow collar pigmentation in hybrid manakins

To characterize genomic introgression from *M. vitellinus* into *M. candei*, HCL and MJB generated resequenced genomes of 26 males from four populations (Figure 1.2A, C). Two

populations represent allopatric *vitellinus* (n = 4) and *candei* (n = 2). The other two populations were white-collared WCCs (n = 10) and introgressed YCC (n = 10), which are 8 km apart but differ in collar color. HCL mapped sequencing reads to a reference genome of *M. vitellinus* (NCBI accession: GCF_00175985.3). Population genomic analyses confirmed that the primary genetic differentiation was between parental *M. vitellinus* and the other three populations, which are all *candei*-like at the genomic level, and secondarily between WCC and YCC (Appendix B, Figure S3.4).

The unique nature of the hybrid zone—genomic similarity but phenotypic disparity between WCC and YCC and relatively deep divergence between *M. vitellinus* and *candei*—provides an opportunity to investigate the genetic mechanisms underlying the introgressed plumage phenotypes. HCL and I applied a non-overlapping 10 kb sliding window across the genome and calculated several metrics of differentiation or introgression between WCC and YCC to reduce the likelihood of one metric producing false positives (Cruickshank and Hahn 2014; Burri 2017) (Appendix B). For each window, we estimated two measures of divergence, F_{ST} and net D_{XY} (Nei and Li 1979; Weir and Cockerham 1984). We also estimated two measures of introgression, f_d and relative node depth (RND) (Feder et al. 2005; Martin et al. 2015; Lopes et al. 2016). f_d is related to Patterson's D (Green et al. 2010) developed for windowed genomic analyses: it is an estimator of the proportion of a window shared due to introgression (Martin et al. 2015). RND describes the divergence between the test populations relative to the divergence of YCC to *M. vitellinus* from central Panama (Feder et al. 2005; Lopes et al. 2016). Values above one indicate windows where YCC shares a more recent common ancestor with *vitellinus* 300 km away than with WCC 8 km away. In addition, I determined the position of all single nucleotide polymorphisms (SNPs) that were diagnostic between allopatric *M. vitellinus* and *M. candei*, had

≥ 0.8 frequency of the *M. candei* allele in WCCs, and ≥ 0.8 frequency of the *M. vitellinus* allele in YCCs, thereby combining expected signatures of differentiation and introgression (hereafter, "dSNPs").

I calculated 99.9% outliers of each windowed statistic. A total of 266 out of 91,913 (0.283%) autosomal and 26 out of 7,079 (0.367%) Z chromosome 10 kb windows were supported as outliers by at least one statistic (Figure 3.2A-E). Among autosomal and Z chromosome outlier windows with support from at least two statistics, a large proportion were supported by only the two differentiation statistics (40.2%) or the two introgression statistics (44.6%), suggesting that these measures are sensitive to different demographic processes (Appendix B, Figure S3.7). HCL and I identified 24 genomic neighborhoods (size: 10-960 kb) in seven chromosomes that contained higher densities of outlier windows supported by multiple statistics (Appendix B, Table S3.4).

One genomic neighborhood contained an 80 kb block of apparently introgressed DNA (Figure 3.2K). This region contained outliers of all four windowed summary statistics, 59 out of 192 dSNPs in the genome, and 46 out of 53 dSNPs that were fixed in either YCC or WCC (Appendix B, Table S3.4). The block of DNA contained four annotated genes, including beta-carotene oxygenase 2 (*BCO2*) (Figure 3.2, Appendix B, Table S3.4, Figure S3.10). It has been implicated in yellow/white polymorphisms in a variety of organisms (Eriksson et al. 2008; Berry et al. 2009; Våge and Boman 2010; Strychalski et al. 2015; Toews et al. 2016; Andrade et al. 2019), and has been shown to introgress across species boundaries in *Setophaga* warblers (Baiz et al. 2021) and junglefowl (*Gallus* spp.) (Eriksson et al. 2008), leading to carotenoid deposition in feathers and bare parts. *BCO2* encodes the enzyme beta-carotene oxygenase 2 that is found in a broad array of vertebrate tissues and catalyzes asymmetric cleavage of a variety of carotenoid

pigments, rendering them colorless (Kiefer et al. 2002; dela Seña et al. 2016). Thus, the yellow-collared phenotype is likely to be associated with reduced *BCO2* activity either due to reduced gene expression or inactivity of the enzyme (Eriksson et al. 2008; Andrade et al. 2019; Lehnert et al. 2019; Enbody et al. 2021). I found no nucleotide substitutions between the white-collared and yellow-collared haplotypes that would cause amino acid changes in *BCO2*; substitutions were concentrated in introns and non-coding regions 5' or 3' of the gene (Appendix B, Fig S3.10). It is therefore likely that functionally relevant mutations cause reduced gene expression constitutively or in key tissues (e.g., liver or growing feathers).

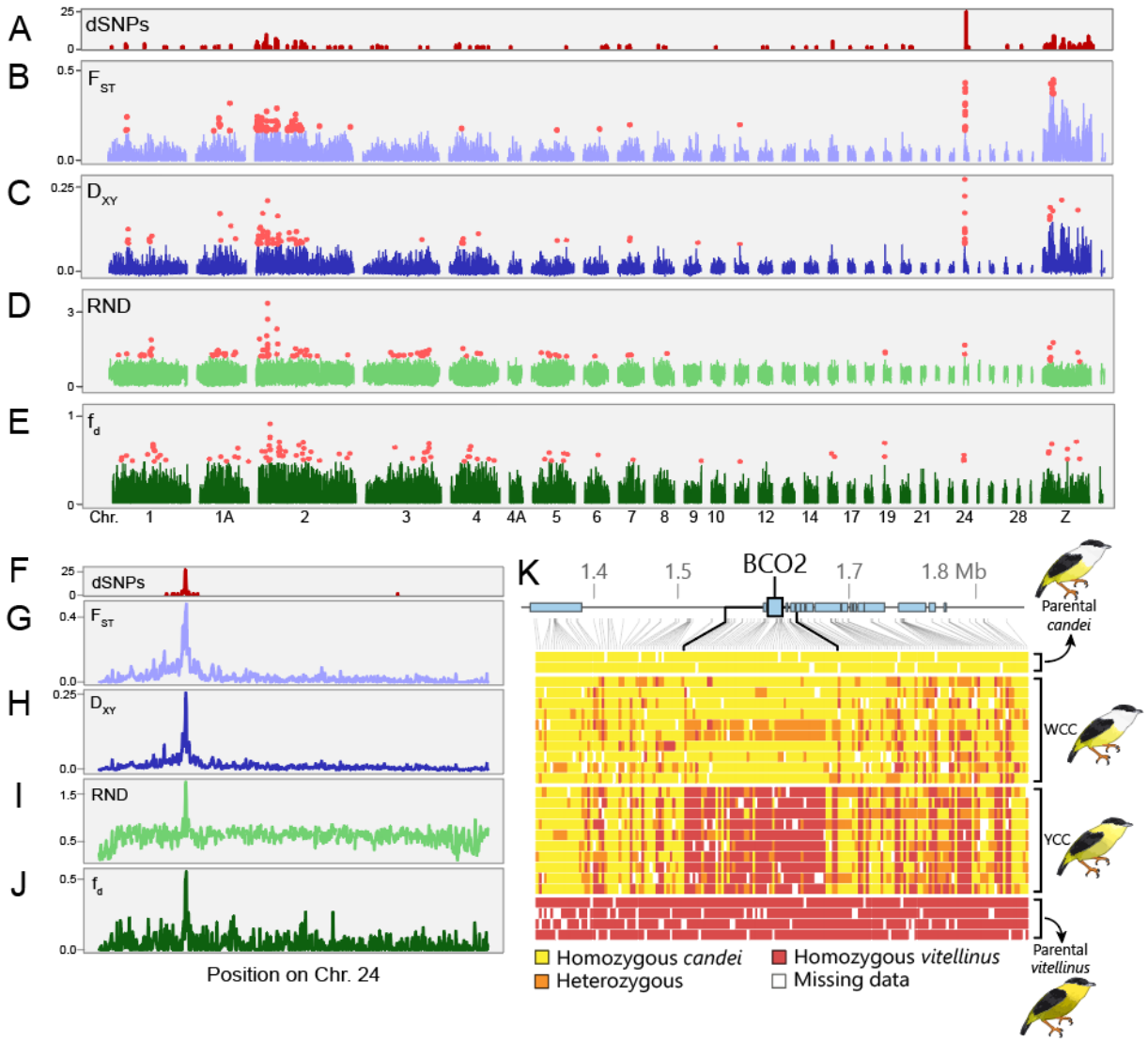

Figure 3.2. Differentiation and introgression analyses between white-collared and yellow-collared *M. candei* (WCC and YCC, respectively). A-E. Genome-wide measures of differentiation (B-C), introgression (D-E), and a combination (A) calculated in 10 kb windows. Autosomal and Z chromosome 99.9% outliers of B-E are indicated in red. F-J. The same measures of differentiation and introgression on chromosome 24. K. Genotypes of SNPs fixed for different alleles in parental *candei* and parental *vitellinus*. Yellow indicates homozygotes for the allele fixed in *candei*; red indicates homozygotes for the allele fixed in *vitellinus*.

Beside the *BCO2*-containing region, the most strongly supported outlier windows were in a region of chromosome 2 adjacent to the genes EIF3E and RSPO2 (Appendix B, Table S3.4, Figure S3.8, S3.8). Neither gene has been clearly linked to coloration. However, the related gene EIF2S2 has been linked with melanin variation in warblers (Wang et al. 2020) and humans (Liu et al. 2015a), and RSPO2 controls dog fur growth patterns (Cadieu et al. 2009), which could share developmental pathways with feather growth. Either or both of these genes could be involved in coloration differences between manakin populations, including general regulation of color patterning or melanin specifically, but further work is needed to confirm their role.

Other 10kb windows supported by differentiation/introgression statistics and/or dSNPs (see Appendix B) contained or were adjacent to annotated genes with a variety of functions, such as transmembrane communication, initiation of protein translation, enhancing Wnt signaling, angiogenesis, solute transportation, spermatogenesis and catalysis of ketolysis (Appendix B, Table S3.4). Several of these genes, or the families they belong to, have been linked to melanin-based color differences or melanin transportation in birds and other animals, including *ASIP* and *SLCO5A1* (Graf et al. 2005; Toews et al. 2016; Campagna et al. 2017; Stryjewski and Sorenson 2017; Abolins-Abols et al. 2018; Wang et al. 2020), and carotenoid metabolism, including *RDH10* (Sandell et al. 2007; Farjo et al. 2011) (Appendix B, Table S3.4).

BCO2 shows signatures of past interspecies introgression

Having identified a gene likely to be involved in collar pigmentation in *M. vitellinus*, my collaborators and I next sought to investigate the history of the trait and the gene in the genus. Because pigmented collars in both *M. vitellinus* and *M. aurantiacus* are due to deposition of lutein, we wondered whether the trait could have a single origin or arose independently in both species. The two are not sister taxa (Brumfield and Braun 2001; Brumfield et al. 2008; Harvey et al. 2020; Leite et al. 2021) nor are they currently in contact, but their ranges are separated by no more than 25 km (Chaves 2020; Sly 2023), so gene flow could have occurred through long-distance dispersal or past periods of contact.

To determine whether the *BCO2* locus had a distinct evolutionary history from the rest of the genome, we sought to compare a gene tree for *BCO2* to the well-established phylogeny of the genus *Manacus* (Harvey et al. 2020). MJB and I resequenced whole genomes of nine additional manakins representing the three remaining major lineages of the genus: three each of *M. aurantiacus*, *M. manacus* east of the Andes (*cis*-Andean), and *M. manacus* west of the Andes (*trans*-Andean) (Figure 1.2A). I used IQ-TREE v2.2 (Minh et al. 2020) to construct phylogenetic trees from a 48 kb region around *BCO2*. As controls, I inferred trees from two other genes on chromosome 24 with no known relationship to coloration (see Appendix B). The two control gene trees were consistent with the species tree (Harvey et al. 2020) (Figure 3.3B,C). In the *BCO2* gene tree *vitellinus* and *aurantiacus* were sister to one another, indicating a more recent common ancestor for the *BCO2* alleles of the pigmented species than the rest of the genus (Figure 3.3A). The *vitellinus* + *aurantiacus* branch of the tree was sister to *candei*, which is the position occupied by *aurantiacus* in the species tree (Figure 1.2B). Both relevant nodes in the *BCO2* tree—*vitellinus* + *aurantiacus* and that branch + *candei*—had high bootstrap support.

Together these results point to a single origin of pigmented collars in *M. aurantiacus,* which spread throughout the range of *vitellinus* and continued into the southernmost portion of the range of *candei*.

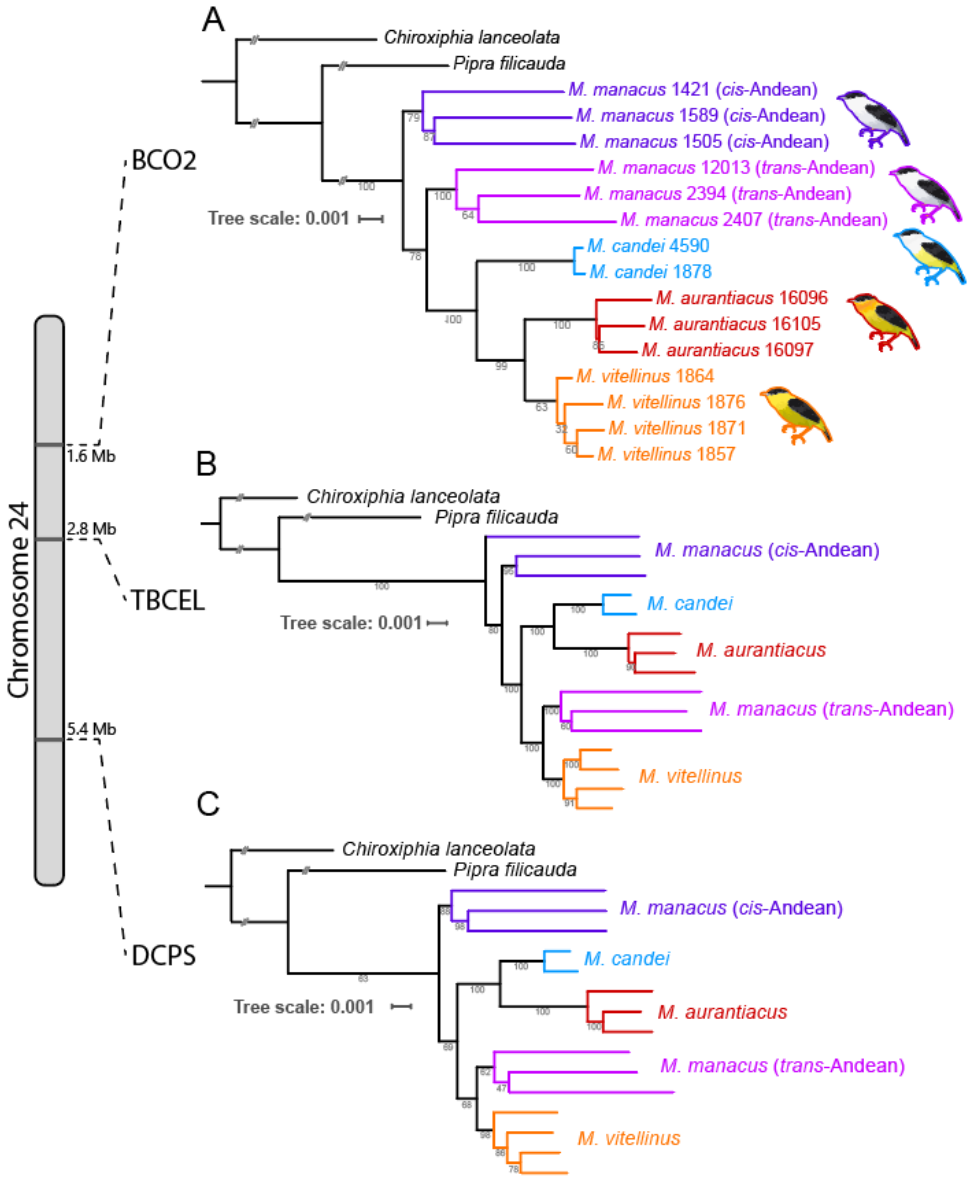

Figure 3.3. Gene trees in *Manacus* at three loci on Chromosome 24. A. *BCO2* gene tree showing sister relationship for M. vitellinus and M. aurantiacus and the sister relationship for the branch with pigmented-collar species and M. candei. B-C. Gene trees for TBCEL and DCPS, respectively. Both show the expected species relationships from Harvey et al. (2020), illustrated above in Figure 1.2.

To further explore this result, I tested for genomic evidence of introgression between *vitellinus* and *aurantiacus* agnostic of candidate genes. I calculated population-level D-statistics

in 10 kb windows (Martin et al. 2015) using *trans*-Andean *M. manacus*, *vitellinus*, *aurantiacus*, and *cis*-Andean *manacus* as test taxa and identified 99.9% outliers (see Appendix B). A window 10 kb upstream of *BCO2* was the fifth-highest of 78 genome-wide 99.9% outliers in f_d (Figure 3.4A,B).

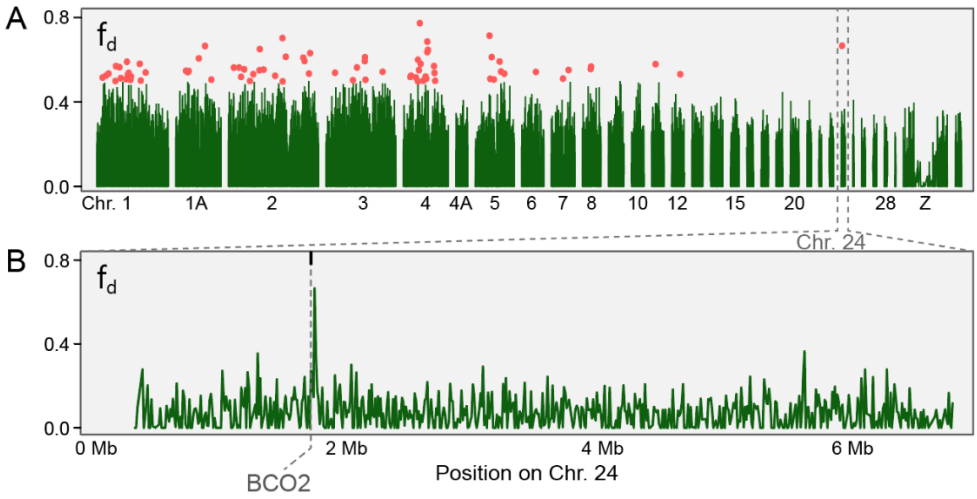

Figure 3.4. Introgression D-statistic f_d between *M. vitellinus* and *M. aurantiacus* calculated in 10 kb windows. A. Genome-wide windows, 99.9% outliers are indicated in red. B. f_d within Chromosome 24.

This finding supports the *BCO2* gene tree as indicative of historical gene flow between *M. aurantiacus* and *vitellinus* despite no previously known contact between the species. It also supports the idea that *BCO2* affects collar color in *aurantiacus*, *vitellinus*, and in *vitellinus* x *candei* hybrids.

Conclusions

These results strongly suggest that the carotenoid metabolism gene, *BCO2*, is implicated in a major coloration difference between *M. vitellinus* and *M. candei* males. The precise molecular mechanism is likely to relate to regulation of gene expression, consistent with results in other species (Andrade et al. 2019; Lehnert et al. 2019; Gazda et al. 2020a). The fact that so far, *BCO2* has so commonly been found to be the gene responsible for simple color differences

between species, particularly in birds (Toews et al. 2016; Gazda et al. 2020b; Baiz et al. 2021; Enbody et al. 2021), points to the prevalence of color evolution operating through single genes of large effect. There is also a strong signal of introgression from *M. aurantiacus* into *M. vitellinus* just upstream of *BCO2*. While the current data cannot conclusively identify the phenotypic consequence of this introgression in *vitellinus*, the fact that the signal has persisted and that male coloration is known to impact sexual selection in *Manacus* (Stein and Uy 2006b,a) together suggest that introgression from *aurantiacus* likely affected coloration in *vitellinus* and may even be responsible for the yellow collar of *vitellinus* males. Methods that are able to detect small genomic signals of ancient introgression are still fairly new, but I believe evidence will continue to accumulate that introgression often spreads genes between species—including genes for sexually selected traits that should aid in species recognition (Baiz et al. 2021)—and results in the patterns of diversity we observe in nature.

Acknowledgements

For valuable discussions and feedback, I thank Jerry Wilkinson and the Wilkinson Lab at UMD, Karen Carleton, Heidi Fisher, Carlos Machado, Shauna Rasband, Luke Anderson, Alice Boyle, Emily DuVal, and the entire Manakin Genomics Research Coordination Network. I thank Steve Mount for the suggestion of historical gene flow between *aurantiacus* and *vitellinus*. For computing technical assistance, I thank Rebecca Dikow, Mike Trizna, and Vanessa Gonzalez. I thank the Smithsonian Laboratories of Analytical Biology for lab assistance, including Jeff Hunt, Tripp McDonald, and Katie Murphy. I thank the NMNH Birds Division, including Chris Milensky and Chris Huddleston, for access to genetic samples and physical specimens.

Appendix A. Supplementary material for Chapter 2

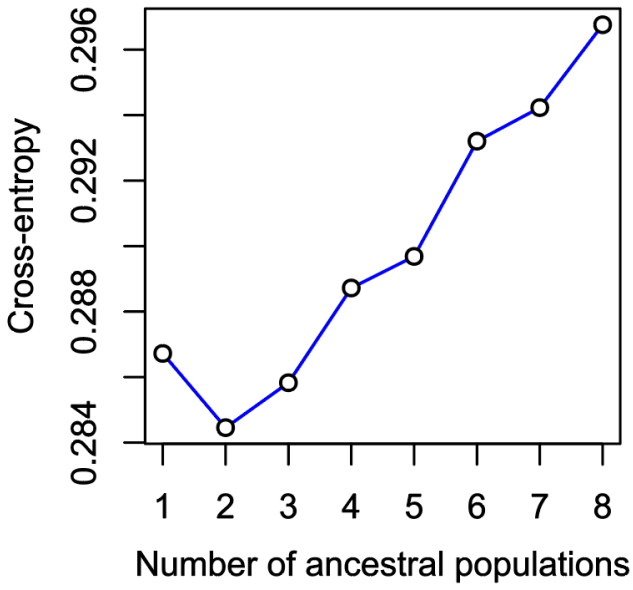

Figure S2.1. Number of genetic clusters ("populations") inferred from admixture analysis.

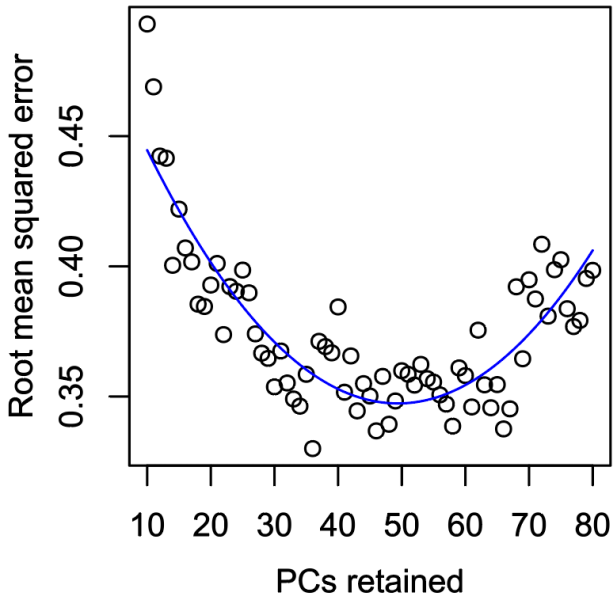

Figure S2.2. Cross-validation of discriminant analysis of principal components (DAPC). Retaining roughly 50 PCs minimizes mean squared error.

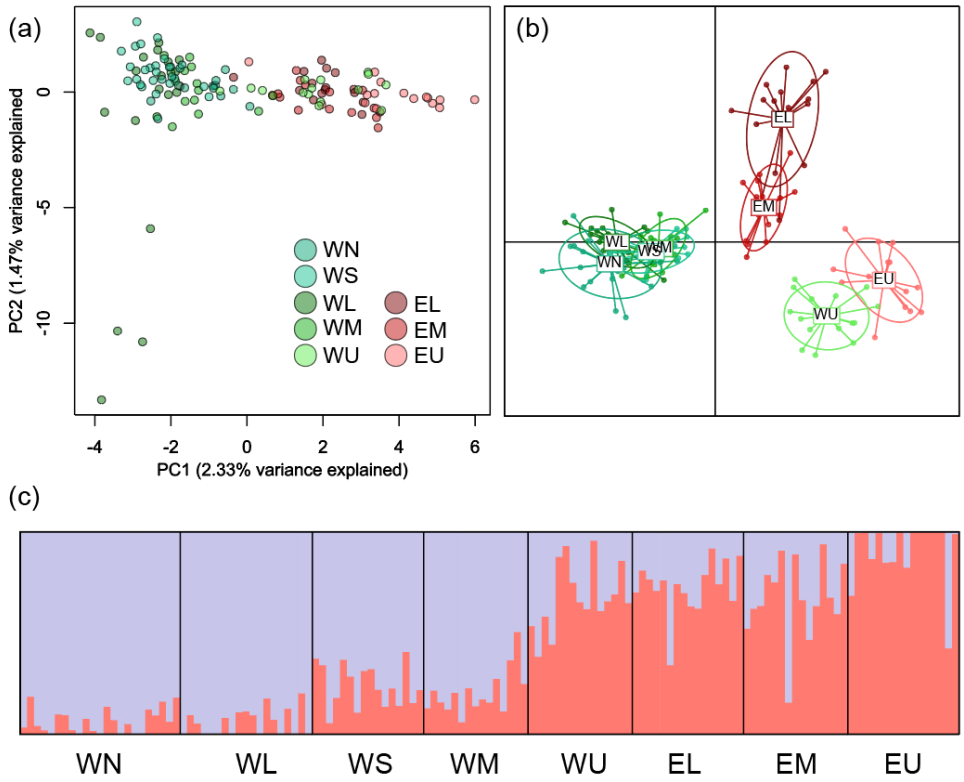

Figure S2.3. Genetic structure in manakin populations using a male-only dataset. **(a)** Principal component analysis (PCA). **(b)** Discriminant analysis of principal components using the first 50 PCs. **(c)** Admixture analysis.

Table S2.1. Manakin samples sequenced for this study. Samples used in the analyses are indicated in the last column.

USNM#	Tissue #	Biorepository ID	Population	Sample	Sex	Age	Color	Date collected	Locality	Lat	Lon	Remained post-filtering
608158	B01896	AB2MY07	EL	EL_1896	M	A	Y	25 Feb 1991	Rio Changuinola, S = E Bank, 3/5 km SE R.R. Bridge	9.4	-82.517	Y
608162	B01897	AB2MY08	EL	EL_1897	M	A	Y	25 Feb 1991	Rio Changuinola, S = E Bank, 3/5 km SE R.R. Bridge	9.4	-82.517	Y
614036	B01898	AB2MY09	EL	EL_1898	M	A	Y	25 Feb 1991	Rio Changuinola, S = E Bank, 3/5 km SE R.R. Bridge	9.4	-82.517	Y
608161	B01899	AB2MY10	EL	EL_1899	M	A	Y	25 Feb 1991	Rio Changuinola, S = E Bank, 3/5 km SE R.R. Bridge	9.4	-82.517	Y
608160	B01900	AB2MY11	EL	EL_1900	M	A	Y	25 Feb 1991	Rio Changuinola, S = E Bank, 3/5 km SE R.R. Bridge	9.4	-82.517	Y
608165	B01902	AB2MY12	EL	EL_1902	M	A	Y	25 Feb 1991	Rio Changuinola, S = E Bank, 3/5 km SE R.R. Bridge	9.4	-82.517	Y
608163	B01903	AB2MY13	EL	EL_1903	M	A	Y	25 Feb 1991	Rio Changuinola, S = E Bank, 3/5 km SE R.R. Bridge	9.4	-82.517	Y
608164	B01904	AB2MY14	EL	EL_1904	M	A	Y	25 Feb 1991	Rio Changuinola, S = E Bank, 3/5 km SE R.R. Bridge	9.4	-82.517	Y
608169	B01905	AB2MY15	EL	EL_1905	U	U	G	25 Feb 1991	Rio Changuinola, S = E Bank, 3/5 km SE R.R. Bridge	9.4	-82.517	N
608166	B01907	AB2MY16	EL	EL_1907	M	I	G	26 Feb 1991	Rio Changuinola, S = E Bank, 3/5 km SE R.R. Bridge	9.4	-82.517	Y
608159	B01908	AB2MY17	EL	EL_1908	M	A	Y	26 Feb 1991	Rio Changuinola, S = E Bank, 3/5 km SE R.R. Bridge	9.4	-82.517	Y
614037	B01909	AB2MY18	EL	EL_1909	M	A	Y	26 Feb 1991	Rio Changuinola, S = E Bank, 3/5 km SE R.R. Bridge	9.4	-82.517	Y
614038	B01910	AB2MY19	EL	EL_1910	M	A	Y	26 Feb 1991	Rio Changuinola, S = E Bank, 3/5 km SE R.R. Bridge	9.4	-82.517	Y
614039	B01911	AB2MY20	EL	EL_1911	M	A	Y	26 Feb 1991	Rio Changuinola, S = E Bank, 3/5 km SE R.R. Bridge	9.4	-82.517	Y
614040	B01912	AB2MY21	EL	EL_1912	M	A	Y	26 Feb 1991	Rio Changuinola, S = E Bank, 3/5 km SE R.R. Bridge	9.4	-82.517	Y
614041	B01913	AB2MY22	EL	EL_1913	F	U	G	26 Feb 1991	Rio Changuinola, S = E Bank, 3/5 km SE R.R. Bridge	9.4	-82.517	Y
614042	B01914	AB2MY23	EL	EL_1914	F	U	G	26 Feb 1991	Rio Changuinola, S = E Bank, 3/5 km SE R.R. Bridge	9.4	-82.517	Y
608170	B01915	AB2MY24	EL	EL_1915	U	U	G	26 Feb 1991	Rio Changuinola, S = E Bank, 3/5 km SE R.R. Bridge	9.4	-82.517	N

608167	B01948	AB2MY25	EL	EL_1948	M	A	Y	03 Mar 1991	Rio Changuinola, S = E Bank, 3/5 km SE R.R. Bridge	9.4	-82.517 Y
608168	B01949	AB2MY26	EL	EL_1949	M	A	Y	03 Mar 1991	Rio Changuinola, S = E Bank, 3/5 km SE R.R. Bridge	9.4	-82.517 Y
656945	B04501	AB2ML12	EM	EM_4501	F	U	G	19 Apr 1994	Boquisco, 1 km S, On E Bank Rio Changuinola	9.333	-82.517 Y
656946	B04502	AB2ML13	EM	EM_4502	M	A	W	19 Apr 1994	Boquisco, 1 km S, On E Bank Rio Changuinola	9.333	-82.517 Y
656947	B04503	AB2ML14	EM	EM_4503	M	A	Y	19 Apr 1994	Boquisco, 1 km S, On E Bank Rio Changuinola	9.333	-82.517 Y
656948	B04504	AB2ML15	EM	EM_4504	M	A	W	20 Apr 1994	Boquisco, 1 km S, On E Bank Rio Changuinola	9.333	-82.517 Y
656949	B04505	AB2ML16	EM	EM_4505	M	A	Y	20 Apr 1994	Boquisco, 1 km S, On E Bank Rio Changuinola	9.333	-82.517 Y
656950	B04506	AB2ML17	EM	EM_4506	M	I	G	20 Apr 1994	Boquisco, 1 km S, On E Bank Rio Changuinola	9.333	-82.517 Y
656951	B04507	AB2ML18	EM	EM_4507	M	I	G	20 Apr 1994	Boquisco, 1 km S, On E Bank Rio Changuinola	9.333	-82.517 Y
656952	B04508	AB2ML19	EM	EM_4508	M	A	W	21 Apr 1994	Boquisco, 1 km S, On E Bank Rio Changuinola	9.333	-82.517 Y
656953	B04509	AB2ML20	EM	EM_4509	F	U	G	21 Apr 1994	Boquisco, 1 km S, On E Bank Rio Changuinola	9.333	-82.517 Y
656954	B04510	AB2ML21	EM	EM_4510	M	I	G	21 Apr 1994	Boquisco, 1 km S, On E Bank Rio Changuinola	9.333	-82.517 Y
656955	B04511	AB2ML22	EM	EM_4511	M	A	Y	21 Apr 1994	Boquisco, 1 km S, On E Bank Rio Changuinola	9.333	-82.517 Y
656956	B04513	AB2ML23	EM	EM_4513	M	A	Y	21 Apr 1994	Boquisco, 1 km S, On E Bank Rio Changuinola	9.333	-82.517 Y
656957	B04514	AB2ML24	EM	EM_4514	F	U	G	21 Apr 1994	Boquisco, 1 km S, On E Bank Rio Changuinola	9.333	-82.517 Y
656958	B04515	AB2ML25	EM	EM_4515	M	A	W	21 Apr 1994	Boquisco, 1 km S, On E Bank Rio Changuinola	9.333	-82.517 Y
656959	B04516	AB2ML26	EM	EM_4516	M	A	Y	22 Apr 1994	Boquisco, 1 km S, On E Bank Rio Changuinola	9.333	-82.517 Y
656960	B04517	AB2ML27	EM	EM_4517	M	I	G	22 Apr 1994	Boquisco, 1 km S, On E Bank Rio Changuinola	9.333	-82.517 N
608986	B04518	AC8CO88	EM	EM_4518	M	A	Y	22 Apr 1994	Boquisco, 1 km S, On E Bank Rio Changuinola	9.333	-82.517 Y

656961	B04520	AB2ML29	EM	EM_4520	F	U	G	23 Apr 1994	Boquisco, 1 km S, On E Bank Rio Changuinola	9.333	-82.517 Y
656962	B04521	AB2ML30	EM	EM_4521	M	A	W	23 Apr 1994	Boquisco, 1 km S, On E Bank Rio Changuinola	9.333	-82.517 Y
656963	B04522	AB2ML31	EM	EM_4522	M	A	Y	23 Apr 1994	Boquisco, 1 km S, On E Bank Rio Changuinola	9.333	-82.517 Y
656964	B04523	AB2ML32	EM	EM_4523	F	U	G	23 Apr 1994	Boquisco, 1 km S, On E Bank Rio Changuinola	9.333	-82.517 Y
657155	B04760	AC8CP63	EU	EU_4760	M	A	W	01 Mar 1996	Arriba, E bank Rio Changuinola	9.2	-82.477 Y
657156	B04761	AC8CP64	EU	EU_4761	M	A	Y	01 Mar 1996	Arriba, E bank Rio Changuinola	9.2	-82.477 Y
657157	B04762	AC8CP65	EU	EU_4762	M	A	Y	01 Mar 1996	Arriba, E bank Rio Changuinola	9.2	-82.477 Y
657158	B04763	AC8CP66	EU	EU_4763	M	A	Y	01 Mar 1996	Arriba, E bank Rio Changuinola	9.2	-82.477 Y
657159	B04764	AC8CP67	EU	EU_4764	M	A	Y	01 Mar 1996	Arriba, E bank Rio Changuinola	9.2	-82.477 Y
657160	B04765	AC8CP68	EU	EU_4765	M	A	Y	01 Mar 1996	Arriba, E bank Rio Changuinola	9.2	-82.477 Y
657161	B04766	AC8CP69	EU	EU_4766	M	A	Y	01 Mar 1996	Arriba, E bank Rio Changuinola	9.2	-82.477 Y
657162	B04767	AC8CP70	EU	EU_4767	M	A	Y	01 Mar 1996	Arriba, E bank Rio Changuinola	9.2	-82.477 Y
657163	B04768	AC8CP71	EU	EU_4768	M	I	G	01 Mar 1996	Arriba, E bank Rio Changuinola	9.2	-82.477 Y
657164	B04769	AC8CP72	EU	EU_4769	M	A	Y	01 Mar 1996	Arriba, E bank Rio Changuinola	9.2	-82.477 Y
657165	B04770	AC8CP73	EU	EU_4770	F	U	G	01 Mar 1996	Arriba, E bank Rio Changuinola	9.2	-82.477 Y
657166	B04771	AC8CP74	EU	EU_4771	F	U	G	01 Mar 1996	Arriba, E bank Rio Changuinola	9.2	-82.477 Y
657167	B04772	AC8CP75	EU	EU_4772	M	A	Y	01 Mar 1996	Arriba, E bank Rio Changuinola	9.2	-82.477 Y
657168	B04773	AC8CP76	EU	EU_4773	F	U	G	01 Mar 1996	Arriba, E bank Rio Changuinola	9.2	-82.477 Y
657169	B04774	AC8CP77	EU	EU_4774	F	U	G	02 Mar 1996	Arriba, E bank Rio Changuinola	9.2	-82.477 Y
657170	B04775	AC8CP78	EU	EU_4775	M	A	Y	02 Mar 1996	Arriba, E bank Rio Changuinola	9.2	-82.477 Y
657171	B04776	AC8CP79	EU	EU_4776	F	U	G	02 Mar 1996	Arriba, E bank Rio Changuinola	9.2	-82.477 Y
657172	B04777	AC8CP80	EU	EU_4777	F	U	G	02 Mar 1996	Arriba, E bank Rio Changuinola	9.2	-82.477 Y
657173	B04778	AC8CP81	EU	EU_4778	F	U	G	02 Mar 1996	Arriba, E bank Rio Changuinola	9.2	-82.477 Y
657174	B04779	AC8CP82	EU	EU_4779	F	U	G	02 Mar 1996	Arriba, E bank Rio Changuinola	9.2	-82.477 Y
657175	B04780	AC8CP83	EU	EU_4780	M	A	Y	02 Mar 1996	Arriba, E bank Rio Changuinola	9.2	-82.477 Y
657176	B04781	AC8CP84	EU	EU_4781	F	U	G	02 Mar 1996	Arriba, E bank Rio Changuinola	9.2	-82.477 Y
657177	B04782	AC8CP85	EU	EU_4782	M	A	Y	02 Mar 1996	Arriba, E bank Rio Changuinola	9.2	-82.477 Y
657178	B04783	AC8CP86	EU	EU_4783	M	A	W	02 Mar 1996	Arriba, E bank Rio Changuinola	9.2	-82.477 Y
657179	B04784	AC8CP87	EU	EU_4784	M	A	Y	02 Mar 1996	Arriba, E bank Rio Changuinola	9.2	-82.477 Y
614056	B01880	AB2MX78	WL	WL_1880	M	A	W	24 Feb 1991	Charagre, 3 km SW, N. Bank Rio Teribe, Quebrada Carbon	9.367	-82.581 Y

608194	B01883	AB2MX82	WL	WL_1883	M	A	W	24 Feb 1991	Charagre, 3 km SW, N. Bank Rio Teribe, Quebrada Carbon	9.367	-82.581	Y
608195	B01884	AB2MX85	WL	WL_1884	M	A	W	24 Feb 1991	Charagre, 3 km SW, N. Bank Rio Teribe, Quebrada Carbon	9.367	-82.581	Y
614058	B01885	AB2MX87	WL	WL_1885	M	A	W	24 Feb 1991	Charagre, 3 km SW, N. Bank Rio Teribe, Quebrada Carbon	9.367	-82.581	Y
614059	B01886	AB2MX89	WL	WL_1886	M	A	W	24 Feb 1991	Charagre, 3 km SW, N. Bank Rio Teribe, Quebrada Carbon	9.367	-82.581	Y
608196	B01887	AB2MX91	WL	WL_1887	M	A	W	24 Feb 1991	Charagre, 3 km SW, N. Bank Rio Teribe, Quebrada Carbon	9.367	-82.581	Y
608197	B01888	AB2MX93	WL	WL_1888	M	A	W	24 Feb 1991	Charagre, 3 km SW, N. Bank Rio Teribe, Quebrada Carbon	9.367	-82.581	Y
614060	B01889	AB2MX94	WL	WL_1889	M	A	W	24 Feb 1991	Charagre, 3 km SW, N. Bank Rio Teribe, Quebrada Carbon	9.367	-82.581	Y
608198	B01890	AB2MX96	WL	WL_1890	M	A	W	24 Feb 1991	Charagre, 3 km SW, N. Bank Rio Teribe, Quebrada Carbon	9.367	-82.581	Y
614061	B01891	AB2MX97	WL	WL_1891	M	A	W	24 Feb 1991	Charagre, 3 km SW, N. Bank Rio Teribe, Quebrada Carbon	9.367	-82.581	Y
608199	B01892	AB2MX98	WL	WL_1892	M	A	W	24 Feb 1991	Charagre, 3 km SW, N. Bank Rio Teribe, Quebrada Carbon	9.367	-82.581	Y
608200	B01893	AB2MX99	WL	WL_1893	M	A	W	24 Feb 1991	Charagre, 3 km SW, N. Bank Rio Teribe, Quebrada Carbon	9.367	-82.581	Y
608201	B01894	AB2MY00	WL	WL_1894	M	I	G	24 Feb 1991	Charagre, 3 km SW, N. Bank Rio Teribe, Quebrada Carbon	9.367	-82.581	Y
608202	B01895	AB2MY01	WL	WL_1895	M	A	W	24 Feb 1991	Charagre, 3 km SW, N. Bank Rio Teribe, Quebrada Carbon	9.367	-82.581	Y
608203	B01920	AB2MY02	WL	WL_1920	M	A	W	28 Feb 1991	Charagre, 3 km SW, N. Bank Rio Teribe, Quebrada Carbon	9.367	-82.581	Y
608204	B01921	AB2MY03	WL	WL_1921	M	A	W	28 Feb 1991	Charagre, 3 km SW, N. Bank Rio Teribe, Quebrada Carbon	9.367	-82.581	Y
614062	B01922	AB2MY04	WL	WL_1922	M	A	W	28 Feb 1991	Charagre, 3 km SW, N. Bank Rio Teribe, Quebrada Carbon	9.367	-82.581	Y
614063	B01923	AB2MY05	WL	WL_1923	M	A	W	28 Feb 1991	Charagre, 3 km SW, N. Bank Rio Teribe, Quebrada Carbon	9.367	-82.581	Y
608205	B01924	AB2MY06	WL	WL_1924	M	A	W	28 Feb 1991	Charagre, 3 km SW, N. Bank Rio Teribe, Quebrada Carbon	9.367	-82.581	Y
656965	B04524	AB2ML33	WM	WM_4524	M	A	W	25 Apr 1994	W Bank Rio Changuinola, between Rios Changuinola and Rio Teribe	9.342	-82.533	Y

656966	B04525	AB2ML34	WM	WM_4525	M	A	W	25 Apr 1994	W Bank Rio Changuinola, between Rios Changuinola and Rio Teribe	9.342	-82.533	Y
656967	B04526	AB2ML35	WM	WM_4526	M	A	W	25 Apr 1994	W Bank Rio Changuinola, between Rios Changuinola and Rio Teribe	9.342	-82.533	Y
656968	B04527	AB2ML36	WM	WM_4527	M	A	W	25 Apr 1994	W Bank Rio Changuinola, between Rios Changuinola and Rio Teribe	9.342	-82.533	Y
656969	B04528	AB2ML37	WM	WM_4528	F	U	G	25 Apr 1994	W Bank Rio Changuinola, between Rios Changuinola and Rio Teribe	9.342	-82.533	Y
656970	B04529	AB2ML38	WM	WM_4529	M	A	W	25 Apr 1994	W Bank Rio Changuinola, between Rios Changuinola and Rio Teribe	9.342	-82.533	Y
656971	B04530	AB2ML39	WM	WM_4530	M	A	W	25 Apr 1994	W Bank Rio Changuinola, between Rios Changuinola and Rio Teribe	9.342	-82.533	N
608990	B04531	AC8CO90	WM	WM_4531	M	A	W	25 Apr 1994	Boquisco, 2 km W, On W Bank Rio Changuinola	9.342	-82.533	Y
656972	B04532	AB2ML41	WM	WM_4532	M	I	G	25 Apr 1994	W Bank Rio Changuinola, between Rios Changuinola and Rio Teribe	9.342	-82.533	Y
656973	B04533	AB2ML42	WM	WM_4533	M	A	W	25 Apr 1994	W Bank Rio Changuinola, between Rios Changuinola and Rio Teribe	9.342	-82.533	Y
656974	B04535	AB2ML43	WM	WM_4535	M	A	W	26 Apr 1994	W Bank Rio Changuinola, between Rios Changuinola and Rio Teribe	9.342	-82.533	N
656975	B04536	AB2ML44	WM	WM_4536	M	A	W	26 Apr 1994	W Bank Rio Changuinola, between Rios Changuinola and Rio Teribe	9.342	-82.533	N
656976	B04537	AB2ML45	WM	WM_4537	M	A	W	26 Apr 1994	W Bank Rio Changuinola, between Rios Changuinola and Rio Teribe	9.342	-82.533	N
656977	B04538	AB2ML46	WM	WM_4538	M	A	W	26 Apr 1994	W Bank Rio Changuinola, between Rios Changuinola and Rio Teribe	9.342	-82.533	Y
656978	B04539	AB2ML47	WM	WM_4539	M	I	G	26 Apr 1994	W Bank Rio Changuinola, between Rios Changuinola and Rio Teribe	9.342	-82.533	Y
656979	B04540	AB2ML48	WM	WM_4540	M	I	G	26 Apr 1994	W Bank Rio Changuinola, between Rios Changuinola and Rio Teribe	9.342	-82.533	Y
656980	B04541	AB2ML49	WM	WM_4541	M	I	G	26 Apr 1994	W Bank Rio Changuinola, between Rios Changuinola and Rio Teribe	9.342	-82.533	N
656981	B04542	AB2ML50	WM	WM_4542	F	U	G	26 Apr 1994	W Bank Rio Changuinola, between Rios Changuinola and Rio Teribe	9.342	-82.533	N
656982	B04543	AB2ML51	WM	WM_4543	M	I	G	26 Apr 1994	W Bank Rio Changuinola, between Rios Changuinola and Rio Teribe	9.342	-82.533	N
656983	B04544	AB2ML52	WM	WM_4544	M	I	G	26 Apr 1994	W Bank Rio Changuinola, between Rios Changuinola and Rio Teribe	9.342	-82.533	Y

656984	B04545	AB2ML53	WM	WM_4545	F	U	G	26 Apr 1994	W Bank Rio Changuinola, between Rios Changuinola and Rio Teribe	9.342	-82.533 N
656985	B04547	AB2ML54	WM	WM_4547	M	A	W	27 Apr 1994	W Bank Rio Changuinola, between Rios Changuinola and Rio Teribe	9.342	-82.533 Y
656986	B04548	AB2ML55	WM	WM_4548	F	U	G	27 Apr 1994	W Bank Rio Changuinola, between Rios Changuinola and Rio Teribe	9.342	-82.533 Y
656987	B04549	AB2ML56	WM	WM_4549	M	A	W	27 Apr 1994	W Bank Rio Changuinola, between Rios Changuinola and Rio Teribe	9.342	-82.533 Y
656988	B04550	AB2ML57	WM	WM_4550	F	U	G	27 Apr 1994	W Bank Rio Changuinola, between Rios Changuinola and Rio Teribe	9.342	-82.533 Y
656989	B04551	AB2ML58	WM	WM_4551	F	U	G	28 Apr 1994	W Bank Rio Changuinola, between Rios Changuinola and Rio Teribe	9.342	-82.533 Y
656991	B04553	AB2ML60	WM	WM_4553	M	A	W	29 Apr 1994	W Bank Rio Changuinola, between Rios Changuinola and Rio Teribe	9.342	-82.533 Y
620103	B03246	AC8CO82	WN	WN5_3246	F	U	G	29 Apr 1994	Guabito, 8 km W	9.45	-82.667 Y
608991	B03248	AC8CO84	WN	WN5_3248	F	U	G	04 May 1994	Guabito, 8 km SW	9.45	-82.667 Y
656992	B04554	AB2ML61	WN	WN6_4554	M	A	W	30 Apr 1994	Rio Sansan, 8 km SW Guabito	9.45	-82.667 Y
656993	B04555	AB2ML62	WN	WN6_4555	M	A	W	30 Apr 1994	Rio Sansan, 8 km SW Guabito	9.45	-82.667 Y
656994	B04556	AB2ML63	WN	WN5_4556	M	A	W	30 Apr 1994	Rio Sansan, 8 km SW Guabito	9.45	-82.667 Y
656995	B04557	AB2ML64	WN	WN6_4557	M	A	W	30 Apr 1994	Rio Sansan, 8 km SW Guabito	9.45	-82.667 Y
656996	B04558	AB2MR56	WN	WN6_4558	M	A	W	30 Apr 1994	Rio Sansan, 8 km SW Guabito	9.45	-82.667 N
656997	B04559	AB2MR57	WN	WN6_4559	F	U	G	30 Apr 1994	Rio Sansan, 8 km SW Guabito	9.45	-82.667 Y
656998	B04560	AB2MR58	WN	WN6_4560	M	A	W	30 Apr 1994	Rio Sansan, 8 km SW Guabito	9.45	-82.667 Y
656999	B04561	AB2ML65	WN	WN6_4561	M	A	W	30 Apr 1994	Rio Sansan, 8 km SW Guabito	9.45	-82.667 Y
657003	B04567	AB2MR59	WN	WN6_4567	M	A	W	30 Apr 1994	Rio Sansan, 8 km SW Guabito	9.45	-82.667 Y
649533	B04569	AB2MW47	WN	WN6_4569	M	A	W	30 Apr 1994	Rio Sansan, 8 km SW Guabito	9.45	-82.667 Y
649534	B04573	AB2MW48	WN	WN6_4573	M	A	W	30 Apr 1994	Rio Sansan, 8 km SW Guabito	9.45	-82.667 Y
649535	B04574	AB2MW49	WN	WN6_4574	M	A	W	01 Mar 1994	Rio Sansan, 8 km SW Guabito	9.45	-82.667 Y
649536	B04575	AB2MW50	WN	WN6_4575	M	A	W	01 Mar 1994	Rio Sansan, 8 km SW Guabito	9.45	-82.667 Y
649537	B04576	AB2MW51	WN	WN6_4576	M	A	W	01 Mar 1994	Rio Sansan, 8 km SW Guabito	9.45	-82.667 Y
649538	B04577	AB2MW52	WN	WN6_4577	M	A	W	01 Mar 1994	Rio Sansan, 8 km SW Guabito	9.45	-82.667 Y
657007	B04578	AB2ML72	WN	WN6_4578	F	U	G	01 Mar 1994	Rio Sansan, 8 km SW Guabito	9.45	-82.667 Y
657008	B04580	AB2ML73	WN	WN6_4580	M	I	G	01 Mar 1994	Rio Sansan, 8 km SW Guabito	9.45	-82.667 Y
657009	B04581	AB2ML74	WN	WN5_4581	M	I	G	01 Mar 1994	Rio Sansan, 8 km SW Guabito	9.45	-82.667 Y
657010	B04583	AB2ML75	WN	WN6_4583	F	U	G	01 Mar 1994	Rio Sansan, 8 km SW Guabito	9.45	-82.667 Y
657014	B04587	AB2ML79	WN	WN5_4587	F	U	G	01 Mar 1994	Rio Sansan, 8 km SW Guabito	9.45	-82.667 Y

657015	B04588	AB2ML80	WN	WN6_4588	M	A	W	02 Mar 1994	Rio Sansan, 8 km SW Guabito	9.45	-82.667	Y
657016	B04589	AB2ML81	WN	WN5_4589	F	U	G	02 Mar 1994	Rio Sansan, 8 km SW Guabito	9.45	-82.667	Y
608988	B04590	AB2MW55	WN	WN5_4590	M	A	W	28 Apr 1994	Guabito, 8 km SW	9.45	-82.667	Y
608989	B04595	AB7RB11	WN	WN5_4595	M	A	W	29 Apr 1994	Guabito, 8 km SW	9.45	-82.667	Y
657019	B04598	AB2ML84	WN	WN6_4598	M	A	W	02 Mar 1994	Rio Sansan, 8 km SW Guabito	9.45	-82.667	Y
657020	B04600	AB2ML85	WN	WN6_4600	F	U	G	02 Mar 1994	Rio Sansan, 8 km SW Guabito	9.45	-82.667	Y
657021	B04602	AB2ML86	WN	WN6_4602	M	A	W	20 Jul 1994	Rio Sansan, 8 km SW Guabito	9.45	-82.667	Y
657082	B04682	AB2MO90	WN	WN5_4682	F	U	G	07 Apr 1995	Rio Sansan, 8 km SW Guabito	9.45	-82.667	N
657083	B04683	AB2MO91	WN	WN5_4683	M	I	G	07 Apr 1995	Rio Sansan, 8 km SW Guabito	9.45	-82.667	Y
657084	B04684	AB2MO92	WN	WN5_4684	M	A	W	07 Apr 1995	Rio Sansan, 8 km SW Guabito	9.45	-82.667	Y
657085	B04685	AB2MO93	WN	WN5_4685	F	U	G	08 Apr 1995	Rio Sansan, 8 km SW Guabito	9.45	-82.667	N
657087	B04688	AB2MO95	WN	WN5_4688	M	A	W	08 Apr 1995	Rio Sansan, 8 km SW Guabito	9.45	-82.667	N
None	B04900	None	WN	WN6_4900	M	A	W	Feb 1997	Rio Sansan, 8 km SW Guabito	9.45	-82.667	Y
657111	B04716	AC8CP19	WS	WS_4716	M	A	W	22 Feb 1996	Wetso, S bank Rio Teribe	9.36	-82.598	Y
657112	B04717	AC8CP20	WS	WS_4717	F	U	G	22 Feb 1996	Wetso, S bank Rio Teribe	9.36	-82.598	Y
657113	B04718	AC8CP21	WS	WS_4718	M	A	W	22 Feb 1996	Wetso, S bank Rio Teribe	9.36	-82.598	Y
657114	B04719	AC8CP22	WS	WS_4719	M	I	G	23 Feb 1996	S bank Rio Teribe at Quebrada Bonyic	9.36	-82.598	Y
657115	B04720	AC8CP23	WS	WS_4720	M	A	W	23 Feb 1996	S bank Rio Teribe at Quebrada Bonyic	9.36	-82.598	Y
657116	B04721	AC8CP24	WS	WS_4721	M	A	W	23 Feb 1996	S bank Rio Teribe at Quebrada Bonyic	9.36	-82.598	Y
657117	B04722	AC8CP25	WS	WS_4722	M	A	W	23 Feb 1996	S bank Rio Teribe at Quebrada Bonyic	9.36	-82.598	Y
657118	B04723	AC8CP26	WS	WS_4723	M	I	G	23 Feb 1996	S bank Rio Teribe at Quebrada Bonyic	9.36	-82.598	N
657119	B04724	AC8CP27	WS	WS_4724	M	A	W	24 Feb 1996	S bank Rio Teribe at Quebrada Bonyic	9.36	-82.598	Y
657120	B04725	AC8CP28	WS	WS_4725	M	I	G	24 Feb 1996	S bank Rio Teribe at Quebrada Bonyic	9.36	-82.598	Y
657121	B04726	AC8CP29	WS	WS_4726	M	A	W	24 Feb 1996	S bank Rio Teribe at Quebrada Bonyic	9.36	-82.598	Y
657122	B04727	AC8CP30	WS	WS_4727	M	A	W	24 Feb 1996	S bank Rio Teribe at Quebrada Bonyic	9.36	-82.598	Y
657123	B04728	AC8CP31	WS	WS_4728	M	A	W	24 Feb 1996	S bank Rio Teribe at Quebrada Bonyic	9.36	-82.598	N
657124	B04729	AC8CP32	WS	WS_4729	M	A	W	24 Feb 1996	S bank Rio Teribe at Quebrada Bonyic	9.36	-82.598	Y
657125	B04730	AC8CP33	WS	WS_4730	M	A	W	24 Feb 1996	S bank Rio Teribe at Quebrada Bonyic	9.36	-82.598	Y
657126	B04731	AC8CP34	WS	WS_4731	M	A	W	24 Feb 1996	S bank Rio Teribe at Quebrada Bonyic	9.36	-82.598	Y
657127	B04732	AC8CP35	WS	WS_4732	M	A	W	24 Feb 1996	S bank Rio Teribe at Quebrada Bonyic	9.36	-82.598	Y
657128	B04733	AC8CP36	WS	WS_4733	M	A	W	24 Feb 1996	S bank Rio Teribe at Quebrada Bonyic	9.36	-82.598	Y
657129	B04734	AC8CP37	WS	WS_4734	M	I	G	24 Feb 1996	S bank Rio Teribe at Quebrada Bonyic	9.36	-82.598	Y
657130	B04735	AC8CP38	WS	WS_4735	F	U	G	24 Feb 1996	S bank Rio Teribe at Quebrada Bonyic	9.36	-82.598	Y
657131	B04736	AC8CP39	WS	WS_4736	F	U	G	24 Feb 1996	S bank Rio Teribe at Quebrada Bonyic	9.36	-82.598	Y

657132	B04737	AC8CP40	WU	WU_4737	M	A	W	28 Feb 1996	Arriba, W bank Rio Changuinola	9.2	-82.478	Y
657133	B04738	AC8CP41	WU	WU_4738	M	A	Y	28 Feb 1996	Arriba, W bank Rio Changuinola	9.2	-82.478	Y
657134	B04739	AC8CP42	WU	WU_4739	M	A	W	28 Feb 1996	Arriba, W bank Rio Changuinola	9.2	-82.478	Y
657135	B04740	AC8CP43	WU	WU_4740	M	A	Y	28 Feb 1996	Arriba, W bank Rio Changuinola	9.2	-82.478	Y
657136	B04741	AC8CP44	WU	WU_4741	M	A	Y	28 Feb 1996	Arriba, W bank Rio Changuinola	9.2	-82.478	Y
657137	B04742	AC8CP45	WU	WU_4742	M	A	Y	28 Feb 1996	Arriba, W bank Rio Changuinola	9.2	-82.478	Y
657138	B04743	AC8CP46	WU	WU_4743	M	A	W	28 Feb 1996	Arriba, W bank Rio Changuinola	9.2	-82.478	Y
657139	B04744	AC8CP47	WU	WU_4744	M	I	Y	28 Feb 1996	Arriba, W bank Rio Changuinola	9.2	-82.478	Y
657140	B04745	AC8CP48	WU	WU_4745	F	U	G	28 Feb 1996	Arriba, W bank Rio Changuinola	9.2	-82.478	Y
657141	B04746	AC8CP49	WU	WU_4746	F	U	G	28 Feb 1996	Arriba, W bank Rio Changuinola	9.2	-82.478	Y
657142	B04747	AC8CP50	WU	WU_4747	M	A	W	28 Feb 1996	Arriba, W bank Rio Changuinola	9.2	-82.478	Y
657143	B04748	AC8CP51	WU	WU_4748	M	A	Y	28 Feb 1996	Arriba, W bank Rio Changuinola	9.2	-82.478	Y
657144	B04749	AC8CP52	WU	WU_4749	F	U	G	28 Feb 1996	Arriba, W bank Rio Changuinola	9.2	-82.478	Y
657145	B04750	AC8CP53	WU	WU_4750	F	U	G	28 Feb 1996	Arriba, W bank Rio Changuinola	9.2	-82.478	N
657146	B04751	AC8CP54	WU	WU_4751	M	I	G	29 Feb 1996	Arriba, W bank Rio Changuinola	9.2	-82.478	Y
657147	B04752	AC8CP55	WU	WU_4752	M	A	W	29 Feb 1996	Arriba, W bank Rio Changuinola	9.2	-82.478	Y
657148	B04753	AC8CP56	WU	WU_4753	M	I	G	29 Feb 1996	Arriba, W bank Rio Changuinola	9.2	-82.478	Y
657149	B04754	AC8CP57	WU	WU_4754	F	U	G	29 Feb 1996	Arriba, W bank Rio Changuinola	9.2	-82.478	Y
657150	B04755	AC8CP58	WU	WU_4755	F	U	G	29 Feb 1996	Arriba, W bank Rio Changuinola	9.2	-82.478	Y
657151	B04756	AC8CP59	WU	WU_4756	M	A	Y	29 Feb 1996	Arriba, W bank Rio Changuinola	9.2	-82.478	Y
657152	B04757	AC8CP60	WU	WU_4757	M	A	Y	29 Feb 1996	Arriba, W bank Rio Changuinola	9.2	-82.478	Y
657153	B04758	AC8CP61	WU	WU_4758	F	U	G	29 Feb 1996	Arriba, W bank Rio Changuinola	9.2	-82.478	Y
657154	B04759	AC8CP62	WU	WU_4759	F	U	G	29 Feb 1996	Arriba, W bank Rio Changuinola	9.2	-82.478	Y

Table S2.2. Geographic and genetic distance between manakin populations. Geographic distance is measured in degrees and kilometers, residuals are measured in degrees, and genetic distance is Weir and Cockerham's F_{ST}.

Pop 1	Pop 2	FST	Distance	Distance-km	Residual	Bank comparison
EL	EM	0.00262	0.06667	7.407037	-0.00352	same
EL	EU	0.00571	0.203961	22.66007	-0.00325	same
EL	WL	0.013694	0.072061	8.005977	0.007447	opposite
EL	WM	0.009262	0.060663	6.739659	0.00325	opposite
EL	WN	0.012641	0.158114	17.56647	0.004623	opposite
EL	WS	0.009604	0.09093	10.10232	0.002969	opposite
EL	WU	0.005522	0.203642	22.62463	-0.00343	opposite
EM	EU	0.003244	0.139201	15.46523	-0.00439	same
EM	WL	0.009829	0.072066	8.006533	0.003582	opposite
EM	WM	0.005821	0.018631	2.069904	0.000674	opposite
EM	WN	0.008648	0.190031	21.11244	-2.81E-05	opposite
EM	WS	0.005309	0.085905	9.544046	-0.00122	opposite
EM	WU	0.002676	0.138733	15.41324	-0.00494	opposite
EU	WL	0.01475	0.196398	21.81982	0.005943	opposite
EU	WM	0.011393	0.15258	16.95164	0.003489	opposite
EU	WN	0.014596	0.314006	34.88607	0.003366	opposite
EU	WS	0.010006	0.201	22.3311	0.001104	opposite
EU	WU	0.003097	0.00166	0.184426	-0.0017	opposite
WL	WM	0.005548	0.053438	5.936962	-0.00032	same
WL	WN	0.004637	0.119828	13.31289	-0.00259	same
WL	WS	0.005382	0.018981	2.108789	0.000228	same
WL	WU	0.01123	0.195525	21.72283	0.00244	same
WM	WN	0.004391	0.171799	19.08687	-0.00391	same
WM	WS	0.003911	0.067535	7.503139	-0.00224	same
WM	WU	0.007358	0.151972	16.88409	-0.00053	same
WN	WS	0.003672	0.113006	12.55497	-0.00342	same
WN	WU	0.010179	0.313005	34.77486	-0.00103	same
WS	WU	0.006289	0.2	22.22	-0.00259	same

Table S2.3 AMOVA results partitioning variation within populations (i.e., sampling locations), between locations, and between riverbanks. The test was performed on samples from west of the Río Changuinola and testing for a riverbank effect of the Río Teribe.

Component	Sigma	% Variance Explained	P-Value
Within-population	1130.50	97.78	0.0001
Between-population	26.93	2.33	0.0001
Between-riverbank	-1.27	-0.11	0.5072

Table S2.4. Geographic and genetic distance between all-male samples of manakin populations. Geographic distance is measured in degrees and kilometers, residuals are measured in degrees, and genetic distance is Weir and Cockerham's F_{ST}.

Pop 1	Pop 2	FST	Distance	Distance-km	Residual	Bank comparison
EL	EM	0.003839	0.06667	7.407037	same	-0.00283
EL	EU	0.007516	0.203961	22.66004	same	-0.00224
EL	WL	0.014264	0.072061	8.006003	opposite	0.00747
EL	WM	0.009355	0.060663	6.739609	opposite	0.002818
EL	WN	0.01293	0.158114	17.56645	opposite	0.004201
EL	WS	0.009949	0.09093	10.10238	opposite	0.002731
EL	WU	0.006623	0.203642	22.6246	opposite	-0.00313
EM	EU	0.004657	0.139201	15.46522	same	-0.00365
EM	WL	0.010673	0.072066	8.006517	opposite	0.00388
EM	WM	0.006212	0.018631	2.069895	opposite	0.00062
EM	WN	0.009749	0.190031	21.11248	opposite	0.000302
EM	WS	0.00593	0.085905	9.54403	opposite	-0.00118
EM	WU	0.003842	0.138733	15.41324	opposite	-0.00445
EU	WL	0.016255	0.196398	21.81977	opposite	0.006665
EU	WM	0.012194	0.15258	16.95167	opposite	0.003589
EU	WN	0.016149	0.314006	34.88611	opposite	0.003914
EU	WS	0.011821	0.201	22.33114	opposite	0.002127
EU	WU	0.004773	0.00166	0.184426	opposite	-0.00044
WL	WM	0.005019	0.053438	5.937017	same	-0.00136
WL	WN	0.004656	0.119828	13.31292	same	-0.00321
WL	WS	0.006063	0.018981	2.108741	same	0.000463
WL	WU	0.011285	0.195525	21.72278	same	0.001714
WM	WN	0.004355	0.171799	19.08688	same	-0.00468
WM	WS	0.003697	0.067535	7.503149	same	-0.003
WM	WU	0.006829	0.151972	16.88405	same	-0.00176
WN	WS	0.003935	0.113006	12.55497	same	-0.00378
WN	WU	0.010444	0.313005	34.77482	same	-0.00177
WS	WU	0.006649	0.2	22.22	same	-0.00302

Table S2.5. AMOVA results partitioning variation within populations (i.e., sampling locations), between locations, and between riverbanks. The test was performed on a dataset containing only males.

Component	Sigma	% Variance Explained	P-Value
Within-population	1129.57	96.36	0.0001
Between-population	23.62	2.02	0.0001
Between-riverbank	19.10	1.63	0.5072

Appendix B. Supplementary material for Chapter 3

Feather analyses

Feather collection

The color quantification and biochemical analysis used feathers plucked from museum specimens of golden-collared manakin (*Manacus vitellinus*), white-bearded manakin (*M. manacus*), orange-collared manakin (*M. aurantiacus*), white-collared manakin (*M. candei*), and *M. candei* males with yellow collars due to introgression from *M. vitellinus* (YCC). I plucked five feathers from both the belly and collar region from six male specimens of each taxon. Museum specimens, housed at the U.S. National Museum of Natural History (USNM), were collected from a variety of locations and from a range of dates (Table S3.1).

Table S3.1. Summary of museum specimens sampled to perform feather analyses. YCC refers to a population of *M. candei* whose adult males have yellow collars due to introgression from *M. vitellinus*.

Species	**USNM**	**Locality**	**Year**
M. vitellinus	608987	Gamboa, Panama	1994
M. vitellinus	608136	Gamboa, Panama	1991
M. vitellinus	608135	Gamboa, Panama	1991
M. vitellinus	608985	Gamboa, Panama	1994
M. vitellinus	534054	Gamboa, Panama	1963
M. vitellinus	470154	Gamboa, Panama	1959
M. candei	608194	N bank Teribe 3 km SW Charagre, Quebrada Carbon, Panama	1991
M. candei	608195	N bank Teribe 3 km SW Charagre, Quebrada Carbon, Panama	1991
M. candei	614059	N bank Teribe 3 km SW Charagre, Quebrada Carbon, Panama	1991
M. candei	608197	N bank Teribe 3 km SW Charagre, Quebrada Carbon, Panama	1991
M. candei	614061	N bank Teribe 3 km SW Charagre, Quebrada Carbon, Panama	1991
M. candei	614062	N bank Teribe 3 km SW Charagre, Quebrada Carbon, Panama	1991
YCC	608161	3/5 km SE RR bridge E (=S) bank Changuinola River, Panama	1991
YCC	608159	3/5 km SE RR bridge E (=S) bank Changuinola River, Panama	1991
YCC	614037	3/5 km SE RR bridge E (=S) bank Changuinola River, Panama	1991
YCC	614038	3/5 km SE RR bridge E (=S) bank Changuinola River, Panama	1991
YCC	608167	3/5 km SE RR bridge E (=S) bank Changuinola River, Panama	1991
YCC	608168	3/5 km SE RR bridge E (=S) bank Changuinola River, Panama	1991
M. aurantiacus	448955	Soná, Rio San Pablo, La Isleta, Veraguas, Panama	1953
M. aurantiacus	448952	Soná, Rio San Pablo, La Isleta, Veraguas, Panama	1953
M. aurantiacus	448945	Soná, Rio San Pablo, La Isleta, Veraguas, Panama	1953
M. aurantiacus	448939	Soná, Rio San Pablo, La Isleta, Veraguas, Panama	1953
M. aurantiacus	448944	Soná, Rio San Pablo, La Isleta, Veraguas, Panama	1953
M. aurantiacus	448942	Soná, Rio San Pablo, La Isleta, Veraguas, Panama	1953
M. manacus	384069	Los Gorros, Colombia	1945

M. manacus	384068	Los Gorros, Colombia	1945
M. manacus	384066	Los Gorros, Colombia	1945
M. manacus	384067	Los Gorros, Colombia	1945
M. manacus	411825	Coloso, Colombia	1948
M. manacus	411826	Coloso, Colombia	1948

Light microscopy

NMJ examined each feather under reflected light before and after pigment extraction. The presence or absence of barbules along the barbs, and the presence of pigmentation in the barbs and barbules was noted for each species. Pictures were taken using an AmScope Microscope Digital Camera at a magnification of 1x and 4x. Photographs shown in figures below are at 4x magnification.

UV-vis Reflectance spectroscopy

NMJ performed UV-vis spectroscopy. Five feathers were overlapped and taped down flat, ventral side up, onto a black cardboard background. This was done to simulate how the feathers may have been placed on the bird during life, and to eliminate any background noise when sampling the feathers. Three measurements were taken in a dark room at a 90° angle of incidence from each set of feathers using an Ocean Optics USB4000 spectrophotometer and an Ocean Optics PX-2 pulsed xenon light source relative to a white reflectance standard (Labsphere Inc., North Sutton, NH, USA). Spectra were measured using OceanView v1.67 (Ocean Insight, FL, USA). A measurement was taken from the left, center, and right of the distal end of the overlapped group of feathers. Capturing multiple measurements from each plumage patch helps account for any variation in color within or between feathers. The resulting spectral data were analyzed and graphed using the pavo package v2.4.0 (Maia et al. 2019) in R v3.6.0 (R Core Team 2021).

Carotenoid extraction and HPLC analysis

Two feathers from each feather patch were sampled from each species. All feathers were cut approximately 1/3 of the way up from the base, removing the bottom portion of the feather that was heavily melanized, and saving the top 2/3 of the feather. Cut feather sections were washed with ethanol and hexane, and then weighed to the nearest 0.1 mg. The feather was then placed in 500 µL acidified pyridine and sealed in a microcentrifuge tube with nitrogen gas to prevent oxidation of any carotenoids (McGraw et al. 2005). NMJ and MJP then placed the samples on a 95 °C hot plate for 1 hour. Carotenoids were extracted from the pyridine with the addition of 250 µL H_20, 500 µL TBME, and 250 µL hexane (McGraw et al. 2002). The upper organic phase, containing carotenoids, was then removed. The solvent of the organic phase was evaporated to dryness under vacuum at 30 °C using a centrifugal concentrator. Dried carotenoid samples were resuspended in 80 µL of mobile phase (100% acetone) for HPLC analysis.

After pigment extraction from the belly and collar feathers, NMJ and MJP confirmed visually that all orange-yellow parts of the feathers were white, or very pale yellow. This indicated that the carotenoid extraction was successful. The barbules that were black remained black after pigment extraction (including the olive-green belly feathers of *M. vitellinus*), which indicated that melanin was not extracted and remained in the feathers. This also allowed us to confirm that melanin was not co-deposited in the barbs of the feathers because the orange-yellow feathers were white and not brown or black after extraction (e.g. red-winged blackbird) (McGraw et al. 2004).

10 µL of suspended carotenoid samples were injected on to a Sonoma C18 column (10 µm, 250 x 4.6 mm, ES Technologies, New Jersey, USA) fitted with a C18 guard cartridge using a Shimadzu Prominence HPLC system. Carotenoids were separated and eluted using mobile phases adapted from S.W. Wright et al. (1991) described briefly here. Mobile phases were A)

80:20 methanol: 0.5M ammonium acetate; B) 90:10 acetonitrile: H_2O; and C) ethyl acetate. A tertiary linear gradient was used that consisted of 100% A to 100% B over 4 min, then 80% C: 20% B over 14 minutes, then 100% B over 3 minutes, ending with 100% A over 11 minutes to re-equilibrate the column. A flow rate of 1 mL/min was used for a total active run lasting 32 minutes per sample. Multiple samples were run consecutively using an autosampler equipped with an automatic internal and external cleaning port to remove cross-contamination. NMJ and MJP visualized and detected carotenoid absorbance using a Prominence UV/Vis detector set to 450 nm. Carotenoids were quantified by comparison to calibration curves of authentic standards that included: astaxanthin, zeaxanthin, β-carotene, lutein, 3-hydroxy echinenone, and canthaxanthin. Pigment identity was confirmed by comparing the shape and retention time of peaks of feather extracts to carotenoid standards after HPLC and UV/Vis (see Figure S3.1 for representative chromatograms of standards and feather pigments). Carotenoid concentration was normalized by the dry weight of each feather sample, and we report carotenoid concentrations as μg carotenoid/mg feather dry weight.

Statistical analysis

MJP performed four sets of statistical analyses in R using linear models corrected for multiple comparisons using the 'emmeans' package v.1.4.5 (Lenth et al. 2023) and linear mixed effects models. The first analysis compared the concentration of lutein (square root transformed to achieve normality) in the belly or collar feathers among the five taxa included in this study. The second analysis compared the concentration of lutein in the belly versus the collar feathers of the three taxa which had yellow pigmentation in both feather patches (YCC, *M. vitellinus*, *M. aurantiacus*). The third analysis investigated the effect of increasing lutein concentration on color components obtained during reflectance spectroscopy of collar feathers only—to remove

the effect of barbule morphology present in belly feathers—using a mixed effects model that incorporated bird identify to account for non-independence of data within species. These components were saturation in the yellow wavelengths of light, UV reflectance saturation, carotenoid chroma, mean sample brightness, and peak sample wavelength hue. The fourth analysis compared the feather brightness (as measured by reflectance spectroscopy) of the collar feathers of each of the five taxa.

From each model analysis we report the estimated effect size (β: the difference between groups or the slope of the relationship between two variables), the confidence interval around the estimated effect size, and the associated p-value. All figures and graphs were built in R using the 'ggpubr' package v.0.2.1 (Kassambara 2023), and 'cowplot' package v.1.0.0 (Wilke 2020).

Presence and concentration of pigments

Based on comparison with analytical standards and carotenoid profiles from the literature, the only carotenoid detectable in the feathers for each of the species was lutein (Figure S3.1). The list of museum specimens and the date each was collected can be found in Table S3.1. The average mass-corrected concentration of lutein in collar feathers for each group were: *M. aurantiacus* 0.422 µg carotenoid/ mg feather, *M. vitellinus* 0.144 µg/ mg, YCC 0.163 µg/ mg, *M. candei* 0 µg/ mg, and *M. manacus* 0 µg/ mg. The adjusted average values for the belly feathers of each bird were: *M. aurantiacus* 0.118 µg/ mg, *M. vitellinus* 0.051 µg/ mg, YCC *M. candei* 0.098 µg/ mg, and white-collared *M. candei* 0.108 µg/ mg (*M. manacus* belly feathers contained no lutein).

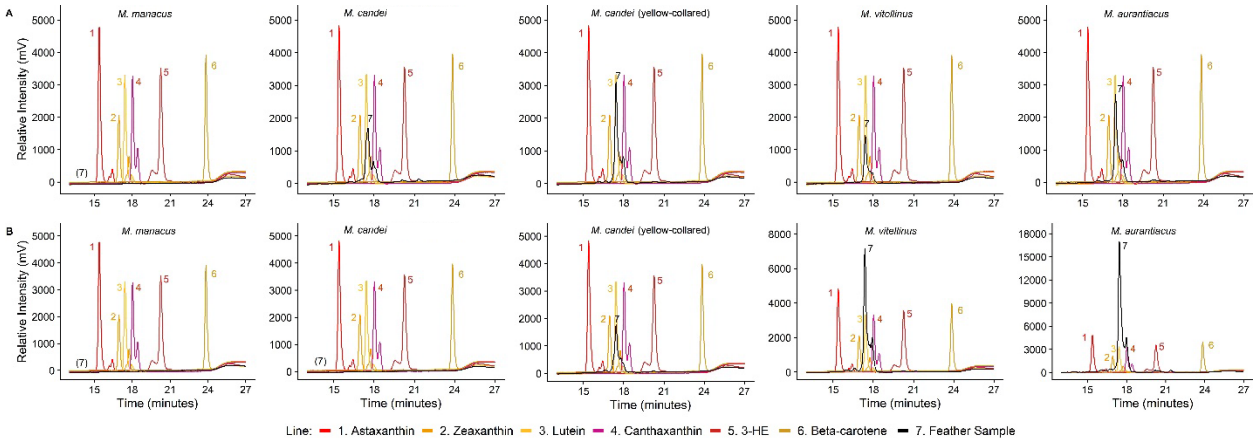

Figure S3.1. Representative HPLC chromatograms of pigment extractions detected at 450 nm using UV-vis. Row A (top) shows belly feather samples and row B (bottom) shows collar feather samples. Peaks are numbered by retention time except for the peak corresponding to the feather samples (this is shown as a black line for contrast). Each colored peak (1-6) corresponds to an authentic carotenoid standard used to identify and quantify feather pigments. If no peak was detected in a feather sample, the black baseline number is noted in parentheses (7). Carotenoid concentrations were quantified by a standard calibration curve for each of the six standards shown above.

In a comparison of lutein concentration in belly and collar feathers belonging to taxa that have both feather patches pigmented yellow (YCC, *M. vitellinus*, *M. aurantiacus*), lutein concentration in the belly feathers was lower than in the collar feathers. However, this was only statistically significant in *M. vitellinus* (β = -0.09, 95%CI: -0.18 to -0.002, $p < 0.05$) and *M. aurantiacus* (β = -0.31, 95%CI: -0.40 to -0.21, $p < 0.001$). Statistical comparison of the lutein concentration in belly and/or collar feathers among each of the five taxa in this study can be found in Table S3.2 and in Figure 3.1A. Notably, the YCCs did not significantly differ in the lutein concentration of either the belly or collar compared to its *M. vitellinus* (Belly: β = -0.08, 95%CI : -0.18 to 0.03, $p = 0.24$; Collar: β = -0.03, 95%CI : -0.17 to 0.12, $p = 0.98$). On average, the pigmented belly feathers had lower concentrations of lutein than the collar feathers. This difference may be due to the reduction in width observed in barbs of belly feathers relative to collar feathers in pigmented species (Figure 3.1).

Table S3.2. Results from statistical models contrasting lutein concentration among species' belly feathers (A), lutein concentration among species' collar feathers (B), feather brightness among species (C), lutein concentrations in species with yellow bellies and collars (D), and models estimating the relationship between lutein concentration and reflectance measurements estimated using the 'pavo' R package (E). Columns are as follows left to right: estimate of effect, standard error, degrees of freedom, t-value, p-value, confidence interval around estimate of effect. YCC refers to a population of *M. candei* whose adult males have yellow collars due to introgression from *M. vitellinus*.

A. Lutein Comparison - BELLY							
contrast	**estimate**	**SE**	**df**	**t.ratio**	**p.value**	**lower.CI**	**upper.CI**
M. vitellinus - YCC	-0.0755	0.0354	25	-2137	0.2365	-0.1794	0.0283
M. vitellinus - M. aurantiacus	-0.1149	0.0354	25	-3.251	0.0248	-0.2188	-0.0111
M. vitellinus - M. manacus	0.2261	0.0354	25	6.394	<0.0001	0.1222	0.3299
M. vitellinus - M. candei	-0.0934	0.0354	25	-2.641	0.0929	-0.1972	0.0105
YCC - M. aurantiacus	-0.0394	0.0354	25	-1.114	0.7975	-0.1432	0.0644
YCC - M. manacus	0.3016	0.0354	25	8.531	<0.0001	0.1978	0.4054
YCC - M. candei	-0.0178	0.0354	25	-0.504	0.9862	-0.1217	0.0860
M. aurantiacus - M. manacus	0.3410	0.0354	25	9.645	<0.0001	0.2372	0.4448
M. aurantiacus - M. candei	0.0216	0.0354	25	0.610	0.9722	-0.0823	0.1254
M. manacus - M. candei	-0.3194	0.0354	25	-9.035	<0.0001	-0.4232	-0.2156
B. Lutein Comparison - COLLAR							
contrast	**estimate**	**SE**	**df**	**t.ratio**	**p.value**	**lower.CI**	**upper.CI**
M. vitellinus - YCC	-0.0281	0.0491	25	-0.572	0.9780	-0.172	0.116
M. vitellinus - M. aurantiacus	-0.2773	0.0491	25	-5.651	0.0001	-0.421	-0.133
M. vitellinus - M. manacus	0.3648	0.0491	25	7.434	<0.0001	0.221	0.509
M. vitellinus - M. candei	0.3648	0.0491	25	7.434	<0.0001	0.221	0.509
YCC - M. aurantiacus	-0.2493	0.0491	25	-5.080	0.0003	-0.393	-0.105
YCC - M. manacus	0.3928	0.0491	25	8.005	<0.0001	0.249	0.537
YCC - M. candei	0.3928	0.0491	25	8.005	<0.0001	0.249	0.537
M. aurantiacus - M. manacus	0.6421	0.0491	25	13.085	<0.0001	0.498	0.786
M. aurantiacus - M. candei	0.6421	0.0491	25	13.085	<0.0001	0498	0.786
M. manacus - M. candei	0.0000	0.0491	25	0.000	1.000	-0.144	0.144
C. Brightness Comparison - COLLAR							
contrast	**estimate**	**SE**	**df**	**t.ratio**	**p.value**	**lower.CI**	**upper.CI**
M. vitellinus - YCC	-6.36668	4.2127	25	-1.51131	0.565017	-20.4933	8.507488
M. vitellinus - M. aurantiacus	-0.99005	4.2127	25	-0.23502	0.999275	-15.1167	13.88412
M. vitellinus - M. manacus	-22.3175	4.2127	25	-5.29768	0.000156	-36.4442	-7.44335
M. vitellinus - M. candei	-4.10449	4.2127	25	-0.97431	0.864138	-18.2311	10.76967
YCC - M. aurantiacus	5.37663	4.2127	25	1.276291	0.707597	-7.59292	18.34618
YCC - M. manacus	-15.9508	4.2127	25	-3.78637	0.006971	-28.9204	-2.98129
YCC - M. candei	2.262186	4.2127	25	0.536992	0.982545	-10.7074	15.23174
M. aurantiacus - M. manacus	-21.3275	4.2127	25	-5.06266	0.000283	-34.297	-8.35792
M. aurantiacus - M. candei	-3.11444	4.2127	25	-0.7393	0.945077	-16.084	9.855108

M. manacus - M. candei		18.21303	4.2127	25	4.323362	0.001841	5.243475	31.18258
D. Lutein Comparison - BELLY vs COLLAR by species								
contrast	**species**	**estimate**	**SE**	**df**	**t.ratio**	**p.value**	**lower.CI**	**upper.CI**
Belly - Collar	*M. vitellinus*	-0.0928	0.0447	30	-2.076	0.0466	-0.184	-0.0015
Belly - Collar	YCC	-0.0647	0.0447	30	-1.447	0.1581	-0.156	0.0266
Belly - Collar	*M. aurantiacus*	-0.30473	0.0447	30	-6.820	<0.0001	-0.396	-0.2135

E. Lutein effect on reflectance color components from pavo						
Dependent variable	**Independent variable**	**estimate**	**SE**	**lower.CI**	**upper.CI**	**p.value**
Yellow saturation (S1Yellow)	Lutein	0.07937	0.02549	0.02533	0.1334	6.69E-03
UV saturation (S1UV)	Lutein	-0.105	0.03187	-0.17256	-0.03745	0.00457
Carotenoid chroma (S1carotchroma)	Lutein	0.14257	0.0664	0.00181	0.283323	0.0474
mean brightness (b2meanbright)	Lutein	-2.87	6.977	-17.6612	11.92124	0.686
Peak Hue (H1peakwavhue)	Lutein	-15.60	13.658	-44.5541	13.35418	0.27

The effect of lutein concentration on reflectance measurements

MJP compared the concentration of lutein in each feather sample with the color values obtained in pavo from reflectance spectroscopy. The brightness (β = -2.87, 95%CI : -17.66 to 11.92, p = 0.69) and peak wavelength hue (β = -15.60, 95%CI : -44.55 to 13.35, p = 0.27) were not significantly affected by the concentration of lutein within the feathers. Interestingly, plumage brightness was previously shown to be associated with male mating success in *M. vitellinus* (Stein and Uy 2006a). Differences in brightness presumably arise from differences in the white microstructural background of yellow feathers (Shawkey and Hill 2005; Shawkey et al. 2006), but that was not investigated in this study. However, an increase in the concentration of lutein in each feather was associated with a statistically significant decrease in UV reflectance saturation (β = -0.11, 95%CI : -0.17 to -0.04, $p < 0.001$, see Figure S3.2). Additionally, an increase in lutein concentration was associated with a statistically significant increase in the carotenoid and yellow chroma component provided by pavo (Figure S3.2, Table S3.2).

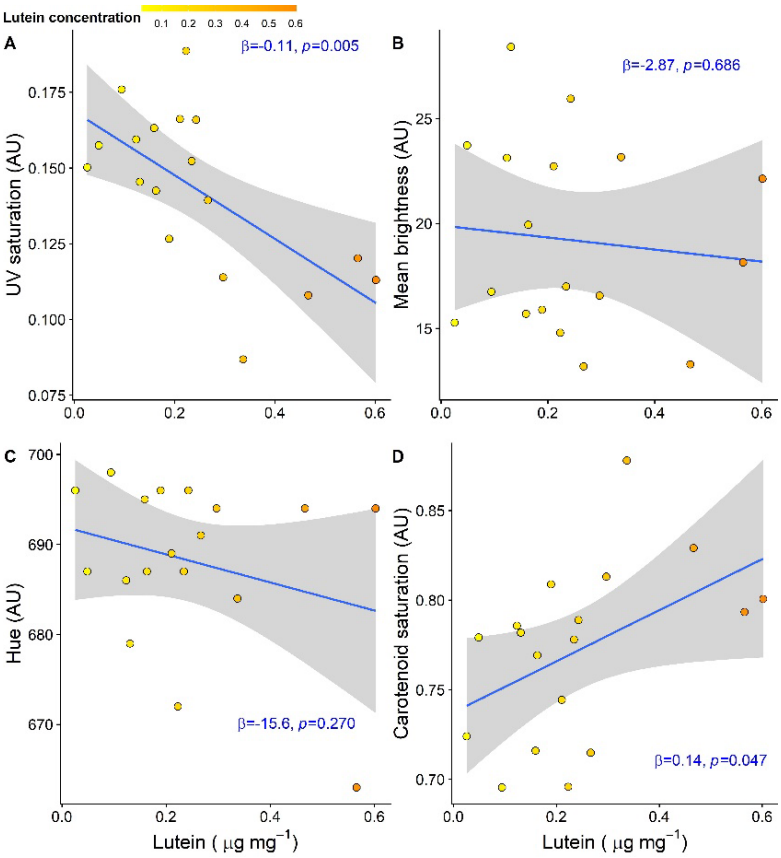

Figure S3.2. The effect of increasing feather lutein concentration (in μg lutein mg^{-1} feather tissue) on A) UV saturation, B) mean feather brightness, C) mean feather hue, and D) carotenoid chroma in pigmented feathers as measured by spectroscopy. All spectroscopy components are expressed in arbitrary units. The blue line shows the slope (β) and the grey shading represents the 95% confidence interval around the slope estimate. Each colored dot represents a single pigmented feather sample. White feathers, melanized feathers, and belly feathers (i.e., feathers with barbules) were not included in this analysis so the effect of lutein could be isolated from other effects.

Previous studies have shown that hue and saturation are often correlated with the concentration of carotenoids within a feather, while brightness is not (Saks et al. 2003). However, the impact that barb and barbule morphology might have on feather coloration is often understudied. Wider barbs can enhance the saturation of a feather containing carotenoids (Hill 1994). Since the deposition of carotenoids is often associated with morphological modifications, it seems likely that the morphology of the barb and barbules also plays an important role in producing the color variation observed between species (Brush 1990). NMJ observed significant

widening of barbs in the collar feathers of manakins containing lutein (Figure S3.3). In addition, collar feathers containing lutein did not have barbules attached to the distal third of the feathers. It is unclear if these feathers develop without barbules, or if the barbules are gradually lost throughout the season, as is the case for some other species of birds (e.g. white-winged crossbill) (Gill 1995). The widening of barbs and absence of barbules in these regions could be important for maximizing this behavioral signaling. Passerines are generally UVS sensitive (Lind et al. 2014); however, the *M. manacus* has previously been predicted to possess violet-sensitive vision based on the amino acid sequence of its SWS1 opsin gene (Aidala et al. 2012; Ödeen and Håstad 2013). This suggests that the manakins would be unable to see the UV peak produced by lutein in their orange-yellow feathers. This may place more importance on the yellow to orange color differences in the collar feathers.

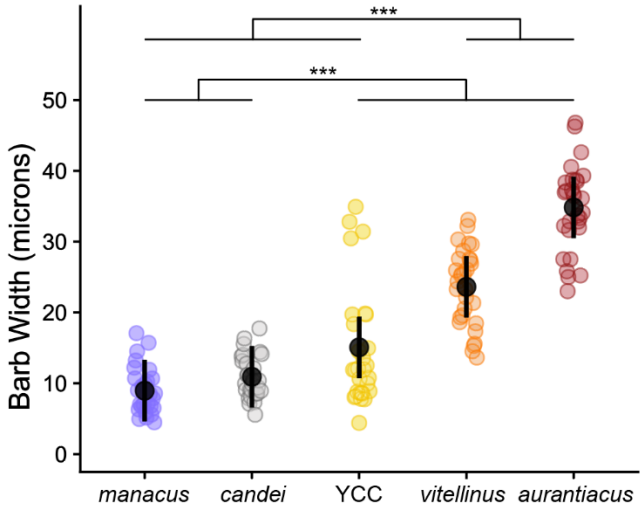

Figure S3.3. Barb width of manakin collar feathers. Pigmented feathers, including those of hybrids, had significantly wider barbs than unpigmented feathers. Feathers of the two pigmented species excluding hybrids also had significantly wider barbs than the other three taxa, hybrids included. YCC refers to a population of *M. candei* whose adult males have yellow collars due to introgression from *M. vitellinus*.

Resequencing and outlier analysis

Resequencing

Samples used for genome resequencing were collected in NW Panama (Table S3.3). All were male birds collected in 1980-90s and preserved as voucher specimens at USNM as round or flat study skins, or skeletal specimens. The samples consisted of 22 *M. candei* and 4 *M. vitellinus*. Two *M. candei* individuals were from a population ~10 km west of the Rio Changuinola (9.44 N, 82.45 W), called population 2 by Brumfield et al. (2001) and WN in Chapter 2; and twenty were from east and west banks of the Rio Changuinola, called populations 3 (N = 10) and 4 (N = 10) by Brumfield et al. (2001), WL and WL in Chapter 2, and WCC and YCC in this chapter. Previous studies indicated that male *M. candei* located east of the Rio Changuinola resembled *M. vitellinus* (i.e., possessing golden collar and olive green belly) in their adult plumage, and this was likely a result of limited genetic introgression from *M. vitellinus* (Parsons et al. 1993; Brumfield et al. 2001; Parchman et al. 2013; Long et al. in review). The four *M. vitellinus* individuals were collected from a population ~250 km east of the Rio Changuinola, ~300 km from the plumage or genomic contact zones (Table S3.3). Plumage form (i.e., coloration of collar and belly) of most of the birds were determined through study of the museum specimens. Study skins of five of the 26 resequenced birds were unavailable, but these birds were collected from populations distant from the plumage transition zone and hence their plumage could be inferred with confidence. DNA, extracted through a phenol-chloroform and ethanol precipitation method, were shipped by HCL to the McDonnell Genome Institute, Washington University, for library preparation and DNA sequencing (2 x 150 bp paired-end reads).

The average number of raw FASTQ reads per individual was 97.6 million (range: 64.4 – 123.6 million). HCL used Cutadapt implemented in TrimGalore v0.6.4 (https://github.com /FelixKrueger/TrimGalore) to conduct quality and adapter trimming (default parameters). The

average read length and number of reads per sample after quality trimming was 145.4 bp and 96.3 million (range: 63.7 – 121.6 million), respectively. HCL used bowtie2 v2.3.5 (Langmead and Salzberg 2012) to map trimmed and filtered reads to the reference genome of *M. vitellinus* (NCBI Genome accession ASM171598v3). Samtools v1.9 was then used to sort and index the bam files (Li et al. 2009). This reference genome (scaffold N50 = 17.9 Mbp, contig N50 = 290.6 Kb) was generated with a combination of Illumina HiSeq short reads and Pacific Biosystem long reads, and assembled with MaSuRCA v3.1.1 (Zimin et al. 2013). HCL used the latest genome annotations to date that was released on July 29, 2019 (*M. vitellinus* Annotation Release 103, NCBI RefSeq assembly accession GCF_00175985.3).

Across all samples, the average overall botwtie2 alignment rate was 94.6% (range: 91.5-96.5%). Next, HCL used GATK v3.8.1 to conduct variant calling (McKenna et al. 2010). Briefly, HCL used the HaplotypeCaller tool to conduct calling of single nucleotide polymorphisms (SNPs) and Indels simultaneously via local *de novo* assembly of haplotypes. This generated per-sample intermediate GVCF files, which were then combined with the GenotypeGVCFs tool to produce the final raw VCF (Variant Call Format) file. HCL then selected for SNPs and used the GATK tool VariantFiltration to conduct both SNP- and genotype-level filtering. HCL used the expressions “QD < 2.0 || FS > 60.0 || SOR > 3.0 || MQ < 40.0 || ReadPosRankSum < -3.0 || ReadPosRankSum > 3.0 || BaseQRankSum < -3.0 || BaseQRankSum > 3.0 || MQRankSum < -3.0 || MQRankSum > 3.0” and " DP < 5.0 || GQ < 13.0" for SNP- and genotype-level filtering, respectively. Finally, HCL retained SNPs that contained genotype information in at least 21 individuals (out of a total of 26), producing a filtered Variant Call Format (VCF) file containing 19.8 million SNPs. At the individual level, the proportion of SNPs with missing genotype information ranged from 2.9% to 22.5%.

Because a downstream analysis (ABBA-BABA analysis) required the use of an outgroup taxon to determined derived-ancestral allelic states, HCL downloaded Illumina HiSeq 2000 FASTQ reads from a whole genome sequencing project of *Pipra filicauda* (NCBI Run Accession: SRR6885520; 105.5 x 10^{12} bp, 349.2 x 10^{6} 150 bp paired-end reads). Following the above workflow, HCL mapped *P. filicauda* reads to the *M. vitellinus* reference genome and generated a separate VCF file with outgroup data.

To place *M. vitellinus* scaffolds in their approximate chromosomal positions, HCL conducted reference-guided chromosome-level scaffolding, using the genome of *Chiroxiphia lanceolata* (lance-tailed manakin) as the reference (NCBI Genome Accession GCA_009829145.1). This high-quality genome assembly consists of full chromosomes, including 33 autosomal macro- and micro-chromosomes, and two sex chromosomes (W and Z). HCL used RaGOO v1 (Alonge et al. 2019), which is based on the Minimap2 alignment software (Li 2016), and default parameters to conduct scaffolding. As expected, given the high level of synteny among bird species, the scaffolding process resulted in high confidence in terms of placing and orienting each *M. vitellinus* scaffold against *C. lanceolata* chromosomes (average positional confidence score = 77.8%, SD = 27.6%; average orientation confidence score = 98.2%, SD = 7.3%).

Table S3.3. Samples used for genome resequencing, and associated plumage, locality and sequencing information. †Historical population designations refer population number in Brumfield et al. (2001).

Species	Population	Sample ID	Throat plumage	Belly plumage	Historical population designations†	Collection locality	Latitude	Longitude	USNM no.	Avg. Sequencing depth	Proportion of missing SNPs (%)
M. candei	allo white-coll	Mc_1878	white	yellow*	2	Bocas del Toro; hills on S bank of Rio Sixaola	9º 27' N	82º 40' W	608193	11.5	6.9
M. candei	allo white-coll	Mc_4590	white	yellow	2	Bocas del Toro; hills on S bank of Rio Sixaola	9º 27' N	82º 40' W	608988	13.2	3.9
M. candei	WCC	Mc_1883	white	yellow	3	Bocas del Toro; N bank Rio Teribe	9º 22' N	82º 34' 50" W	608194	10.6	7.5
M. candei	WCC	Mc_1884	white	yellow	3	Bocas del Toro; N bank Rio Teribe	9º 22' N	82º 34' 50" W	608195	11.4	6.7
M. candei	WCC	Mc_1886	white	yellow	3	Bocas del Toro; N bank Rio Teribe	9º 22' N	82º 34' 50" W	614059	9.8	10.2
M. candei	WCC	Mc_1888	white	yellow	3	Bocas del Toro; N bank Rio Teribe	9º 22' N	82º 34' 50" W	608197	11.3	7.5

M. candei	WCC	Mc_1890	white (hints of yellow)	yellow	3	Bocas del Toro; N bank Rio Teribe	9º 22' N	82º 34' 50" W	608198	12.0	5.3
M. candei	WCC	Mc_1891	white (hints of yellow)	yellow	3	Bocas del Toro; N bank Rio Teribe	9º 22' N	82º 34' 50" W	614061	13.0	4.6
M. candei	WCC	Mc_1894	white	yellow	3	Bocas del Toro; N bank Rio Teribe	9º 22' N	82º 34' 50" W	608201	12.2	5.2
M. candei	WCC	Mc_1921	white (hints of yellow)	yellow	3	Bocas del Toro; N bank Rio Teribe	9º 22' N	82º 34' 50" W	608204	7.6	22.5
M. candei	WCC	Mc_1922	white	yellow	3	Bocas del Toro; N bank Rio Teribe	9º 22' N	82º 34' 50" W	614062	10.4	9.6
M. candei	WCC	Mc_1924	white	yellow	3	Bocas del Toro; N bank Rio Teribe	9º 22' N	82º 34' 50" W	608205	11.8	6.1
M. candei	YCC	Mc_1897	yellow	olive green	4	Bocas del Toro; S bank Changuinola River	9º 24' N	82º 31' W	608162	10.4	8.5
M. candei	YCC	Mc_1898	yellow	olive green	4	Bocas del Toro; S bank Changuinola River	9º 24' N	82º 31' W	614036	11.5	6.4
M. candei	YCC	Mc_1899	yellow	yellow-olive green intermediate	4	Bocas del Toro; S bank Changuinola River	9º 24' N	82º 31' W	608161	12.8	4.3
M. candei	YCC	Mc_1903	yellow	olive green	4	Bocas del Toro; S bank Changuinola River	9º 24' N	82º 31' W	608163	11.3	6.9
M. candei	YCC	Mc_1908	yellow	yellow	4	Bocas del Toro; S bank Changuinola River	9º 24' N	82º 31' W	608159	13.4	4.2
M. candei	YCC	Mc_1909	yellow	olive green	4	Bocas del Toro; S bank Changuinola River	9º 24' N	82º 31' W	614037	9.3	12.4
M. candei	YCC	Mc_1910	yellow	yellow-olive green intermediate	4	Bocas del Toro; S bank Changuinola River	9º 24' N	82º 31' W	614038	14.3	2.9
M. candei	YCC	Mc_1911	yellow	olive green	4	Bocas del Toro; S bank Changuinola River	9º 24' N	82º 31' W	614039	12.2	4.9
M. candei	YCC	Mc_1948	yellow	yellow-olive green intermediate	4	Bocas del Toro; S bank Changuinola River	9º 24' N	82º 31' W	608167	9.2	13.4
M. candei	YCC	Mc_1949	yellow	olive green	4	Bocas del Toro; S bank Changuinola River	9º 24' N	82º 31' W	608168	13.2	4.5
M. vitellinus	allo yellow-col	Mv_1857	yellow	olive green*	12	Canal Zone; Pipeline Road, near Gamboa	9º 7' 50" N	79º 42' W	614019	13.6	5.0
M. vitellinus	allo yellow-col	Mv_1864	yellow	olive green*	12	Canal Zone; Pipeline Road, near Gamboa	9º 7' 50" N	79º 42' W	614025	11.3	10.6
M. vitellinus	allo yellow-col	Mv_1874	yellow	olive green*	12	Canal Zone; Pipeline Road, near Gamboa	9º 7' 50" N	79º 42' W	608137	9.1	15.4
M. vitellinus	allo yellow-col	Mv_1876	yellow	olive green*	12	Canal Zone; Pipeline Road, near Gamboa	9º 7' 50" N	79º 42' W	614035	12.1	7.5

To conduct principal component analysis (PCA), HCL first used ANGSD v0.918 (Korneliussen et al. 2014) to generate filtered genotype posterior probabilities (command: -doMaf 1 -doMajorMinor 1 -SNP_pval 1e-6 -uniqueOnly 1 -remove_bads 1 -only_propoer_pairs 1 -C 50 – baq 1 -minMapQ 20 -minQ 13 -minMaf 0.05 -minind 21 -GL 1 -doGeno 32 -doPost 1). This created a genotype posterior probabilities output containing 13.1 million SNPs. Following this, ngsCovar v1 (Fumagalli et al. 2013) was used to randomly subsample 1 million SNPs to reduce linkage disequilibrium, and to calculate the covariance matrix among individuals. Eigenvector decomposition was then conducted in R to calculate the principal components (R Core Team 2021). The first five principal components explained 40.89% of the

total genetic variation. PC1 demarcated the two species while PC5 separated YCC from WCC and allopatric *M. candei*. (Figure S3.4).

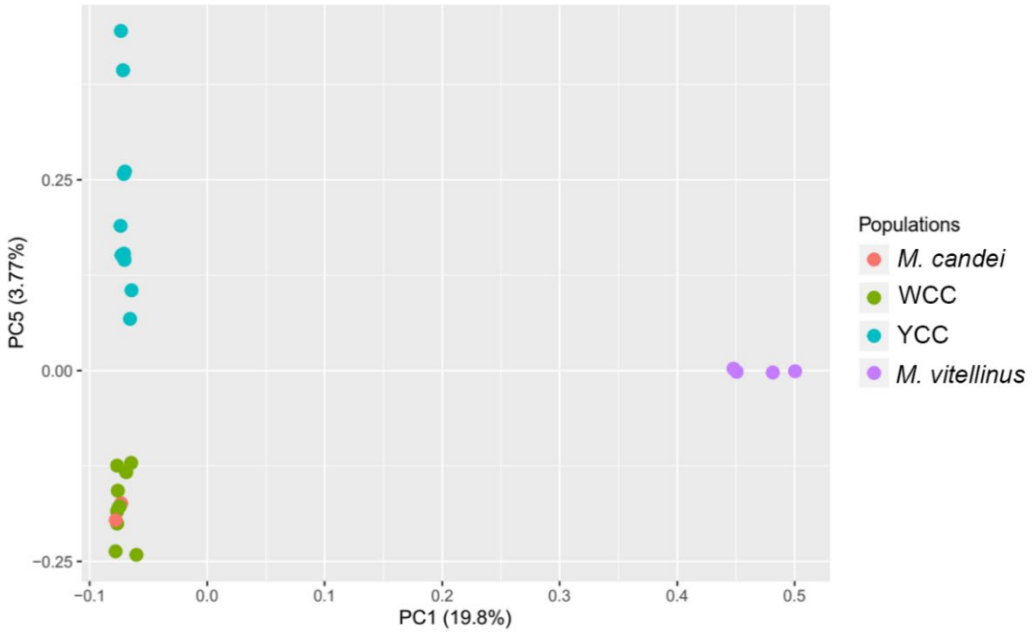

Figure S3.4. Plot of principal component axes 1 and 5, with each filled circle representing one individual. Axis 1 separates *M. vitellinus* from *M. candei* populations. Axis 5 accounts for variation between white-collared *candei* and yellow-collared *candei*.

Outlier Analysis

To locate genomic regions underlying plumage color difference between populations, I calculated differentiation and introgression statistics in sliding windows along genomic scaffolds. Because any single population genetic statistic may be affected by confounding factors, I used two different analysis methods to assess both differentiation and introgression (Cruickshank and Hahn 2014; Burri 2017). I calculated these statistics in non-overlapping windows of 10 kb. I omitted all scaffolds smaller than 10 kb, which accounted for 0.25% of the total genome length. I identified focal regions potentially underlying the plumage color difference by selecting windows that fall above the 99.9th percentile of the differentiation and introgression statistics (details described below). The avian Z Chromosome has a smaller

effective population size than autosomes (macro- and micro-chromosomes) and as a result, differentiation and introgression statistics behaved differently on Z than on autosomes (Figure S3.5). Therefore, I calculated Z Chromosome 99.9th percentile thresholds separately from autosome thresholds.

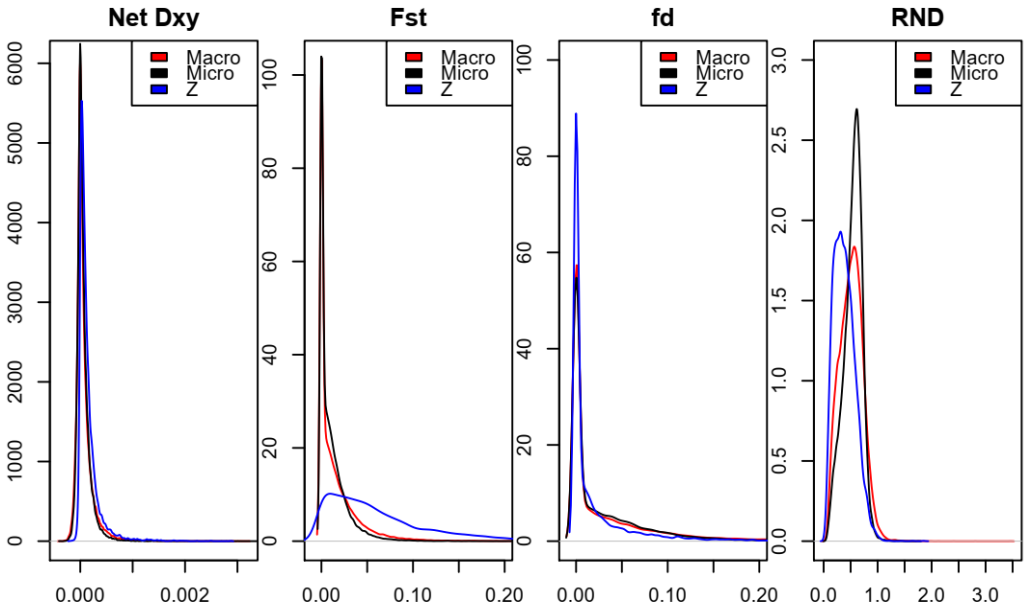

Figure S3.5. Density plot of differentiation (between white- and yellow-collared *M. candei* populations, net D_{XY} and F_{ST}) and introgression statistics (from *M. vitellinus* into yellow-collared *M. candei* populations, f_d and RND) in 10 kb genomic windows across macro-chromosomes (chromosome 1-5), micro-chromosomes (other autosomes), and the Z chromosome.

Genomic regions underlying the plumage color differences between *M. vitellinus* and *M. candei* should show substantial genetic differentiation between WCC and YCC populations on either side of the river (Populations 3 and 4, respectively, in Table S3.3). I used the popgenWindows.py script (github.com/simonhmartin/genomics_general) to calculate F_{ST} (Weir and Cockerham 1984) and sequence divergence, D_{XY} (Nei 1987) in between the two populations in 10 kb windows. F_{ST} is the proportion of total genetic variation accounted for by differences between populations, while D_{XY} is the average of the pairwise sequence divergence between population samples. Because D_{XY} is heavily influenced by nucleotide diversity, π, (Pearson's r =

0.984, Figure S3.6A) I instead used net D_{XY} (Nei and Li 1979), which I calculated by subtracting the mean π of the two populations from D_{XY} (Figure S3.6B).

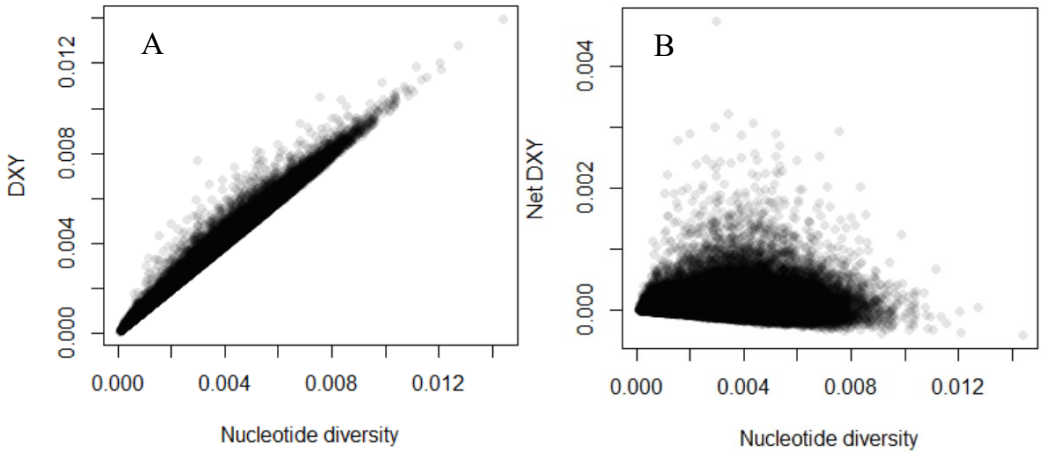

Figure S3.6. Relationships between average nucleotide diversity of white-and yellow-collared *M. candei* (populations 3 and 4, respectively, from Table S3.3) and two differentiation statistics, D_{XY} and net D_{XY}. The calculations were based on non-overlapping sliding windows of 10 kb.

Because the plumage differences between WCC and YCC are likely due to introgression of these traits from *M. vitellinus* into YCC (Parsons et al. 1993; Brumfield et al. 2001), HCL and I calculated introgression statistics to identify genomic regions in YCC that originated in *M. vitellinus*. Genomic regions underlying the plumage color differences should show signatures of both differentiation and introgression. HCL and I calculated f_d, which is a modified version of the ABBA-BABA D statistic intended to be applied to small genomic windows (Martin et al. 2015), using the ABBABABAwindows.py script (github.com/simonhmartin/genomics_general). f_d is an estimator of the proportion of a genomic region that is shared due to introgression between populations P2 and P3 in a set of populations with the relationship (((P1, P2), P3), O). f_d is a more sensitive and less biased statistic than D when applied to small genomic regions (Martin et al. 2015), and unlike F_{ST} and D_{XY}, f_d is not sensitive to local recombination rate variation since it depends on the ratio of various allelic states across a tree, rather than measures of genetic diversity (Booker et al. 2020). In these calculations, we used P1 = WCC (n = 10), P2 =

YCC (n = 10), P3 = *M. vitellinus* (n = 4), and the outgroup was *Pipra filicauda*. We omitted windows with fewer than 100 biallelic SNPs used to calculate f_d, as recommended by the author.

In addition to f_d, HCL and I estimated the relative node depth (RND) of the split between WCC and YCC to the split between YCC and *M. vitellinus* by calculating D_{XY} between the former two populations ÷ D_{XY} between the latter two (Feder et al. 2005; Lopes et al. 2016). Assuming a consistent substitution rate across lineages, values above one represent genomic windows where the divergence between YCC and *M. vitellinus* is more recent than the yellow-collared/white-collared *M. candei* divergence, indicating introgression.

A total of 266 autosomal (out of 91,913) and 26 Z chromosome (out of 7,079) 10 kb windows were considered 99.9th percentile outliers for at least one of the four summary statistics. A substantial proportion of these windows were flagged as outliers by two or more summary statistics (autosomes: 32.3%; Z chromosome: 23.1%). Among the windows flagged by two summary statistics (n = 75), the majority were flagged by either the two introgression statistics, f_d and RND (autosomes: 37 out of 75; Z chromosome: 4 out of 6), or the two differentiation statistics, F_{ST} and net D_{XY} (autosomes: 36 out of 75; Z chromosome: 1 out of 6). The fact that outlier windows for introgression statistics did not often overlap with differentiation statistics outliers suggests that high differentiation (between white- and yellow-collared *M. candei*) of some windows might have arisen from processes other than introgression (from *M. vitellinus* into yellow-collared *M. candei*), including local selection or drift in one of the two *M. candei* populations after their lineages diverged or increased F_{ST} or net D_{XY} due to low π and/or recombination rates (Booker et al. 2020). Nevertheless, a number of autosomal outlier windows were supported by three or all four summary statistics, indicating these were strong candidates for windows that contain loci that underlie the plumage introgression (Figure S3.7).

Additionally, I identified sites that fit the expected allele frequency pattern from introgressed regions responsible for the plumage differences: sites that were fixed for different alleles between allopatric *M. candei* and *M. vitellinus* populations and with a ≥ 80% *M. candei* allele frequency WCC and ≥ 80% *M. vitellinus* allele frequency in YCC. These sites (termed dSNPs) have the highest density in outlier autosomal windows supported by all four summary statistics (mean = 8.2 per 10 kb window; Figure S3.7A).

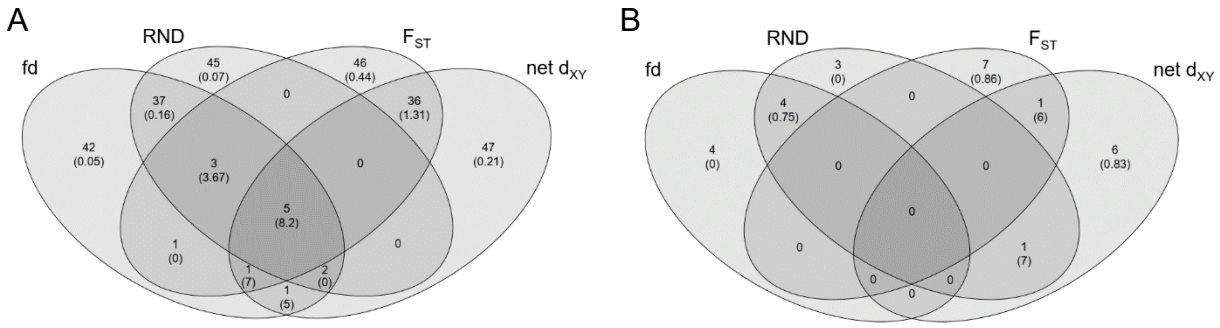

Figure S3.7. Venn diagram showing the number of 10 kb outlier windows supported by 1-4 summary statistics in (A) autosomes and (B) Chromosome Z. Numbers in parentheses represent the average number of dSNPs per 10 kb window of each category.

To facilitate the inspection of gene content of genomic regions that received strong support from window-based analyses, HCL selected focal windows based on the following approach. An autosomal window was considered a focal window if it was marked as a 99.9th percentile outlier by at least three of the four summary statistics (num_outliers ≥ 3). In addition, the rollmean function of the R package zoo (Zeileis et al. 2023) was used to calculate centered moving average of num_outliers; for each window, the average of its num_outliers and those of the two windows that were immediately up or downstream (MAV3) were calculated. An autosomal window was considered a focal window if its num_outliers ≥ 3 or MAV3 ≥ 1. The use of moving averages as a criterion for identifying focal windows provided for the identification of

genomic regions of interest where outlier windows for the various introgression/differentiation statistics were not exactly coincident but could be found in adjacent windows.

Using these criteria, we found a total of 74 focal windows. HCL and I further organized the focal windows into 24 genomic neighborhoods where focal windows were contiguous or no more than 1 Mb (100-window length) from each other (Table S3.4). These genomic neighborhoods were found in six autosomes. They each spanned 10 kb to 960 kb, containing zero to eight *ab initio* annotated protein coding genes. Three such genomic neighborhoods stood out as being highly prominent in that they each contained one (genomic neighborhood 11) or two (genomic neighborhoods 9 and 19) 10 kb windows that were outliers for all four summary statistics (Table S3.4).

Table S3.4. Genomic neighborhoods comprising blocks of focal windows (10 kb) separated by less than 1 Mb and genes that lie within or intersect with these neighborhoods. Genes shown in bold were adjacent to or contained 10 kb focal windows that were determined as outliers by all four summary statistics.

No	Chrom	Scaffold	Start	End	Length	Out Ws[1]	MAV Ws[2]	Genes
1	Chr 1	NW_021940813.1	25040001	25060000	20kb	0	2	FHL2
2	Chr 1	NW_021940208.1	24140001	24160000	20kb	0	2	
3	Chr 1	NW_021940208.1	25920001	25960000	40kb	1	4	LOC108639407
4	Chr 1A	NW_021940682.1	9040001	9080000	40kb	1	3	CHRM2
5	Chr 1A	NW_021940682.1	32830001	32860000	30kb	0	3	CAND1
6	Chr 2	NW_021939396.1	3010001	3250000	240kb	0	3	DENND3, LOC108640223, PTK2
7	Chr 2	NW_021939396.1	5320001	5340000	20kb	0	2	
8	Chr 2	NW_021939396.1	9770001	9860000	90kb	1	6	
9	Chr 2	NW_021939396.1	16860001	17550000	690kb	4	14	TMEM74, EMC2, LOC108640531, LOC108640531, LOC108640532, **EIF3E, RSPO2, ANGPT1**
10	Chr 2	NW_021939396.1	31250001	31390000	140kb	0	5	STAU2, RDH10, RPL7
11	Chr 2	NW_021939396.1	32770001	32800000	30kb	1	3	**SLCO5A1**
12	Chr 2	NW_021939396.1	49260001	50220000	960kb	0	4	DLGAP1, AKAIN1, ZBTB14,

								EPB41L3, TMEM200C, ARHGAP28, LAMA1
13	Chr 2	NW_021939256.1	10160001	10170000	10kb	0	1	
14	Chr 2	NW_021939256.1	12560001	12580000	20kb	0	2	CUNH7orf57, LOC103756761 (myosin-6-like)
15	Chr 2	NW_021940651.1	3830001	3850000	20kb	0	2	
16	Chr 3	NW_021940604.1	42710001	42730000	20kb	0	2	KHDRBS2
17	Chr 3	NW_021938895.1	15770001	15790000	20kb	0	2	TPO
18	Chr 19	NW_021940460.1	2650001	2660000	10kb	0	1	LOC103759492 (claudin-3-like), LOC115307618
19	Chr 24	NW_021940545.1	5530001	5670000	140kb	3	13	DIXDC1, DLAT, NKAPD, SDHD, IL18, TEX12, **BCO2**, PTS

[1] number of 10 kb windows satisfying the number of outliers criterion (num_outliers ≥ 3)
[2] number of 10 kb windows satisfying the moving average criterion (MAV3 ≥ 1)

One focal window in genomic neighborhood 9, (Table S3.4, Figure S3.8) with outliers in all four statistics calculated was located between the genes *EIF3E* and *RSPO2*, and it might contain *cis*-regulatory element(s) of one or both of these two genes. *EIF3E* (Eukaryotic Translation Initiation Factor 3 subunit E) is involved in initiation and regulation of protein synthesis by organizing the interactions of ribosomes and initiation factors (Lee et al. 2015). A closely related protein, *EIF2S*, which is also involved in the initiation of protein synthesis, was found to relate significantly with plumage color variation in two *Setophaga* warbler species, along with two adjacent genes *ASIP* and *RALY* (Wang et al. 2020). These two warbler species (*S. occidentalis* and *S. townsendii*) have different amounts of melanin-based coloration in their cheek, crown, flank and breast. *EIF2S2* was also found to be differentially expressed in darker melanocytes derived from Europeans with different skin colors (Liu et al. 2015a). *RSPO2* (R-Spondin 2), on the other hand, functions as an enhancer of the *Wnt* signaling pathway through the inhibition of Ubiquitin E3 ligases, and the pathway is known to be involved in the control of feather bud growth and patterning (Chang et al. 2004; Widelitz et al. 2019).

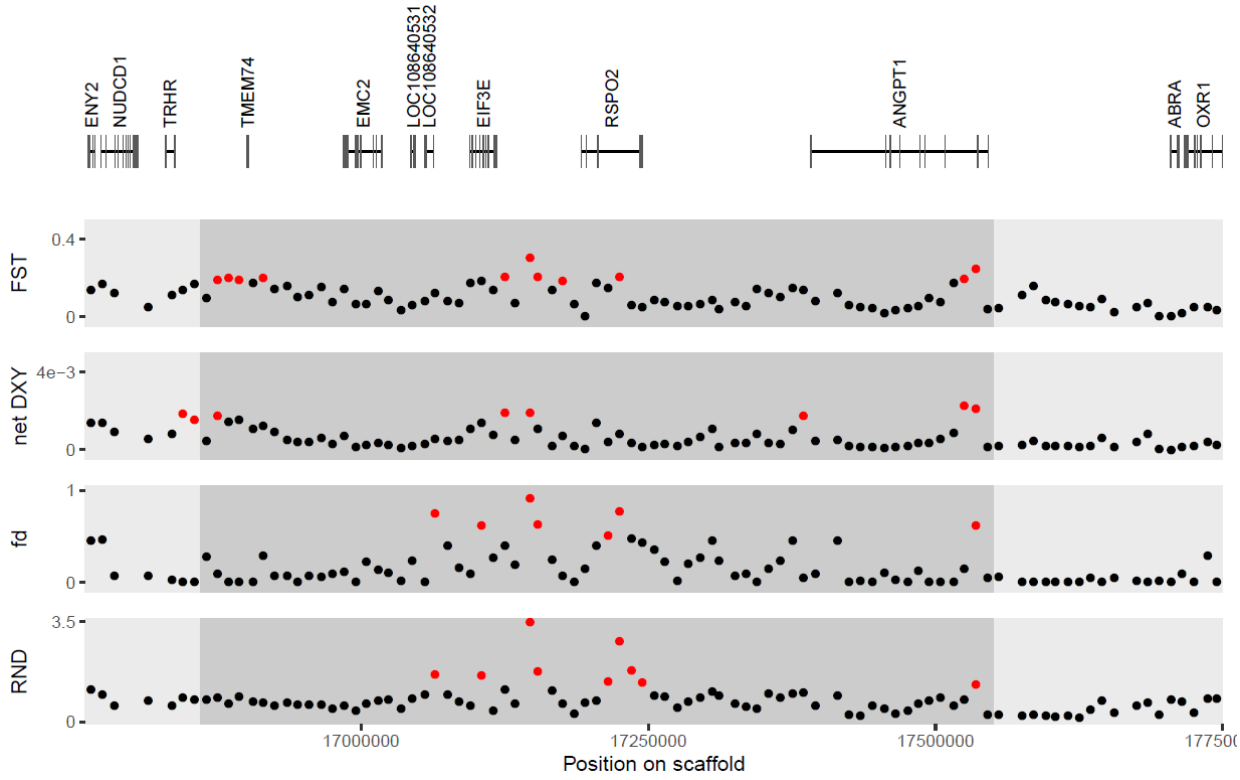

Figure S3.8. Differentiation and introgression statistics in and around genomic neighborhood 9 (Chromosome 2, scaffold NW_021939396.1, 16860001-17550000 bp). Differentiation (top two panel) and introgression statistics (bottom two panels) are plotted in 10 kb windows. 99.9th percentile outlier windows are shown in red. The gray highlighted region is the genomic neighborhood comprising focal windows separated by less than 1 Mb. The top panel shows genes with vertical bars representing exons.

These two genes were associated with a genomic region roughly 200 kb long that shows clear signs of introgression from *vitellinus* into YCC within it (Figure S3.9). This region has been broken up through recombination with parental *candei* DNA or involves two to three separate introgression blocks.

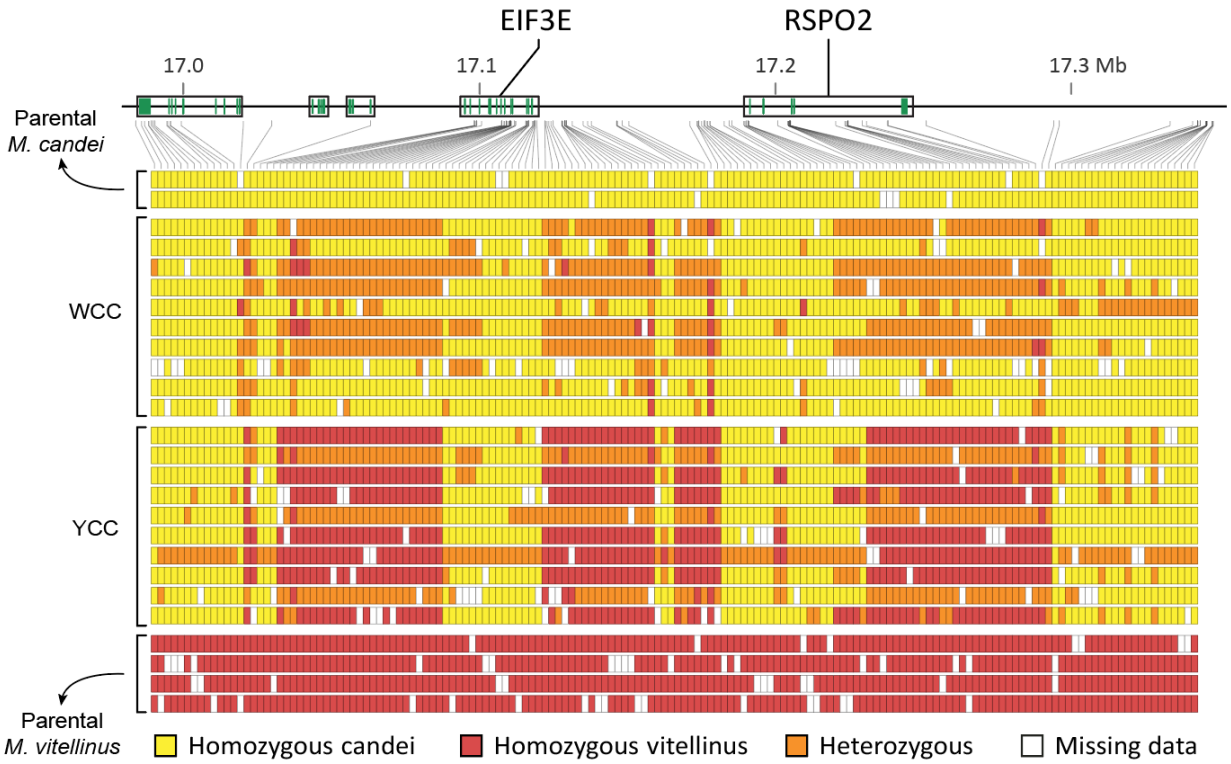

Figure S3.9. Introgression blocks in yellow-collared vs. white-collared *M. candei* (YCC and WCC, respectively). Positions indicate location on scaffold NW_021939396.1. SNPs represented on the figure are only those fixed for different alleles between parental *vitellinus* (max two missing genotypes) and parental *candei* (max one missing genotype).

The other focal windows with strongest support were two adjacent windows located in genomic neighborhood 19 on Chromosome 24 (Table S3.4). The two focal windows were within the *BCO2* (Beta-Carotene Oxygenase 2) gene (Figure S3.10). dSNPs were clustered up- and downstream of the gene and in its largest intron (Figure S3.11). *BCO2* codes for an enzyme responsible for metabolism of carotenoids (Kiefer et al. 2002) and has broad substrate specificity (dela Seña et al. 2016). In mice, it is localized in the mitochondria (Amengual et al. 2011) and protects against oxidative stress in mice (Amengual et al. 2011), zebrafish, and humans (Lobo et al. 2012). *BCO2* has been implicated in several cases of yellow/white polymorphism. Loss-of-function mutations have resulted in yellow coloration to mammal fat (Berry et al. 2009; Våge and Boman 2010; Strychalski et al. 2015), and a regulatory change to *BCO2* expression has resulted in domestic chicken skin being yellow rather than gray, as is found in wild junglefowl

(Eriksson et al. 2008). Most interestingly, *BCO2* has been implicated in bird plumage polymorphisms, as well. Differentiation upstream of *BCO2* is associated with plumage differences between blue-winged warblers, which are mostly yellow, and golden-winged warblers, which are mostly gray (Toews et al. 2016). An amino acid substitution in *BCO2* is responsible for carotenoid coloration changes in canary bills (Gazda et al. 2020b), and trans-regulation of *BCO2* expression is responsible for sexual dichromatism in canaries and related species (Gazda et al. 2020a). Finally, introgression in and around the *BCO2* genomic region is implicated in color differences among *Setophaga* warblers (Baiz et al. 2021).

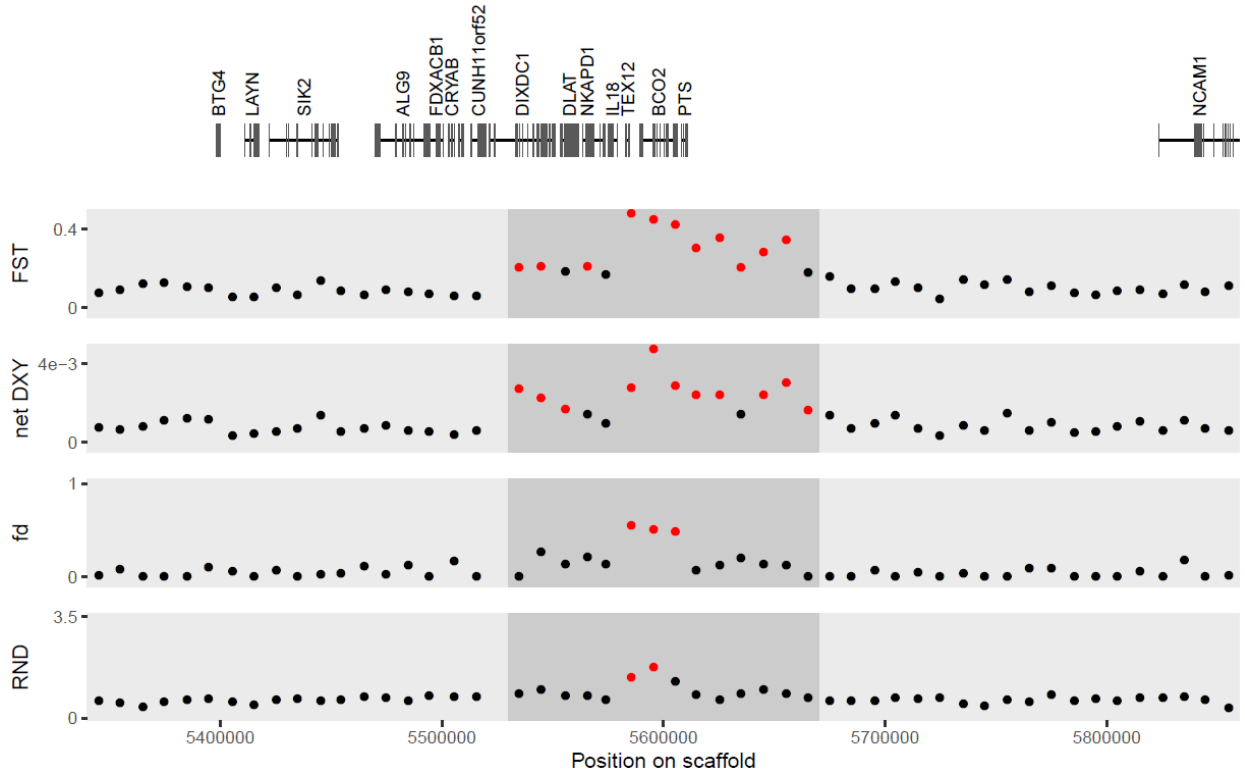

Figure S3.10. Differentiation and introgression statistics in and around genomic neighborhood 19 (Chromosome 24, scaffold NW_021940545.1, 5530001-5670000 bp). Differentiation (top two panels) and introgression statistics (bottom two panels) are plotted in 10 kb windows. 99.9th percentile outlier windows are shown in red. The gray highlighted region is the genomic neighborhood comprising focal windows separated by less than 1 Mb. The top panel shows genes with vertical bars representing exons.

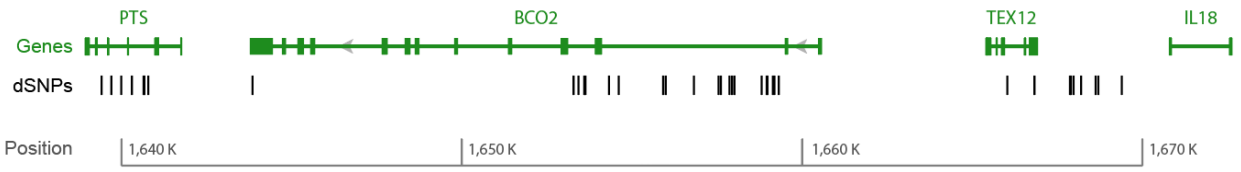

Figure S3.11. Concentration of dSNPs nearby and within *BCO2*.

Together, these results and those of previous studies provide strong evidence that *BCO2* is a common regulator of carotenoid coloration in birds. The results additionally suggest that this gene is principally responsible for the yellow-white collar dichromatism between golden-collared (*M. vitellinus*) and white-collared manakins (*M. candei*).

Two WCC individuals were heterozygous across the *BCO2* region (Figure 3.2K), indicating that introgression has partially penetrated into this population. However, no fully yellow-collared males have been found there despite repeated population sampling (MJB, *personal obs.*). It therefore appears that the yellow-collared phenotype is recessively inherited.

Ancient *BCO2* gene flow

I prepared WGS libraries for nine additional individuals to encompass the major lineages within *Manacus*, including three *M. aurantiacus*, three *M. manacus* from east of the Andes (*cis*-Andean), and three *M. manacus* from west of the Andes (*trans*-Andean) (Table S9.1). The libraries were sequenced by Novogene Corp. on one Illumina HiSeq lane, producing 217M total reads, averaging 23.8M reads per sample. Reads were trimmed using Cutadapt implemented in TrimGalore v0.6.4 and aligned to the *M. vitellinus* reference genome using bwa v0.7.1 (Li 2013). I marked duplicates using Picard v.2.20 MarkDuplicates (http://broadinstitute.github.io/picard/). I followed the GATK best practices workflow, including to produce and filter a VCF file, then use the filtered VCF to apply a recalibration table to the original bam files using GATK v3.8.1.0 (McKenna et al. 2010). The terms I used for VCF filtering were "QD < 2.0 || FS > 60.0 || SOR >

3.0 || MQ < 40.0 || ReadPosRankSum < -3.0 || ReadPosRankSum > 3.0 || BaseQRankSum < -3.0 || BaseQRankSum > 3.0 || MQRankSum < -3.0 || MQRankSum > 3.0" and "DP < 4.0 || DP > 45.0 || GQ < 3.0," followed by a filter to remove indels and sites missing in more than five out of nine individuals in VCFtools v0.1.16.

Table S3.5. Sample information for ancient *Manacus* gene flow analyses

Genus	Species	Subsp	Institution	Tissue Num	Collection location	Andes
Manacus	manacus	interior	ANSP	1589	Morona-Santiago, Ecuador	cis-Andean
Manacus	manacus	interior	ANSP	1505	Morona-Santiago, Ecuador	cis-Andean
Manacus	manacus	interior	ANSP	1421	Morona-Santiago, Ecuador	cis-Andean
Manacus	manacus	bangsi	LSU	12013	Esmeraldas, Ecuador	trans-Andean
Manacus	manacus	bangsi	ANSP	2394	Esmeraldas, Ecuador	trans-Andean
Manacus	manacus	bangsi	ANSP	2407	Esmeraldas, Ecuador	trans-Andean
Manacus	aurantiacus		LSU	16097	Puntarenas, Costa Rica	NA
Manacus	aurantiacus		LSU	16096	Puntarenas, Costa Rica	NA
Manacus	aurantiacus		LSU	16105	Puntarenas, Costa Rica	NA

I haphazardly chose two "control" genes on Chromosome 24 similar in size to *BCO2* and with no known connection to coloration, *DCPS* and *TBCEL*. I identified genomic regions to use for building gene trees by anchoring the ends of the regions of interest in exons of flanking genes to aid sequence alignment. I used a much shorter sequence for the *BCO2* gene tree (48 kb, from 26 kb upstream to 5 kb downstream) than the control trees (306 kb and 384 kb, respectively) because of the likelihood that recombination has reduced signals of shared ancestry that may have been present if introgression occurred at *BCO2*.

Using bam files from each individual, including two *M. candei* and four *M. vitellinus* whole genome resequencing samples used in the above analyses, I produced a single consensus sequence per individual using Samtools v1.17 consensus (Li et al. 2009) then aligned the sequences using Mafft v7.407 (Katoh and Standley 2013) To facilitate tree rooting, I included

the corresponding genomic regions from the reference genomes of *Pipra filicauda* (Accession ASM394559v2) and *Chiroxiphia lanceolata* (Accession bChiLan1.pri) in the alignments.

Finally, I used IQ-Tree v2.1.3 (Minh et al. 2020) to produce gene trees from each alignment with 10,000 bootstrap replicates. The resulting trees were visualized using the Interactive Tree of Life v6 (Letunic and Bork 2021) and rooted at the midpoints.

The two control trees largely recapitulated the phylogeny of the genus from Harvey et al. (2020). On the *BCO2* gene tree, *M. aurantiacus* and *M. vitellinus* were sister to one another, indicating more recent shared ancestry in that region of the genome. The branch including those two species was sister to *M. candei*, which is the location of *M. aurantiacus* in the phylogeny of the genus. If ancient gene flow is responsible for the observed patterns, the two species sharing gene flow should occupy the location on the tree of the "donor" species, since evolution of the gene would have followed the normal evolutionary trajectory of the "donor" species before subsequently spreading into the "recipient" species. Therefore, the results support gene flow from *M. aurantiacus* into *M. vitellinus* at *BCO2* but not at other locations on Chromosome 24.

Next, to place the evidence of gene flow at *BCO2* in the context of genome-wide signals of introgression between *M. aurantiacus* and *M. vitellinus*, I calculated ABBA-BABA D-statistics. To produce a VCF file for this analysis, I used the recalibrated bam files from the above analysis as inputs for GATK HaplotypeCaller and CombineGVCFs, then filtered using the terms: "QD < 2.0 || FS > 60.0 || SOR > 3.0 || MQ < 40.0 || ReadPosRankSum < -3.0 || ReadPosRankSum > 3.0 || BaseQRankSum < -3.0 || BaseQRankSum > 3.0 || MQRankSum < -3.0 || MQRankSum > 3.0" and "DP < 4.0 || GQ < 3.0". Finally, I filtered out indels and any sites missing in more than 10 out of 15 individuals using VCFtools.

ABBA-BABA statistics require a four-species tree. To maximize power to detect signals of introgression, I used the combination of study taxa with the largest sample size: in the structure (((P1,P2),P3,)P4), I used *trans*-Andean *M. manacus* as P1, *M. vitellinus* as P2, *M. aurantiacus* as P3, and *cis*-Andean *M. manacus* as P4. I used the genomics_general package (https://github.com/simonhmartin/genomics_general) to calculate f_d across the genome in 10 kb windows (Martin et al. 2015). I changed values of f_d to zero in windows where D was negative, where f_d was negative, or where f_d was greater than one, as recommended by the author. Removing windows with fewer than 100 sites used to calculate f_d is recommended to reduce stochastic variation in f_d (https://github.com/simonhmartin/genomics_general, Figure S3.12A), but this cutoff was not feasible for this dataset (Figure S3.12B). Instead, I used a 50-site cutoff.

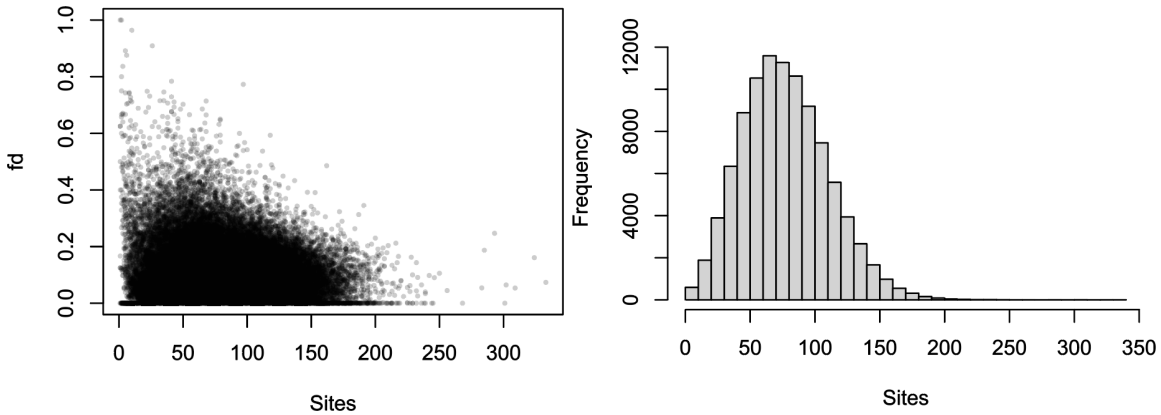

Figure S3.12. Information used to determine sites cutoff in fd analysis. A. relationship between sites used to calculate f_d and values of f_d in 10 kb genomic windows. B. Histogram of sites used to calculate fd.

One 10 kb window upstream from the start of *BCO2* was among the 99.9% outliers in f_d across the genome. This window had the fifth-highest f_d value in the genome out of 77.7k windows after filtering, and it overlapped with the introgressing block of DNA from *vitellinus* into *candei* (Figure 3.2K).

The code for this chapter is available at https://github.com/kfpbennett/color_genes.

References

Abolins-Abols, M., E. Kornobis, P. Ribeca, K. Wakamatsu, M. P. Peterson, E. D. Ketterson, and B. Milá. 2018. Differential gene regulation underlies variation in melanic plumage coloration in the dark-eyed junco (*Junco hyemalis*). Mol Ecol 27:4501–4515.

Aguillon, S. M., J. Walsh, and I. J. Lovette. 2021. Extensive hybridization reveals multiple coloration genes underlying a complex plumage phenotype. Proc Biol Sci 288:20201805.

Aidala, Z., L. Huynen, P. L. R. Brennan, J. Musser, A. Fidler, N. Chong, G. E. Machovsky Capuska, M. G. Anderson, A. Talaba, D. Lambert, and M. E. Hauber. 2012. Ultraviolet visual sensitivity in three avian lineages: paleognaths, parrots, and passerines. J. Comp. Physiol. A 198:495–510.

Alatalo, R. V., J. Höglund, A. Lundberg, and W. J. Sutherland. 1992. Evolution of black grouse leks: female preferences benefit males in larger leks. Behav Ecol 3:53–59.

Alonge, M., S. Soyk, S. Ramakrishnan, X. Wang, S. Goodwin, F. J. Sedlazeck, Z. B. Lippman, and M. C. Schatz. 2019. RaGOO: fast and accurate reference-guided scaffolding of draft genomes. Genome Biol. 20:224.

Alves, W. B., C. Albano, W. A. de G. e Silva, J. Araripe, and P. S. do Rêgo. 2016. Confirmation of the hybridization of *Chiroxiphia* Cabanis, 1847 and *Antilophia* Reichenbach, 1850 (Passeriformes: Pipridae) using molecular markers. Rev Bras Ornitol 24:185–190.

Amengual, J., G. P. Lobo, M. Golczak, H. N. M. Li, T. Klimova, C. L. Hoppel, A. Wyss, K. Palczewski, and J. von Lintig. 2011. A mitochondrial enzyme degrades carotenoids and protects against oxidative stress. FASEB J. 25:948–959.

Anderson, R. P., and C. O. Handley Jr. 2002. Dwarfism in insular sloths: biogeography, selection, and evolutionary rate. Evolution 56:1045–1058.

Andersson, M. 1994. Sexual Selection. Princeton University Press, Princeton, NJ.

Andrade, P., C. Pinho, G. Pérez i de Lanuza, S. Afonso, J. Brejcha, C.-J. Rubin, O. Wallerman, P. Pereira, S. J. Sabatino, A. Bellati, D. Pellitteri-Rosa, Z. Bosakova, I. Bunikis, M. A. Carretero, N. Feiner, P. Marsik, F. Paupério, D. Salvi, L. Soler, G. M. While, T. Uller, E. Font, L. Andersson, and M. Carneiro. 2019. Regulatory changes in pterin and carotenoid genes underlie balanced color polymorphisms in the wall lizard. Proc. Natl. Acad. Sci. 116:5633–5642.

Angehr, G. R., and R. Dean. 2010. The Birds of Panama: A Field Guide. Cornell University Press, Ithaca, New York.

Arnold, M. L. 1997. Natural Hybridization and Evolution. Oxford University Press, New York, NY.

Arntzen, J. W., W. de Vries, D. Canestrelli, and I. Martínez-Solano. 2017. Hybrid zone formation and contrasting outcomes of secondary contact over transects in common toads. Mol. Ecol. 26:5663–5675.

Ayres, J. M., and T. H. Clutton-Brock. 1992. River boundaries and species range size in Amazonian primates. Am Nat 140:531–537.

Baiz, M. D., A. W. Wood, A. Brelsford, I. J. Lovette, and D. P. L. Toews. 2021. Pigmentation genes show evidence of repeated divergence and multiple bouts of introgression in *Setophaga* warblers. Curr Biol 31:643-649.e3.

Baldassarre, D. T., and M. S. Webster. 2013. Experimental evidence that extra-pair mating drives asymmetrical introgression of a sexual trait. Proc Biol Sci 280:20132175.

Baldassarre, D. T., T. A. White, J. Karubian, and M. S. Webster. 2014. Genomic and morphological analysis of a semipermeable avian hybrid zone suggests asymmetrical introgression of a sexual signal. Evolution 68:2644–2657.

Barrera-Guzmán, A. O., A. Aleixo, M. D. Shawkey, and J. T. Weir. 2018. Hybrid speciation leads to novel male secondary sexual ornamentation of an Amazonian bird. Proc Natl Acad Sci USA 115:E218–E225.

Barske, J., M. J. Fuxjager, C. Ciofi, C. Natali, B. A. Schlinger, T. Billo, and L. Fusani. 2023. Beyond plumage: acrobatic courtship displays show intermediate patterns in manakin hybrids. Anim Behav 198:195–205.

Barske, J., B. A. Schlinger, M. Wikelski, and L. Fusani. 2011. Female choice for male motor skills. Proc Biol Sci 278:3523–3528.

Barton, N. H. 1979. The dynamics of hybrid zones. Heredity 43:341–359.

Barton, N. H., and K. S. Gale. 1993. Genetic analysis of hybrid zones. Pp. 13–45 *in* R. G. Harrison, ed. Hybrid zones and the evolutionary process. Oxford University Press, Oxford, UK.

Barton, N. H., R. B. Halliday, and G. M. Hewitt. 1983. Rare electrophoretic variants in a hybrid zone. Heredity 50:139–146.

Barton, N. H., and G. M. Hewitt. 1985. Analysis of Hybrid Zones. Annu Rev Ecol Syst 16:113–148.

Bates, H. W. 1892. The Naturalist on the River Amazons. 2nd ed. John Murray, London, UK.

Bennett, K. F. P., H. C. Lim, and M. J. Braun. 2021. Sexual selection and introgression in avian hybrid zones: Spotlight on *Manacus*. Integr Comp Biol 61:1291–1309.

Berry, S. D., S. R. Davis, E. M. Beattie, N. L. Thomas, A. K. Burrett, H. E. Ward, A. M. Stanfield, M. Biswas, A. E. Ankersmit-Udy, P. E. Oxley, J. L. Barnett, J. F. Pearson, Y. van der Does, A. H. K. MacGibbon, R. J. Spelman, K. Lehnert, and R. G. Snell. 2009. Mutation in Bovine β-carotene oxygenase 2 affects milk color. Genetics 182:923–926.

Billo, T. J. 2011. Sexual selection, vocal signals, and plumage introgression in an avian hybrid zone. University of Washington.

Bímová, B. V., M. Macholán, S. J. E. Baird, P. Munclinger, P. Dufková, C. M. Laukaitis, R. C. Karn, K. Luzynski, P. K. Tucker, and J. Piálek. 2011. Reinforcement selection acting on the European house mouse hybrid zone. Mol. Ecol. 20:2403–2424.

Bodony, D. J., L. Day, A. R. Friscia, L. Fusani, A. Karon, G. W. Swenson Jr, M. Wikelski, and B. A. Schlinger. 2016. Determination of the wingsnap sonation mechanism of the golden-collared manakin (*Manacus vitellinus*). J Exp Biol 219:1524–1534.

Booker, T. R., S. Yeaman, and M. C. Whitlock. 2020. Variation in recombination rate affects detection of outliers in genome scans under neutrality. Mol. Ecol. 29:4274–4279.

Brelsford, A., and D. E. Irwin. 2009. Incipient speciation despite little assortative mating: the yellow-rumped warbler hybrid zone. Evolution 63:3050–3060.

Brelsford, A., B. Milá, and D. E. Irwin. 2011. Hybrid origin of Audubon's warbler. Mol Ecol 20:2380–2389.

Brelsford, A., D. P. L. Toews, and D. E. Irwin. 2017. Admixture mapping in a hybrid zone reveals loci associated with avian feather coloration. Proc Biol Sci 284.

Bronson, C. L., T. C. Grubb Jr, and M. J. Braun. 2003. A test of the endogenous and exogenous selection hypotheses for the maintenance of a narrow avian hybrid zone. Evolution 57:630–637.

Bronson, C. L., T. C. Grubb, G. D. Sattler, and M. J. Braun. 2005. Reproductive success across the Black-capped Chickadee (*Poecile atricapillus*) and Carolina Chickadee (*P. carolinensis*) hybrid zone in Ohio. Auk 122:759–772.

Brumfield, R. T. 1999. Evolution of brilliant male plumage traits in Manacus: Hybrid zones, molecular systematics, and riverine barriers. University of Maryland, College Park.

Brumfield, R. T., and M. J. Braun. 2001. Phylogenetic relationships in bearded manakins (Pipridae: *Manacus*) indicate that male plumage color is a misleading taxonomic marker. Condor 103:248–258.

Brumfield, R. T., R. W. Jernigan, D. B. McDonald, and M. J. Braun. 2001. Evolutionary implications of divergent clines in an avian (*Manacus*: Aves) hybrid zone. Evolution 55:2070–2087.

Brumfield, R. T., L. Liu, D. E. Lum, and S. V. Edwards. 2008. Comparison of species tree methods for reconstructing the phylogeny of bearded manakins (Aves: Pipridae, *Manacus*) from multilocus sequence data. Syst Biol 57:719–731.

Brush, A. H. 1990. Metabolism of carotenoid pigments in birds. FASEB J 4:2969–2977.

Brush, A. H., and H. Seifried. 1968. Pigmentation and feather structure in genetic variants of the Gouldian Finch, *Poephila gouldiae*. The Auk 85:416–430.

Buggs, R. J. A. 2007. Empirical study of hybrid zone movement. Heredity 99:301–312.

Burley, N., and C. B. Coopersmith. 2010. Bill color preferences of zebra finches. Ethology 76:133–151.

Burney, C. W., and R. T. Brumfield. 2009. Ecology predicts levels of genetic differentiation in neotropical birds. Am Nat 174:358–368.

Burri, R. 2017. Interpreting differentiation landscapes in the light of long-term linked selection. Evol. Lett. 1:118–131.

Butlin, R. K., and R. M. Neems. 1994. Hybrid zones and sexual selection. Science 265:122.

Butlin, R. K., and C. M. Smadja. 2018. Coupling, reinforcement, and speciation. Am. Nat. 191:155–172.

Cadieu, E., M. W. Neff, P. Quignon, K. Walsh, K. Chase, H. G. Parker, B. M. VonHoldt, A. Rhue, A. Boyko, A. Byers, A. Wong, D. S. Mosher, A. G. Elkahloun, T. C. Spady, C. André, K. G. Lark, M. Cargill, C. D. Bustamante, R. K. Wayne, and E. A. Ostrander. 2009. Coat variation in the domestic dog is governed by variants in three genes. Science 326:150–153.

Campagna, L., M. Repenning, L. F. Silveira, C. S. Fontana, P. L. Tubaro, and I. J. Lovette. 2017. Repeated divergent selection on pigmentation genes in a rapid finch radiation. Sci. Adv. 3:e1602404.

Capparella, A. P. 1988. Genetic variation in Neotropical birds: implications for the speciation process. Acta Congr. Int. Ornithol. 19:1658–1664.

Carneiro, M., S. J. E. Baird, S. Afonso, E. Ramirez, P. Tarroso, H. Teotónio, R. Villafuerte, M. W. Nachman, and N. Ferrand. 2013. Steep clines within a highly permeable genome across a hybrid zone between two subspecies of the European rabbit. Mol. Ecol. 22:2511–2525.

Caves, E. M., L. E. Schweikert, P. A. Green, M. N. Zipple, C. Taboada, S. Peters, S. Nowicki, and S. Johnsen. 2020. Variation in carotenoid-containing retinal oil droplets correlates with variation in perception of carotenoid coloration. Behav Ecol Sociobiol 74:93.

Cestari, C., and M. A. Pizo. 2014. Court cleaning behavior of the White-bearded Manakin (*Manacus manacus*) and a test of the anti-predation hypothesis. Wilson J Ornithol 126:98–104.

Chang, C.-H., T.-X. Jiang, C.-M. Lin, L. W. Burrus, C.-M. Chuong, and R. Widelitz. 2004. Distinct Wnt members regulate the hierarchical morphogenesis of skin regions (spinal tract) and individual feathers. Mech. Dev. 121:157–171.

Chapman, F. M. 1935. The courtship of Gould's manakin (*Manacus vitellinus vitellinus*) on Barro Colorado Island, Canal Zone. Bull. AMNH 68:471–525.

Chaves, N. 2020. Orange-collared Manakin (*Manacus aurantiacus*), version 1.0. Cornell Lab of Ornithology, Ithaca, NY.

Chessel, D., A. B. Dufour, and J. Thioulouse. 2004. The ade4 package - I: One-table methods. R News 4:5–10.

Clarke, A. L., B.-E. Sæther, and E. Røskaft. 1997. Sex biases in avian dispersal: A reappraisal. Oikos 79:429–438.

Concannon, M. R., A. C. Stein, and J. A. C. Uy. 2012. Kin selection may contribute to lek evolution and trait introgression across an avian hybrid zone. Mol Ecol 21:1477–1486.

Coyne, J. A., and H. A. Orr. 2004. Speciation. Sinauer Associates, Sunderland, MA.

Cruickshank, T. E., and M. W. Hahn. 2014. Reanalysis suggests that genomic islands of speciation are due to reduced diversity, not reduced gene flow. Mol. Ecol. 23:3133–3157.

Davidson, B. S., G. D. Sattler, S. Via, and M. J. Braun. 2013. Reproductive isolation and cryptic introgression in a sky island enclave of Appalachian birds. Ecol Evol 3:2485–2496.

Day, L. B., W. Helmhout, G. Pano, U. Olsson, J. D. Hoeksema, and W. R. Lindsay. 2021. Correlated evolution of acrobatic display and both neural and somatic phenotypic traits in manakins (Pipridae). Integr. Comp. Biol. 61:1343–1362.

dela Seña, C., J. Sun, S. Narayanasamy, K. M. Riedl, Y. Yuan, R. W. Curley, S. J. Schwartz, and E. H. Harrison. 2016. Substrate specificity of purified recombinant chicken β-carotene 9′,10′-oxygenase (BCO2). J Biol Chem 291:14609–14619.

Delmore, K. E., R. A. Brenneman, R. Lei, C. A. Bailey, A. Brelsford, E. E. Louis Jr, and S. E. Johnson. 2013. Clinal variation in a brown lemur (*Eulemur* spp.) hybrid zone: Combining morphological, genetic and climatic data to examine stability. J. Evol. Biol. 26:1677–1690.

Delmore, K. E., S. Hübner, N. C. Kane, R. Schuster, R. L. Andrew, F. Câmara, R. Guigó, and D. E. Irwin. 2015. Genomic analysis of a migratory divide reveals candidate genes for migration and implicates selective sweeps in generating islands of differentiation. Mol Ecol 24:1873–1888.

DeRaad, D. A., E. E. Applewhite, W. L. E. Tsai, R. S. Terrill, S. E. Kingston, M. J. Braun, and J. E. McCormack. 2023. Hybrid zone or hybrid lineage: a genomic reevaluation of Sibley's classic species conundrum in *Pipilo* towhees. Evolution 77:852–869.

Dobzhansky, T. 1937. Genetics and the Origin of Species. Columbia University Press.

Dowell, N. L., M. W. Giorgianni, S. Griffin, V. A. Kassner, J. E. Selegue, E. E. Sanchez, and S. B. Carroll. 2018. Extremely divergent haplotypes in two toxin gene complexes encode alternative venom types within rattlesnake species. Curr Biol 28:1016-1026.e4.

Ducrest, A.-L., L. Keller, and A. Roulin. 2008. Pleiotropy in the melanocortin system, coloration and behavioural syndromes. Trends Ecol Evol 23:502–510.

Edelman, N. B., P. B. Frandsen, M. Miyagi, B. Clavijo, J. Davey, R. B. Dikow, G. García-Accinelli, S. M. Van Belleghem, N. Patterson, D. E. Neafsey, R. Challis, S. Kumar, G. R. P. Moreira, C. Salazar, M. Chouteau, B. A. Counterman, R. Papa, M. Blaxter, R. D. Reed, K. K. Dasmahapatra, M. Kronforst, M. Joron, C. D. Jiggins, W. O. McMillan, F. Di Palma, A. J. Blumberg, J. Wakeley, D. Jaffe, and J. Mallet. 2019. Genomic architecture and introgression shape a butterfly radiation. Science 366:594–599.

Elgvin, T. O., C. N. Trier, O. K. Tørresen, I. J. Hagen, S. Lien, A. J. Nederbragt, M. Ravinet, H. Jensen, and G.-P. Sætre. 2017. The genomic mosaicism of hybrid speciation. Sci Adv 3:e1602996.

Eliason, C. M., J. C. Cooper, S. J. Hackett, E. Zahnle, T. Z. Pequeño Saco, J. D. Maddox, T. Hains, M. E. Hauber, and J. M. Bates. 2023. Interspecific hybridization explains rapid gorget colour divergence in *Heliodoxa* hummingbirds (Aves: Trochilidae). R Soc Open Sci 10:221603.

Emlen, S. T., and P. H. Wrege. 2004. Size dimorphism, intrasexual competition, and sexual selection in Wattled Jacana (*Jacana jacana*), a sex-role-reversed shorebird in Panama. The Auk 121:391–403.

Enbody, E. D., C. G. Sprehn, A. Abzhanov, H. Bi, M. P. Dobreva, O. G. Osborne, C.-J. Rubin, P. R. Grant, B. R. Grant, and L. Andersson. 2021. A multispecies BCO2 beak color polymorphism in the Darwin's finch radiation. Curr. Biol. 31:5597-5604.e7.

Enciso-Romero, J., C. Pardo-Díaz, S. H. Martin, C. F. Arias, M. Linares, W. O. McMillan, C. D. Jiggins, and C. Salazar. 2017. Evolution of novel mimicry rings facilitated by adaptive introgression in tropical butterflies. Mol. Ecol. 26:5160–5172.

Endler, J. A., and M. Théry. 1996. Interacting effects of lek placement, display behavior, ambient light, and color patterns in three Neotropical forest-dwelling birds. Am Nat 148:421–452.

Eriksson, J., G. Larson, U. Gunnarsson, B. Bed'hom, M. Tixier-Boichard, L. Strömstedt, D. Wright, A. Jungerius, A. Vereijken, E. Randi, P. Jensen, and L. Andersson. 2008. Identification of the yellow skin gene reveals a hybrid origin of the domestic chicken. PLoS Genet 4:e1000010.

Etter, P. D., S. Bassham, P. A. Hohenlohe, E. A. Johnson, and W. A. Cresko. 2011. SNP discovery and genotyping for evolutionary genetics using RAD sequencing. Methods Mol Biol 772:157–178.

Farjo, K. M., G. Moiseyev, O. Nikolaeva, L. L. Sandell, P. A. Trainor, and J. Ma. 2011. RDH10 is the primary enzyme responsible for the first step of embryonic Vitamin A metabolism and retinoic acid synthesis. Dev. Biol. 357:347–355.

Feder, J. L., X. Xie, J. Rull, S. Velez, A. Forbes, B. Leung, H. Dambroski, K. E. Filchak, and M. Aluja. 2005. Mayr, Dobzhansky, and Bush and the complexities of sympatric speciation in *Rhagoletis*. Proc. Natl. Acad. Sci. 102:6573–6580.

Felsenstein, J. 1981. Skepticism towards Santa Rosalia, or why are there so few kinds of animals? Evolution 35:124–138.

Fisher, R. A. 1930. The genetical theory of natural selection. Clarendon Press, Oxford, UK.

Fisher, R. A. 1937. The wave of advance of advantageous genes. Ann Eugen 7:355–369.

Foster, M. S. 1977. Odd couples in manakins: A study of social organization and cooperative breeding in *Chiroxiphia linearis*. Am Nat 111:845–853.

Frichot, E., and O. François. 2015. LEA: An R package for landscape and ecological association studies. Methods Ecol Evol 6:925–929.

Frost, P. 2006. European hair and eye color: A case of frequency-dependent sexual selection? Evol Hum Behav 27:85–103.

Fumagalli, M., F. G. Vieira, T. S. Korneliussen, T. Linderoth, E. Huerta-Sánchez, A. Albrechtsen, and R. Nielsen. 2013. Quantifying population genetic differentiation from next-generation sequencing data. Genetics 195:979–992.

Funk, E. R., and S. A. Taylor. 2019. High-throughput sequencing is revealing genetic associations with avian plumage color. The Auk 136:ukz048.

Fusani, L., J. Barske, C. Natali, G. Chelazzi, and C. Ciofi. 2018. Relatedness within and between leks of golden-collared manakin differ between sexes and age classes. Behav Ecol 29:1390–1401.

Fuxjager, M. J., F. Goller, A. Dirkse, G. D. Sanin, and S. Garcia. 2016. Select forelimb muscles have evolved superfast contractile speed to support acrobatic social displays. Elife 5:e13544.

Fuxjager, M. J., and E. R. Schuppe. 2018. Androgenic signaling systems and their role in behavioral evolution. J Steroid Biochem Mol Biol 184:47–56.

Gazda, M. A., P. M. Araújo, R. J. Lopes, M. B. Toomey, P. Andrade, S. Afonso, C. Marques, L. Nunes, P. Pereira, S. Trigo, G. E. Hill, J. C. Corbo, and M. Carneiro. 2020a. A genetic mechanism for sexual dichromatism in birds. Science 368:1270–1274.

Gazda, M. A., M. B. Toomey, P. M. Araújo, R. J. Lopes, S. Afonso, C. A. Myers, K. Serres, P. D. Kiser, G. E. Hill, J. C. Corbo, and M. Carneiro. 2020b. Genetic basis of de novo

appearance of carotenoid ornamentation in bare parts of canaries. Mol Biol Evol 37:1317–1328.

Gill, F. B. 1995. Ornithology. 2nd ed. W. H. Freeman, New York, NY.

Goldberg, E. E., and R. Lande. 2006. Ecological and reproductive character displacement of an environmental gradient. Evolution 60:1344–1357.

Gompert, Z., E. G. Mandeville, and A. C. Buerkle. 2017. Analysis of population genomic data from hybrid zones. Annu Rev Ecol Evol S 48:207–229.

Goudet, J., and T. Jombart. 2022. hierfstat: Estimation and tests of hierarchical F-statistics. https://CRAN.R-project.org/package=hierfstat.

Graf, J., R. Hodgson, and A. van Daal. 2005. Single nucleotide polymorphisms in the MATP gene are associated with normal human pigmentation variation. Hum. Mutat. 25:278–284.

Grau-Bové, X., S. Tomlinson, A. O. O'Reilly, N. J. Harding, A. Miles, D. Kwiatkowski, M. J. Donnelly, D. Weetman, and and The Anopheles gambiae 1000 Genomes Consortium. 2020. Evolution of the insecticide target Rdl in African *Anopheles* is driven by interspecific and interkaryotypic introgression. Mol. Biol. Evol. 37:2900–2917.

Graves, G. R. 1993. A new hybrid manakin (*Dixiphia pipra* x *Pipra filicauda*)(Aves, Pipridae) from the Andean foothills of eastern Ecuador. Proc Biol Soc Wash 106:436–441.

Green, R. E., J. Krause, A. W. Briggs, T. Maricic, U. Stenzel, M. Kircher, N. Patterson, H. Li, W. Zhai, M. H.-Y. Fritz, N. F. Hansen, E. Y. Durand, A.-S. Malaspinas, J. D. Jensen, T. Marques-Bonet, C. Alkan, K. Prüfer, M. Meyer, H. A. Burbano, J. M. Good, R. Schultz, A. Aximu-Petri, A. Butthof, B. Höber, B. Höffner, M. Siegemund, A. Weihmann, C. Nusbaum, E. S. Lander, C. Russ, N. Novod, J. Affourtit, M. Egholm, C. Verna, P. Rudan,

D. Brajkovic, Ž. Kucan, I. Gušic, V. B. Doronichev, L. V. Golovanova, C. Lalueza-Fox, M. de la Rasilla, J. Fortea, A. Rosas, R. W. Schmitz, P. L. F. Johnson, E. E. Eichler, D. Falush, E. Birney, J. C. Mullikin, M. Slatkin, R. Nielsen, J. Kelso, M. Lachmann, D. Reich, and S. Pääbo. 2010. A Draft sequence of the Neandertal genome. Science 328:710–722.

Greenwood, P. J. 1980. Mating systems, philopatry and dispersal in birds and mammals. Anim Behav 28:1140–1162.

Gross, M. R., P. H. Harvey, L. Partridge, and S. R. Southwood. 1991. Evolution of alternative reproductive strategies: frequency-dependent sexual selection in male bluegill sunfish. Philos Trans R Soc Lond B Biol Sci 332:59–66.

Guruvayoorappan, C., and G. Kuttan. 2007. [beta]-Carotene inhibits tumor-specific angiogenesis by altering the cytokine profile and inhibits the nuclear translocation of transcription factors in B16F-10 melanoma cells. Integr. Cancer Ther. 6:258–271.

Haas, F., and A. Brodin. 2005. The crow *Corvus corone* hybrid zone in southern Denmark and northern Germany. Ibis 147:649–656.

Haffer, J. 1970. Art-Entstehung bei einigen Waldvögeln Amazoniens. J. Für Ornithol. 111:285–331.

Haffer, J. 1974. Avian Speciation in Tropical South America. Nuttall Ornithological Club Publication, Cambridge, MA.

Haffer, J. 1997. Contact zones between birds of southern Amazonia. Ornithol Monogr 281–305.

Haffer, J. 1969. Speciation in Amazonian forest birds. Science 165:131–137.

Haffer, J. 1967. Speciation in Colombian forest birds west of the Andes. Am Mus Novit 1–57.

Harrison, R. G. (ed). 1993. Hybrid Zones and the Evolutionary Process. Oxford University Press, Oxford, UK.

Harvey, M. G., G. A. Bravo, S. Claramunt, A. M. Cuervo, G. E. Derryberry, J. Battilana, G. F. Seeholzer, J. S. McKay, B. C. O'Meara, B. C. Faircloth, S. V. Edwards, J. Pérez-Emán, R. G. Moyle, F. H. Sheldon, A. Aleixo, B. T. Smith, R. T. Chesser, L. F. Silveira, J. Cracraft, R. T. Brumfield, and E. P. Derryberry. 2020. The evolution of a tropical biodiversity hotspot. Science 370:1343–1348.

Harvey, M. G., and R. T. Brumfield. 2015. Genomic variation in a widespread Neotropical bird (Xenops minutus) reveals divergence, population expansion, and gene flow. Mol Phylogenet Evol 83:305–316.

Hellmayr, C. E. 1910. The birds of the Rio Madeira. Novit. Zool. 17:257–428.

Hermansen, J. S., S. A. Saether, T. O. Elgvin, T. Borge, E. Hjelle, and G.-P. Saetre. 2011. Hybrid speciation in sparrows I: phenotypic intermediacy, genetic admixture and barriers to gene flow. Mol Ecol 20:3812–3822.

Hewitt, G. M. 1988. Hybrid zones-natural laboratories for evolutionary studies. Trends Ecol Evol 3:158–167.

Hill, G. E. 2006. Female mate choice for ornamental coloration. Pp. 137–200 *in* G. E. Hill and K. J. McGraw, eds. Bird Coloration Volume II. Function and Evolution. Harvard University Press, Cambridge, MA.

Hill, G. E. 2019. Mitonuclear Ecology. Oxford University Press, Oxford, UK.

Hill, G. E. 1991. Plumage coloration is a sexually selected indicator of male quality. Nature 350:337–339.

Hill, G. E. 1994. Trait elaboration via adaptive mate choice: sexual conflict in the evolution of signals of male quality. Ethol. Ecol. Evol. 6:351–370.

Hooper, D. M., S. C. Griffith, and T. D. Price. 2019. Sex chromosome inversions enforce reproductive isolation across an avian hybrid zone. Mol Ecol 28:1246–1262.

Hooper, D. M., and T. D. Price. 2017. Chromosomal inversion differences correlate with range overlap in passerine birds. Nat Ecol Evol 1:1526–1534.

Hoskin, C. J., M. Higgie, K. R. McDonald, and C. Moritz. 2005. Reinforcement drives rapid allopatric speciation. Nature 437:1353–1356.

Hudon, J., A. Storni, E. Pini, M. Anciães, and R. Stradi. 2012. Rhodoxanthin as a characteristic keto-carotenoid of manakins (Pipridae). Auk 129:491–499.

Hudson, E. J., and T. D. Price. 2014. Pervasive reinforcement and the role of sexual selection in biological speciation. J Hered 105:821–833.

Huerta-Sánchez, E., X. Jin, Asan, Z. Bianba, B. M. Peter, N. Vinckenbosch, Y. Liang, X. Yi, M. He, M. Somel, P. Ni, B. Wang, X. Ou, Huasang, J. Luosang, Z. X. P. Cuo, K. Li, G. Gao, Y. Yin, W. Wang, X. Zhang, X. Xu, H. Yang, Y. Li, J. Wang, J. Wang, and R. Nielsen. 2014. Altitude adaptation in Tibetans caused by introgression of Denisovan-like DNA. Nature 512:194–197.

Irisarri, I., P. Singh, S. Koblmüller, J. Torres-Dowdall, F. Henning, P. Franchini, C. Fischer, A. R. Lemmon, E. M. Lemmon, G. G. Thallinger, C. Sturmbauer, and A. Meyer. 2018. Phylogenomics uncovers early hybridization and adaptive loci shaping the radiation of Lake Tanganyika cichlid fishes. Nat. Commun. 9:3159.

Irwin, D. E. 2002. Phylogeographic breaks without geographic barriers to gene flow. Evolution 56:2383–2394.

Jaarola, M., H. Tegelström, and K. Fredga. 1997. A contact zone with noncoincident clines for sex-specific markers in the field vole (*Microtus agrestis*). Evolution 51:241–249.

Johnson, B. B., T. A. White, C. A. Phillips, and K. R. Zamudio. 2015. Asymmetric introgression in a spotted salamander hybrid zone. J. Hered. 106:608–617.

Johnson, O., C. C. Ribas, A. Aleixo, L. N. Naka, M. G. Harvey, and R. T. Brumfield. 2023. Amazonian birds in more dynamic habitats have less population genetic structure and higher gene flow. Mol. Ecol. 32:2186–2205.

Jombart, T. 2008. adegenet: a R package for the multivariate analysis of genetic markers. Bioinformatics 24:1403–1405.

Jombart, T., S. Devillard, and F. Balloux. 2010. Discriminant analysis of principal components: a new method for the analysis of genetically structured populations. BMC Genet 11:94.

Jones, M. R., L. S. Mills, P. C. Alves, C. M. Callahan, J. M. Alves, D. J. R. Lafferty, F. M. Jiggins, J. D. Jensen, J. Melo-Ferreira, and J. M. Good. 2018. Adaptive introgression underlies polymorphic seasonal camouflage in snowshoe hares. Science 360:1355–1358.

Jordan, D. S. 1908. The law of geminate species. Am Nat 42:73–80.

Kamvar, Z. N., J. F. Tabima, and N. J. Grünwald. 2014. Poppr: an R package for genetic analysis of populations with clonal, partially clonal, and/or sexual reproduction. PeerJ 2:e281.

Karubian, J. 2002. Costs and benefits of variable breeding plumage in the red-backed fairy-wren. Evolution 56:1673–1682.

Kassambara, A. 2023. ggpubr: "ggplot2" Based Publication Ready Plots. https://cran.r-project.org/web/packages/ggpubr/index.html.

Katoh, K., and D. M. Standley. 2013. MAFFT multiple sequence alignment software version 7: improvements in performance and usability. Mol. Biol. Evol. 30:772–780.

Kearns, A. M., M. Restani, I. Szabo, A. Schrøder-Nielsen, J. A. Kim, H. M. Richardson, J. M. Marzluff, R. C. Fleischer, A. Johnsen, and K. E. Omland. 2018. Genomic evidence of speciation reversal in ravens. Nat Commun 9:906.

Khalil, S., J. F. Welklin, K. J. McGraw, J. Boersma, H. Schwabl, M. S. Webster, and J. Karubian. 2020. Testosterone regulates CYP2J19-linked carotenoid signal expression in male red-backed fairywrens (*Malurus melanocephalus*). Proc Biol Sci 287:20201687.

Kiefer, C., E. Sumser, M. F. Wernet, and J. Von Lintig. 2002. A class B scavenger receptor mediates the cellular uptake of carotenoids in *Drosophila*. Proc Natl Acad Sci USA 99:10581–10586.

Kingston, S. E., R. W. Jernigan, W. F. Fagan, D. Braun, and M. J. Braun. 2012. Genomic variation in cline shape across a hybrid zone. Ecol Evol 2:2737–2748.

Kingston, S. E., A. G. Navarro-Sigüenza, E. A. García-Trejo, H. Vázquez-Miranda, W. F. Fagan, and M. J. Braun. 2014. Genetic differentiation and habitat connectivity across towhee hybrid zones in Mexico. Evol Ecol 28:277–297.

Kingston, S. E., T. L. Parchman, Z. Gompert, C. A. Buerkle, and M. J. Braun. 2017. Heterogeneity and concordance in locus-specific differentiation and introgression between species of towhees. J Evol Biol 30:474–485.

Kirschel, A. N. G., D. T. Blumstein, and T. B. Smith. 2009. Character displacement of song and morphology in African tinkerbirds. Proc Natl Acad Sci USA 106:8256–8261.

Kirwan, G. M., and G. Green. 2011. Cotingas and Manakins. Princeton University Press, Princeton, NJ.

Kleindorfer, S., J. A. O'Connor, R. Y. Dudaniec, S. A. Myers, J. Robertson, and F. J. Sulloway. 2014. Species collapse via hybridization in Darwin's tree finches. Am Nat 183:325–341.

Kopuchian, C., L. Campagna, D. A. Lijtmaer, G. S. Cabanne, N. C. García, P. D. Lavinia, P. L. Tubaro, I. Lovette, and A. S. Di Giacomo. 2020. A test of the riverine barrier hypothesis in the largest subtropical river basin in the Neotropics. Mol Ecol 29:2137–2149.

Korneliussen, T. S., A. Albrechtsen, and R. Nielsen. 2014. ANGSD: Analysis of Next Generation Sequencing Data. BMC Bioinformatics 15:356.

Kozak, K. M., M. Joron, W. O. McMillan, and C. D. Jiggins. 2021. Rampant genome-wide admixture across the *Heliconius* radiation. Genome Biol. Evol. 13:evab099.

Küpper, C., M. Stocks, J. E. Risse, N. Dos Remedios, L. L. Farrell, S. B. McRae, T. C. Morgan, N. Karlionova, P. Pinchuk, Y. I. Verkuil, A. S. Kitaysky, J. C. Wingfield, T. Piersma, K. Zeng, J. Slate, M. Blaxter, D. B. Lank, and T. Burke. 2016. A supergene determines highly divergent male reproductive morphs in the ruff. Nat Genet 48:79–83.

Lamichhaney, S., G. Fan, F. Widemo, U. Gunnarsson, D. S. Thalmann, M. P. Hoeppner, S. Kerje, U. Gustafson, C. Shi, H. Zhang, W. Chen, X. Liang, L. Huang, J. Wang, E. Liang, Q. Wu, S. M.-Y. Lee, X. Xu, J. Höglund, X. Liu, and L. Andersson. 2016. Structural genomic changes underlie alternative reproductive strategies in the ruff (*Philomachus pugnax*). Nat Genet 48:84–88.

Langmead, B., and S. L. Salzberg. 2012. Fast gapped-read alignment with Bowtie 2. Nat. Methods 9:357–359.

Lee, A. S. Y., P. J. Kranzusch, and J. H. D. Cate. 2015. eIF3 targets cell-proliferation messenger RNAs for translational activation or repression. Nature 522:111–114.

Lehnert, S. J., K. A. Christensen, W. E. Vandersteen, D. Sakhrani, T. E. Pitcher, J. W. Heath, B. F. Koop, D. D. Heath, and R. H. Devlin. 2019. Carotenoid pigmentation in salmon:

variation in expression at BCO2-l locus controls a key fitness trait affecting red coloration. Proc. R. Soc. B Biol. Sci. 286:20191588.

Lehtonen, P. K., T. Laaksonen, A. V. Artemyev, E. Belskii, P. R. Berg, C. Both, L. Buggiotti, S. Bureš, M. D. Burgess, A. V. Bushuev, I. Krams, J. Moreno, M. Mägi, A. Nord, J. Potti, P.-A. Ravussin, P. M. Sirkiä, G.-P. Sætre, W. Winkel, and C. R. Primmer. 2012. Candidate genes for colour and vision exhibit signals of selection across the pied flycatcher (*Ficedula hypoleuca*) breeding range. Heredity 108:431–440.

Leite, R. N., R. T. Kimball, E. L. Braun, E. P. Derryberry, P. A. Hosner, G. E. Derryberry, M. Anciães, J. S. McKay, A. Aleixo, C. C. Ribas, R. T. Brumfield, and J. Cracraft. 2021. Phylogenomics of manakins (Aves: Pipridae) using alternative locus filtering strategies based on informativeness. Mol Phylogenet Evol 155:107013.

Lemmon, A. R., and E. M. Lemmon. 2008. A likelihood framework for estimating phylogeographic history on a continuous landscape. Syst Biol 57:544–561.

Lenth, R. V., B. Bolker, P. Buerkner, I. Giné-Vázquez, M. Herve, M. Jung, J. Love, F. Miguez, H. Riebl, and H. Singmann. 2023. emmeans: Estimated Marginal Means, aka Least-Squares Means. https://cran.r-project.org/web/packages/emmeans/index.html.

Letunic, I., and P. Bork. 2021. Interactive Tree Of Life (iTOL) v5: an online tool for phylogenetic tree display and annotation. Nucleic Acids Res. 49:W293–W296.

Li, H. 2013. Aligning sequence reads, clone sequences and assembly contigs with BWA-MEM. arXiv: http://arxiv.org/abs/1303.3997.

Li, H. 2016. Minimap and miniasm: fast mapping and de novo assembly for noisy long sequences. Bioinformatics 32:2103–2110.

Li, H., B. Handsaker, A. Wysoker, T. Fennell, J. Ruan, N. Homer, G. Marth, G. Abecasis, R. Durbin, and 1000 Genome Project Data Processing Subgroup. 2009. The Sequence Alignment/Map format and SAMtools. Bioinformatics 25:2078–2079.

Ligon, J. D. 1999. The Evolution of Avian Breeding Systems. Oxford University Press, New York, NY.

Lill, A. 1974. Sexual behavior of the lek-forming white-bearded manakin (*Manacus manacus trinitatis* Hartert). Z. Für Tierpsychol. 36:1–36.

Lin, S.-J., R. B. Wideliz, Z. Yue, A. Li, X. Wu, T.-X. Jiang, P. Wu, and C.-M. Chuong. 2013. Feather regeneration as a model for organogenesis. Dev. Growth Differ. 55:139–148.

Lind, O., M. Mitkus, P. Olsson, and A. Kelber. 2014. Ultraviolet vision in birds: the importance of transparent eye media. Proc. R. Soc. B Biol. Sci. 281:20132209.

Lindsay, W. R., J. T. Houck, C. E. Giuliano, and L. B. Day. 2015. Acrobatic courtship display coevolves with brain size in manakins (Pipridae). Brain Behav Evol 85:29–36.

Liou, L. W., and T. D. Price. 1994. Speciation by reinforcement of premating isolation. Evolution 48:1451–1459.

Lipshutz, S. E., J. I. Meier, G. E. Derryberry, M. J. Miller, O. Seehausen, and E. P. Derryberry. 2019. Differential introgression of a female competitive trait in a hybrid zone between sex-role reversed species. Evolution 73:188–201.

Lipshutz, S. E., I. A. Overcast, M. J. Hickerson, R. T. Brumfield, and E. P. Derryberry. 2017. Behavioural response to song and genetic divergence in two subspecies of white-crowned sparrows (*Zonotrichia leucophrys*). Mol Ecol 26:3011–3027.

Liu, F., M. Visser, D. L. Duffy, P. G. Hysi, L. C. Jacobs, O. Lao, K. Zhong, S. Walsh, L. Chaitanya, A. Wollstein, G. Zhu, G. W. Montgomery, A. K. Henders, M. Mangino, D.

Glass, V. Bataille, R. A. Sturm, F. Rivadeneira, A. Hofman, W. F. J. van IJcken, A. G. Uitterlinden, R.-J. T. S. Palstra, T. D. Spector, N. G. Martin, T. E. C. Nijsten, and M. Kayser. 2015a. Genetics of skin color variation in Europeans: genome-wide association studies with functional follow-up. Hum. Genet. 134:823–835.

Liu, K. J., E. Steinberg, A. Yozzo, Y. Song, M. H. Kohn, and L. Nakhleh. 2015b. Interspecific introgressive origin of genomic diversity in the house mouse. Proc Natl Acad Sci U A 112:196–201.

Lobo, G. P., A. Isken, S. Hoff, D. Babino, and J. von Lintig. 2012. BCDO2 acts as a carotenoid scavenger and gatekeeper for the mitochondrial apoptotic pathway. Development 139:2966–2977.

Long, K. M., A. G. Rivera-Colón, K. F. P. Bennett, J. M. Catchen, M. J. Braun, and J. D. Brawn. in review. Ongoing introgression of a secondary sexual plumage trait in a stable avian hybrid zone. bioRxiv: https://www.biorxiv.org/content/10.1101/2023.03.30.535000v1.

Lopes, R. J., J. D. Johnson, M. B. Toomey, M. S. Ferreira, P. M. Araujo, J. Melo-Ferreira, L. Andersson, G. E. Hill, J. C. Corbo, and M. Carneiro. 2016. Genetic basis for red coloration in birds. Curr Biol 26:1427–1434.

Maia, R., H. Gruson, J. A. Endler, and T. E. White. 2019. pavo 2: New tools for the spectral and spatial analysis of colour in R. Methods Ecol. Evol. 10:1097–1107.

Marini, M. Â., and S. J. Hackett. 2002. A multifaceted approach to the characterization of an intergeneric hybrid manakin (Pipridae) from Brazil. Auk 119:1114–1120.

Martin, S. H., J. W. Davey, and C. D. Jiggins. 2015. Evaluating the use of ABBA–BABA statistics to locate introgressed loci. Mol. Biol. Evol. 32:244–257.

Martin, S. H., and C. D. Jiggins. 2017. Interpreting the genomic landscape of introgression. Curr Opin Genet Dev 47:69–74.

Martinsen, G. D., T. G. Whitham, R. J. Turek, and P. Keim. 2001. Hybrid populations selectively filter gene introgression between species. Evolution 55:1325–1335.

Mayr, E. 1963. Animal Species and Evolution. Harvard University Press, Cambridge, MA.

Mayr, E. 1942. Systematics and the Origin of Species. Harvard University Press, Cambridge, MA.

McDonald, D. B., R. P. Clay, R. T. Brumfield, and M. J. Braun. 2001. Sexual selection on plumage and behavior in an avian hybrid zone: experimental tests of male-male interactions. Evolution 55:1443–1451.

McGraw, K. J., E. Adkins-Regan, and R. S. Parker. 2002. Anhydrolutein in the zebra finch: a new, metabolically derived carotenoid in birds. Comp. Biochem. Physiol. B Biochem. Mol. Biol. 132:811–818.

McGraw, K. J., J. Hudon, G. E. Hill, and R. S. Parker. 2005. A simple and inexpensive chemical test for behavioral ecologists to determine the presence of carotenoid pigments in animal tissues. Behav. Ecol. Sociobiol. 57:391–397.

McGraw, K. J., K. Wakamatsu, A. B. Clark, and K. Yasukawa. 2004. Red-winged blackbirds Agelaius phoeniceus use carotenoid and melanin pigments to color their epaulets. J. Avian Biol. 35:543–550.

McKenna, A., M. Hanna, E. Banks, A. Sivachenko, K. Cibulskis, A. Kernytsky, K. Garimella, D. Altshuler, S. Gabriel, M. Daly, and M. A. DePristo. 2010. The Genome Analysis Toolkit: a MapReduce framework for analyzing next-generation DNA sequencing data. Genome Res. 20:1297–1303.

McQuillan, M. A., and A. M. Rice. 2015. Differential effects of climate and species interactions on range limits at a hybrid zone: potential direct and indirect impacts of climate change. Ecol Evol 5:5120–5137.

McQuillan, M. A., T. C. Roth 2nd, A. V. Huynh, and A. M. Rice. 2018. Hybrid chickadees are deficient in learning and memory. Evolution 72:1155–1164.

Meier, J. I., R. B. Stelkens, D. A. Joyce, S. Mwaiko, N. Phiri, U. K. Schliewen, O. M. Selz, C. E. Wagner, C. Katongo, and O. Seehausen. 2019. The coincidence of ecological opportunity with hybridization explains rapid adaptive radiation in Lake Mweru cichlid fishes. Nat. Commun. 10:5391.

Menon, M., E. Landguth, A. Leal-Saenz, J. C. Bagley, A. W. Schoettle, C. Wehenkel, L. Flores-Renteria, S. A. Cushman, K. M. Waring, and A. J. Eckert. 2020. Tracing the footprints of a moving hybrid zone under a demographic history of speciation with gene flow. Evol. Appl. 13:195–209.

Metzler, D., U. Knief, J. V. Peñalba, and J. B. W. Wolf. 2021. Assortative mating and epistatic mating-trait architecture induce complex movement of the crow hybrid zone. Evolution 75:3154–3174.

Miles, M. C., F. Goller, and M. J. Fuxjager. 2018. Physiological constraint on acrobatic courtship behavior underlies rapid sympatric speciation in bearded manakins. Elife 7:e40630.

Minh, B. Q., H. A. Schmidt, O. Chernomor, D. Schrempf, M. D. Woodhams, A. von Haeseler, and R. Lanfear. 2020. IQ-TREE 2: New models and efficient methods for phylogenetic inference in the genomic era. Mol. Biol. Evol. 37:1530–1534.

Møller, A. P., C. Biard, J. D. Blount, D. C. Houston, P. Ninni, N. Saino, and P. F. Surai. 2000. Carotenoid-dependent signals: indicators of foraging efficiency, immunocompetence or detoxification ability? Poult. Avian Biol. Rev. 11:137–160.

Moore, R. P., W. D. Robinson, I. J. Lovette, and T. R. Robinson. 2008. Experimental evidence for extreme dispersal limitation in tropical forest birds. Ecol Lett 11:960–968.

Mundy, N. I., J. Stapley, C. Bennison, R. Tucker, H. Twyman, K.-W. Kim, T. Burke, T. R. Birkhead, S. Andersson, and J. Slate. 2016. Red carotenoid coloration in the Zebra Finch Is controlled by a cytochrome P450 gene cluster. Curr Biol 26:1435–1440.

Murphy, T. G., M. F. Rosenthal, R. Montgomerie, and K. A. Tarvin. 2009. Female American goldfinches use carotenoid-based bill coloration to signal status. Behav Ecol 20:1348–1355.

Naka, L. N., C. L. Bechtoldt, L. M. P. Henriques, and R. T. Brumfield. 2012. The role of physical barriers in the location of avian suture zones in the Guiana Shield, northern Amazonia. Am Nat 179:E115-32.

Naka, L. N., and R. T. Brumfield. 2018. The dual role of Amazonian rivers in the generation and maintenance of avian diversity. Sci Adv 4:eaar8575.

Naka, L. N., and M. W. Pil. 2020. Moving beyond the riverine barrier vicariant paradigm. Mol Ecol 29:2129–2132.

Nei, M. 1987. Molecular Evolutionary Genetics. Columbia University Press, New York, NY.

Nei, M., and W. H. Li. 1979. Mathematical model for studying genetic variation in terms of restriction endonucleases. Proc. Natl. Acad. Sci. 76:5269–5273.

Newton, I. 2003. Speciation and Biogeography of Birds. Academic Press, San Diego, CA.

Nosil, P., J. L. Feder, and Z. Gompert. 2021. How many genetic changes create new species? Science 371:777–779.

Ödeen, A., and O. Håstad. 2013. The phylogenetic distribution of ultraviolet sensitivity in birds. BMC Evol. Biol. 13:36.

O'Donald, P., and M. E. N. Majerus. 1984. Polymorphism of melanic ladybirds maintained by frequency-dependent sexual selection. Biol J Linn Soc Lond 23:101–111.

O'Leary, S. J., J. B. Puritz, S. C. Willis, C. M. Hollenbeck, and D. S. Portnoy. 2018. These aren't the loci you'e looking for: Principles of effective SNP filtering for molecular ecologists. Mol Ecol 27:3193–3206.

Olson, J. R., S. J. Cooper, D. L. Swanson, M. J. Braun, and J. B. Williams. 2010. The relationship of metabolic performance and distribution in black-capped and Carolina chickadees. Physiol Biochem Zool 83:263–275.

Olson, S. L. 1970. Specializations of some carotenoid-bearing feathers. The Condor 72:424–430.

Orteu, A., and C. D. Jiggins. 2020. The genomics of coloration provides insights into adaptive evolution. Nat Rev Genet 21:461–475.

Owens, G. L., M. Todesco, N. Bercovich, J.-S. Légaré, N. Mitchell, K. D. Whitney, and L. H. Rieseberg. 2021. Standing variation rather than recent adaptive introgression probably underlies differentiation of the texanus subspecies of *Helianthus annuus*. Mol. Ecol. 30:6229–6245.

Parchman, T. L., Z. Gompert, M. J. Braun, R. T. Brumfield, D. B. McDonald, J. A. C. Uy, G. Zhang, E. D. Jarvis, B. A. Schlinger, and C. A. Buerkle. 2013. The genomic consequences of adaptive divergence and reproductive isolation between species of manakins. Mol Ecol 22:3304–3317.

Parker, T. A., T. S. Schulenberg, G. R. Graves, and M. J. Braun. 1985. The avifauna of the Huancabamba Region, northern Peru. Ornithol Monogr 169–197.

Parkes, K. C. 1961. Intergeneric hybrids in the family Pipridae. Condor 63:345–350.

Parsons, T. J., S. L. Olson, and M. J. Braun. 1994. Hybrid zones and sexual selection: response to Butlin and Neems. Science 265:122–123.

Parsons, T. J., S. L. Olson, and M. J. Braun. 1993. Unidirectional spread of secondary sexual plumage traits across an avian hybrid zone. Science 260:1643–1646.

Payseur, B. A., J. G. Krenz, and M. W. Nachman. 2004. Differential patterns of introgression across the X chromosome in a hybrid zone between two species of house mice. Evolution 58:2064–2078.

Peres, C. A., J. L. Patton, and M. N. da Silva. 1996. Riverine barriers and gene flow in Amazonian saddle-back tamarins. Folia Primatol 67:113–124.

Peters, J. L. 1927. A new manakin from Panama. Proc N Engl Zool Club 10:9–10.

Pflugbeil, G., M. Affenzeller, A. Tribsch, and H. P. Comes. 2021. Primary hybrid zone formation in *Tephroseris helenitis* (Asteraceae), following postglacial range expansion along the central Northern Alps. Mol. Ecol. 30:1704–1720.

Poelstra, J. W., N. Vijay, C. M. Bossu, H. Lantz, B. Ryll, I. Müller, V. Baglione, P. Unneberg, M. Wikelski, M. G. Grabherr, and J. B. W. Wolf. 2014. The genomic landscape underlying phenotypic integrity in the face of gene flow in crows. Science 344:1410–1414.

Poelstra, J. W., N. Vijay, M. P. Hoeppner, and J. B. W. Wolf. 2015. Transcriptomics of colour patterning and coloration shifts in crows. Mol Ecol 24:4617–4628.

Potticary, A. L., E. S. Morrison, and A. V. Badyaev. 2020. Turning induced plasticity into refined adaptations during range expansion. Nat. Commun. 11:3254.

Prado, F., T. J. Billo, and B. Kerr. 2009. Introgression of sexually selected traits in lek-mating species. Evol Ecol Res 11:1235–1250.

Price, T. 2008. Speciation in Birds. Roberts and Co., Greenwood Village, CO.

Price-Waldman, R., and M. C. Stoddard. 2021. Avian coloration genetics: recent advances and emerging questions. J Hered 112:395–416.

Prum, R. O. 1994. Phylogenetic analysis of the evolution of alternative social behavior in the manakins (Aves: Pipridae). Evolution 48:1657–1675.

Prum, R. O. 1998. Sexual selection and the evolution of mechanical sound production in manakins (Aves: Pipridae). Anim. Behav. 55:977–994.

Prum, R. O. 2017. The Evolution of Beauty: How Darwin's Forgotten Theory of Mate Choice Shapes the Animal World - and Us. Doubleday, New York, NY.

Pryke, S. R., and S. Andersson. 2003. Carotenoid-based epaulettes reveal male competitive ability: experiments with resident and floater red-shouldered widowbirds. Anim Behav 66:217–224.

Pyron, A. R., and F. T. Burbrink. 2009. Lineage diversification in a widespread species: roles for niche divergence and conservatism in the common kingsnake, *Lampropeltis getula*. Mol Ecol 18:3443–3457.

Quinlan, A. R., and I. M. Hall. 2010. BEDTools: a flexible suite of utilities for comparing genomic features. Bioinformatics 26:841–842.

R Core Team. 2021. R: a language and environment for statistical computing. R Foundation for Statistical Computing, Vienna, Austria.

Reudink, M. W., S. G. Mech, S. P. Mullen, and R. L. Curry. 2007. Structure and dynamics of the hybrid zone between Black-capped Chickadee (*Poecile atricapillus)* and Carolina Chickadee (*P. carolinensis*) in southeastern Pennsylvania. Auk 124:463–478.

Rheindt, F. E., and S. V. Edwards. 2011. Genetic introgression: An integral but neglected component of speciation in birds. Auk 128:620–632.

Ridgely, R. S., and J. A. Gwynne. 1989. A Guide to the Birds of Panama. Princeton University Press, Princeton, NJ.

Rieseberg, L. H., R. Carter, and S. Zona. 1990. Molecular tests of the hypothesized hybrid origin of two diploid *Helianthus species* (Asteraceae). Evolution 44:1498–1511.

Roberts, N. S., and T. C. Mendelson. 2020. Reinforcement in the banded darter Etheostoma zonale: The effect of sex and sympatry on preferences. Ecol. Evol. 10:2499–2512.

Rochette, N. C., A. G. Rivera-Colón, and J. M. Catchen. 2019. Stacks 2: Analytical methods for paired-end sequencing improve RADseq-based population genomics. Mol Ecol 28:4737–4754.

Rohwer, S. A. 1973. Significance of sympatry to behavior and evolution of Great Plains meadowlarks. Evolution 27:44–57.

Rosser, N., L. M. Queste, B. Cama, N. B. Edelman, F. Mann, R. Mori Pezo, J. Morris, C. Segami, P. Velado, S. Schulz, J. L. B. Mallet, and K. K. Dasmahapatra. 2019. Geographic contrasts between pre- and postzygotic barriers are consistent with reinforcement in *Heliconius* butterflies. Evolution 73:1821–1838.

Rowe, L., and H. D. Rundle. 2021. The alignment of natural and sexual selection. Annu. Rev. Ecol. Evol. Syst. 52:499–517.

Ruokolainen, K., G. M. Moulatlet, G. Zuquim, C. Hoorn, and H. Tuomisto. 2019. Geologically recent rearrangements in central Amazonian river network and their importance for the riverine barrier hypothesis. Front. Biogeogr. 11.

Ryan, S. F., M. C. Fontaine, J. M. Scriber, M. E. Pfrender, S. T. O'Neil, and J. J. Hellmann. 2017. Patterns of divergence across the geographic and genomic landscape of a butterfly hybrid zone associated with a climatic gradient. Mol. Ecol. 26:4725–4742.

Sæther, S. A., G.-P. Sætre, T. Borge, C. Wiley, N. Svedin, G. Andersson, T. Veen, J. Haavie, M. R. Servedio, S. Bureš, M. Král, M. B. Hjernquist, L. Gustafsson, J. Träff, and A. Qvarnström. 2007. Sex chromosome-linked species recognition and evolution of reproductive isolation in flycatchers. Science 318:95–97.

Sætre, G.-P., T. Moum, S. Bureš, M. Král, M. Adamjan, and J. Moreno. 1997. A sexually selected character displacement in flycatchers reinforces premating isolation. Nature 387:589–592.

Saks, L., K. McGraw, and P. Hõrak. 2003. How feather colour reflects its carotenoid content. Funct. Ecol. 17:555–561.

Sakudoh, T., S. Kuwazaki, T. Iizuka, J. Narukawa, K. Yamamoto, K. Uchino, H. Sezutsu, Y. Banno, and K. Tsuchida. 2013. CD36 homolog divergence is responsible for the selectivity of carotenoid species migration to the silk gland of the silkworm *Bombyx mori*. J Lipid Res 54:482–495.

Salisbury, C. L., N. Seddon, C. R. Cooney, and J. A. Tobias. 2012. The latitudinal gradient in dispersal constraints: ecological specialisation drives diversification in tropical birds. Ecol Lett 15:847–855.

Sampaio, L., D. O. Ferraz, A. C. M. da Costa, A. Aleixo, P. V. Cerqueira, J. Araripe, and P. S. do Rêgo. 2020. Analyses of plumage coloration and genetic variation confirm the hybridization of *Pipra fasciicauda* and *Pipra aureola* in the Brazilian Amazon basin. J Ornithol 161:503–508.

Sandell, L. L., B. W. Sanderson, G. Moiseyev, T. Johnson, A. Mushegian, K. Young, J.-P. Rey, J. Ma, K. Staehling-Hampton, and P. A. Trainor. 2007. RDH10 is essential for synthesis of embryonic retinoic acid and is required for limb, craniofacial, and organ development. Genes Dev. 21:1113–1124.

Sattler, G. D., P. Sawaya, and M. J. Braun. 2007. An assessment of song admixture as an indicator of hybridization in Black-capped Chickadees (*Poecile atricapillus*) and Carolina Chickadees (*P. carolinensis*). Auk 124:926–944.

Schlinger, B. A., J. Barske, L. Day, L. Fusani, and M. J. Fuxjager. 2013. Hormones and the neuromuscular control of courtship in the golden-collared manakin (*Manacus vitellinus*). Front Neuroendocr. 34:143–156.

Seddon, N. 2005. Ecological adaptation and species recognition drives vocal evolution in neotropical suboscine birds. Evolution 59:200–215.

Semenov, G. A., E. Linck, E. D. Enbody, R. B. Harris, D. R. Khaydarov, P. Alström, L. Andersson, and S. A. Taylor. 2021. Asymmetric introgression reveals the genetic architecture of a plumage trait. Nat Commun 12:1019.

Semenov, G. A., E. S. C. Scordato, D. R. Khaydarov, C. C. R. Smith, N. C. Kane, and R. J. Safran. 2017. Effects of assortative mate choice on the genomic and morphological structure of a hybrid zone between two bird subspecies. Mol Ecol 26:6430–6444.

Sendell-Price, A. T., K. C. Ruegg, B. C. Robertson, and S. M. Clegg. 2021. An island-hopping bird reveals how founder events shape genome-wide divergence. Mol Ecol 30:2495–2510.

Sequeira, F., J. W. Arntzen, D. van Gulik, S. Hajema, R. L. Diaz, M. Wagt, and I. van Riemsdijk. 2022. Genetic traces of hybrid zone movement across a fragmented habitat. J. Evol. Biol. 35:400–412.

Sequeira, F., A. Bessa-Silva, P. Tarroso, T. Sousa-Neves, M. Vallinoto, H. Gonçalves, and I. Martínez-Solano. 2020. Discordant patterns of introgression across a narrow hybrid zone between two cryptic lineages of an Iberian endemic newt. J. Evol. Biol. 33:202–216.

Servedio, M. R., G. S. V. Doorn, M. Kopp, A. M. Frame, and P. Nosil. 2011. Magic traits in speciation: 'magic' but not rare? Trends Ecol. Evol. 26:389–397.

Shawkey, M. D., and G. E. Hill. 2005. Carotenoids need structural colours to shine. Biol. Lett. 1:121–124.

Shawkey, M. D., G. E. Hill, K. J. McGraw, W. R. Hood, and K. Huggins. 2006. An experimental test of the contributions and condition dependence of microstructure and carotenoids in yellow plumage coloration. Proc. R. Soc. B Biol. Sci. 273:2985–2991.

Shorey, L. 2002. Mating success on white-bearded manakin (*Manacus manacus*) leks: male characteristics and relatedness. Behav Ecol Sociobiol 52:451–457.

Sibley, C. G. 1957. The evolutionary and taxonomic significance of sexual dimorphism and hybridization in birds. Condor 59:166–191.

Sick, H. 1967. Rios e enchentes na Amazônia como obstáculo para a avifauna. Pp. 495–520 *in* Atas Do Simpósio Sobre a Biota Amazônica, Conselho de Pesquisas, Rio de Janeiro. Conselho de Pesquisas Rio de Janeiro, Brazil.

Skutch, A. F. 1969. Life histories of Central American birds III: Families Cotingidae, Pipridae, Formicariidae, Furnariidae, Dendrocolaptidae, and Picidae. Pac. Coast Avifauna 35:1–580.

Slatkin, M. 1985. Gene flow in natural populations. Annu Rev Ecol Syst 16:393–430.

Sly, N. D. 2023. Golden-collared Manakin (*Manacus vitellinus*), version 2.0. Cornell Lab of Ornithology, Ithaca, NY.

Smith, B. T., J. E. McCormack, A. M. Cuervo, M. J. Hickerson, A. Aleixo, C. D. Cadena, J. Pérez-Emán, C. W. Burney, X. Xie, M. G. Harvey, B. C. Faircloth, T. C. Glenn, E. P. Derryberry, J. Prejean, S. Fields, and R. T. Brumfield. 2014. The drivers of tropical speciation. Nature 515:406–409.

Snow, D. W. 2004. Family Pipridae (Manakins). Pp. 110–169 *in* J. del Hoyo, A. Elliott, and D. A. Christie, eds. Handbook of the Birds of the World. Lynx Ediciones, Barcelona, Spain.

Stein, A. C., and J. A. C. Uy. 2006a. Plumage brightness predicts male mating success in the lekking golden-collared manakin, *Manacus vitellinus*. Behav Ecol 17:41–47.

Stein, A. C., and J. A. C. Uy. 2006b. Unidirectional introgression of a sexually selected trait across an avian hybrid zone: A role for female choice? Evolution 60:1476–1485.

Stewart, K. A., J. D. Austin, K. R. Zamudio, and S. C. Lougheed. 2016. Contact zone dynamics during early stages of speciation in a chorus frog (*Pseudacris crucifer*). Heredity 116:239–247.

Stotz, D. F. 1993. A hybrid manakin (Pipra) from Roraima, Brazil, and a phylogenetic perspective on hybridization in the Pipridae. Wilson Bull 105:348–351.

Strychalski, J., P. Brym, U. Czarnik, and A. Gugołek. 2015. A novel AAT-deletion mutation in the coding sequence of the BCO2 gene in yellow-fat rabbits. J. Appl. Genet. 56:535–537.

Stryjewski, K. F., and M. D. Sorenson. 2017. Mosaic genome evolution in a recent and rapid avian radiation. Nat Ecol Evol 1:1912–1922.

Sugawara, T., K. Matsubara, R. Akagi, M. Mori, and T. Hirata. 2006. Antiangiogenic activity of brown algae fucoxanthin and Its deacetylated product, fucoxanthinol. J. Agric. Food Chem. 54:9805–9810.

Suvorov, A., B. Y. Kim, J. Wang, E. E. Armstrong, D. Peede, E. R. R. D'Agostino, D. K. Price, P. J. Waddell, M. Lang, V. Courtier-Orgogozo, J. R. David, D. Petrov, D. R. Matute, D. R. Schrider, and A. A. Comeault. 2022. Widespread introgression across a phylogeny of 155 *Drosophila* genomes. Curr. Biol. 32:111-123.e5.

Taylor, E. B., J. W. Boughman, M. Groenenboom, M. Sniatynski, D. Schluter, and J. L. Gow. 2006. Speciation in reverse: morphological and genetic evidence of the collapse of a three-spined stickleback (*Gasterosteus aculeatus*) species pair. Mol Ecol 15:343–355.

Taylor, S. A., and E. L. Larson. 2019. Insights from genomes into the evolutionary importance and prevalence of hybridization in nature. Nat Ecol Evol 3:170–177.

Taylor, S. A., T. A. White, W. M. Hochachka, V. Ferretti, R. L. Curry, and I. Lovette. 2014. Climate-mediated movement of an avian hybrid zone. Curr Biol 24:671–676.

Teeter, K. C., L. M. Thibodeau, Z. Gompert, C. A. Buerkle, M. W. Nachman, and P. K. Tucker. 2010. The variable genomic architecture of isolation between hybridizing species of house mice. Evolution 64:472–485.

Theron, E., K. Hawkins, E. Bermingham, R. E. Ricklefs, and N. I. Mundy. 2001. The molecular basis of an avian plumage polymorphism in the wild: a melanocortin-1-receptor point mutation is perfectly associated with the melanic plumage morph of the bananaquit, *Coereba flaveola*. Curr Biol 11:550–557.

Théry, M. 1992. The evolution of leks through female choice: differential clustering and space utilization in six sympatric manakins. Behav Ecol Sociobiol 30:227–237.

Titcomb, M., and A. O'Dea. 2020. Post-glacial sea level rise on the isthmus of Panama.

Toews, D. P. L., and A. Brelsford. 2012. The biogeography of mitochondrial and nuclear discordance in animals. Mol Ecol 21:3907–3930.

Toews, D. P. L., N. R. Hofmeister, and S. A. Taylor. 2017. The evolution and genetics of carotenoid processing in animals. Trends Genet 33:171–182.

Toews, D. P. L., S. A. Taylor, H. M. Streby, G. R. Kramer, and I. J. Lovette. 2019. Selection on VPS13A linked to migration in a songbird. Proc. Natl. Acad. Sci. 116:18272–18274.

Toews, D. P. L., S. A. Taylor, R. Vallender, A. Brelsford, B. G. Butcher, P. W. Messer, and I. J. Lovette. 2016. Plumage genes and little else distinguish the genomes of hybridizing warblers. Curr Biol 26:2313–2318.

Toomey, M. B., and J. C. Corbo. 2017. Evolution, development and function of vertebrate cone oil droplets. Front Neural Circuits 11:97.

Toomey, M. B., R. J. Lopes, P. M. Araújo, J. D. Johnson, M. A. Gazda, S. Afonso, P. G. Mota, R. E. Koch, G. E. Hill, J. C. Corbo, and M. Carneiro. 2017. High-density lipoprotein receptor SCARB1 is required for carotenoid coloration in birds. Proc Natl Acad Sci USA 114:5219–5224.

Toomey, M. B., C. I. Marques, P. Andrade, P. M. Araújo, S. Sabatino, M. A. Gazda, S. Afonso, R. J. Lopes, J. C. Corbo, and M. Carneiro. 2018. A non-coding region near Follistatin controls head colour polymorphism in the Gouldian finch. Proc Biol Sci 285.

Troy, D. M., and A. H. Brush. 1983. Pigments and feather structure of the redpolls, *Carduelis flammea* and *C. hornemanni*. The Condor 85:443–446.

Tuttle, E. M., A. O. Bergland, M. L. Korody, M. S. Brewer, D. J. Newhouse, P. Minx, M. Stager, A. Betuel, Z. A. Cheviron, W. C. Warren, R. A. Gonser, and C. N. Balakrishnan. 2016. Divergence and functional degradation of a sex chromosome-like supergene. Curr Biol 26:344–350.

Uy, J. A. C., and J. A. Endler. 2004. Modification of the visual background increases the conspicuousness of golden-collared manakin displays. Behav Ecol 15:1003–1010.

Uy, J. A. C., and A. C. Stein. 2007. Variable visual habitats may influence the spread of colourful plumage across an avian hybrid zone. J Evol Biol 20:1847–1858.

Våge, D. I., and I. A. Boman. 2010. A nonsense mutation in the beta-carotene oxygenase 2 (BCO2) gene is tightly associated with accumulation of carotenoids in adipose tissue in sheep (*Ovis aries*). BMC Genet. 11:10.

Via, S. 2009. Natural selection in action during speciation. Proc. Natl. Acad. Sci. 106:9939–9946.

Vickrey, A. I., R. Bruders, Z. Kronenberg, E. Mackey, R. J. Bohlender, E. T. Maclary, R. Maynez, E. J. Osborne, K. P. Johnson, C. D. Huff, M. Yandell, and M. D. Shapiro. 2018. Introgression of regulatory alleles and a missense coding mutation drive plumage pattern diversity in the rock pigeon. Elife 7:e34803.

Wagner, D. N., R. L. Curry, N. Chen, I. J. Lovette, and S. A. Taylor. 2020. Genomic regions underlying metabolic and neuronal signaling pathways are temporally consistent in a moving avian hybrid zone. Evolution 74:1498–1513.

Wallace, A. R. 1889. Darwinism: An Exposition of the Theory of Natural Selection, with Some of Its Applications. 2nd ed. Macmillan and Co, London, UK.

Wallace, A. R. 1852. On the monkeys of the Amazon. Proc. Zool. Soc. Lond. 20:107–110.

Wang, S., S. Rohwer, D. R. de Zwaan, D. P. L. Toews, I. J. Lovette, J. Mackenzie, and D. Irwin. 2020. Selection on a small genomic region underpins differentiation in multiple color traits between two warbler species. Evol Lett 4:502–515.

Weir, B. S., and C. C. Cockerham. 1984. Estimating F-statistics for the analysis of population structure. Evolution 38:1358–1370.

Weir, J. T., M. S. Faccio, P. Pulido-Santacruz, A. O. Barrera-Guzmán, and A. Aleixo. 2015. Hybridization in headwater regions, and the role of rivers as drivers of speciation in Amazonian birds. Evolution 69:1823–1834.

Wetmore, A. 1959. The birds of Isla Escudo de Veraguas, Panama. Smithson. Misc. Collect. 139:1–27.

Wetmore, A. 1972. The birds of the Republic of Panama. Part 3. Passeriformes: Dendrocolaptidae (woodcreepers) to Oxyruncidae (sharpbills). Smithson. Misc. Collect. 150:334–343.

Whitney, K. D., R. A. Randell, and L. H. Rieseberg. 2006. Adaptive introgression of herbivore resistance traits in the weedy sunflower *Helianthus annuus*. Am. Nat. 167:794–807.

Widelitz, R. B., G.-W. Lin, Y.-C. Lai, J. A. Mayer, P.-C. Tang, H.-C. Cheng, T.-X. Jiang, C.-F. Chen, and C.-M. Chuong. 2019. Morpho-regulation in diverse chicken feather formation: Integrating branching modules and sex hormone-dependent morpho-regulatory modules. Dev. Growth Differ. 61:124–138.

Wiens, B. J., F. J. Combe, B. Dickerson, L. M. Divine, V. M. Padula, G. K. Sage, S. L. Talbot, and A. G. Hope. 2022. Genetic drift drives rapid speciation of an Arctic insular endemic shrew (*Sorex pribilofensis*). Mol Ecol 31:5231–5248.

Wilke, C. O. 2020. cowplot: Streamlined Plot Theme and Plot Annotations for "ggplot2." https://cran.r-project.org/web/packages/cowplot/index.html.

Wilkinson, G. S., F. Breden, J. E. Mank, M. G. Ritchie, A. D. Higginson, J. Radwan, J. Jaquiery, W. Salzburger, E. Arriero, S. M. Barribeau, P. C. Phillips, S. C. P. Renn, and L. Rowe. 2015. The locus of sexual selection: moving sexual selection studies into the post-genomics era. J. Evol. Biol. 28:739–755.

Wirtz, P. 1999. Mother species–father species: unidirectional hybridization in animals with female choice. Anim. Behav. 58:1–12.

Wright, S. 1931. Evolution in Mendelian populations. Genetics 16:97–159.

Wright, S. W., S. W. Jeffrey, R. F. C. Mantoura, C. A. Llewellyn, T. Bjørnland, D. Repeta, and N. Welschmeyer. 1991. Improved HPLC method for the analysis of chlorophylls and carotenoids from marine phytoplankton. Mar. Ecol. Prog. Ser. 77:183–196.

Wu, C.-I. 2001. The genic view of the process of speciation. J. Evol. Biol. 14:851–865.

Yang, W., N. Feiner, C. Pinho, G. M. While, A. Kaliontzopoulou, D. J. Harris, D. Salvi, and T. Uller. 2021. Extensive introgression and mosaic genomes of Mediterranean endemic lizards. Nat. Commun. 12:2762.

Yeaman, S. 2013. Hybridization and the porous genome: patterns of isolation and introgression in manakins. Mol Ecol 22:3195–3197.

Yuri, T., R. W. Jernigan, R. T. Brumfield, N. K. Bhagabati, and M. J. Braun. 2009. The effect of marker choice on estimated levels of introgression across an avian (Pipridae: *Manacus*) hybrid zone. Mol Ecol 18:4888–4903.

Zeileis, A., G. Grothendieck, J. A. Ryan, J. M. Ulrich, and F. Andrews. 2023. zoo: S3 Infrastructure for Regular and Irregular Time Series (Z's Ordered Observations). https://cran.r-project.org/web/packages/zoo/index.html.

Zimin, A. V., G. Marçais, D. Puiu, M. Roberts, S. L. Salzberg, and J. A. Yorke. 2013. The MaSuRCA genome assembler. Bioinformatics 29:2669–2677.

Zouros, E., and C. J. d'Entremont. 1980. Sexual isolation among populations of *Drosophila mojavensis*: Response to pressure from a related species. Evolution 34:421–430.